

Waitaki District Coastal Hazards

Prepared for the Otago Regional Council

January 2019



Prepared by:
Cyprien Bosserelle
Murray Hicks
Jo Bind




For any information regarding this report please contact:

Cyprien Bosserelle
Hydrodynamics Modeller
Hydrodynamics
+64-3-341 2840
cyprien.bosserelle@niwa.co.nz

National Institute of Water & Atmospheric Research Ltd
PO Box 8602
Riccarton
Christchurch 8011

Phone +64 3 348 8987

NIWA CLIENT REPORT No: 2018035CH
Report date: January 2019
NIWA Project: ORC18502

Quality Assurance Statement		
	Reviewed by:	Richard Measures
	Formatting checked by:	Rachel Wright
	Approved for release by:	Helen Rouse

Front page: View of the coastline between Bridge Point and Orore Point. [Jo Bind, NIWA]

© All rights reserved. This publication may not be reproduced or copied in any form without the permission of the copyright owner(s). Such permission is only to be given in accordance with the terms of the client's contract with NIWA. This copyright extends to all forms of copying and any storage of material in any kind of information retrieval system.

Whilst NIWA has used all reasonable endeavours to ensure that the information contained in this document is accurate, NIWA does not give any express or implied warranty as to the completeness of the information contained herein, or that it will be suitable for any purpose(s) other than those specifically contemplated during the Project or agreed by NIWA and the Client.

Contents

- Executive summary 6**

- 1 Introduction 7**
 - 1.1 Project overview 7

- 2 Coastal inundation hazard..... 10**
 - 2.1 Review of Lane et al. (2008) 10
 - 2.2 Updated sea-level rise scenarios 15
 - 2.3 Methodology for updated mapping of inundation hazard zones 16
 - 2.4 Results..... 17

- 3 Coastal erosion hazard 28**
 - 3.1 Introduction 28
 - 3.2 Methodology 29
 - 3.3 Results..... 49

- 4 Discussion 74**
 - 4.1 Overview of the results..... 74
 - 4.2 Impact of accelerated sea-level rise on the erosion hazard 74
 - 4.3 Effectiveness of coastal protection to reduce erosion hazard 75
 - 4.4 Coastal monitoring..... 75

- 5 Conclusion 78**

- 6 Acknowledgements 79**

- 7 References..... 80**

- 8 List of supplementary material supplied separately from this report 83**

Tables

Table 2-1:	Wave runup prediction.	12
Table 2-2:	Sea-level scenarios for coastal inundation prediction.	16
Table 2-3:	Predicted extreme water levels (m above MSL) for four average recurrence interval (ARI).	17
Table 2-4:	Inundation depth for different extreme water level scenarios and sea level rise scenarios at Esplanade Road.	19
Table 3-1:	Imagery data source used in the shoreline detection.	30
Table 3-2:	Wide gravel barrier geometry parameters used in equation 3.6 for the Waitaki River mouth.	46
Table 3-3:	Location of cliff top on profiles surveyed by Otago Regional Council.	64

Figures

Figure 1-1:	Location of the study area.	8
Figure 2-1:	Comparison of measured and predicted inundation extent in Kakanui.	14
Figure 2-2:	Predicted inundation depth for the 100-year ARI storm and +0.0 m SLR for Oamaru.	18
Figure 2-3:	Predicted inundation depth for the 100-year ARI storm and +1.3 m SLR for Oamaru.	19
Figure 2-4:	Predicted inundation depth for the 100-year ARI storm and +0.0 m SLR for Kakanui.	20
Figure 2-5:	Predicted inundation depth for the 100-year ARI storm and +1.3 m SLR for Kakanui.	21
Figure 2-6:	Inundation depth for the 100-year ARI storm and +0.0 m SLR for Hampden.	22
Figure 2-7:	Inundation depth for the 100-year ARI storm and +1.3 m SLR for Hampden.	23
Figure 2-8:	Inundation depth for the 100-year ARI storm and +0.0 m SLR for Moeraki.	24
Figure 2-9:	Inundation depth for the 100-year ARI storm and +1.3 m SLR for Moeraki.	24
Figure 2-10:	Coastal inundation hazard zone extents for Oamaru.	25
Figure 2-11:	Coastal inundation hazard zone extents for Kakanui.	26
Figure 2-12:	Coastal inundation hazard zone extents for Hampden.	26
Figure 2-13:	Coastal inundation hazard zone extents for Moeraki.	27
Figure 3-1:	Armouring of the backshore cliff on Katiki Road (7/12/2017).	29
Figure 3-2:	Example of shoreline detection along Beach Road, south of Oamaru.	31
Figure 3-3:	Example of transects perpendicular to the coast.	32
Figure 3-4:	Example of intersection point between the transects and detected shorelines.	32
Figure 3-5:	Example of shoreline trend analysis.	33
Figure 3-6:	Oamaru (central) beach profiles surveyed by Otago Regional Council.	34
Figure 3-7:	Erosion rates simulated for Oamaru using SCAPE+.	35
Figure 3-8:	Example of probabilistic coastal hazard zone prediction.	37
Figure 3-9:	Coastal morphology types along the Waitaki District coast.	38
Figure 3-10:	Example of bedrock cliff morphology.	40

Figure 3-11:	Example of unconsolidated cliff morphology: north of Oamaru.	41
Figure 3-12:	Example of unconsolidated cliff morphology: Beach Road.	42
Figure 3-13:	Example of unconsolidated cliff morphology: Hampden.	42
Figure 3-14:	Four main types of perched beaches.	44
Figure 3-15:	Example of geologically controlled beach: South Katiki Beach.	45
Figure 3-16:	Example of thin sand/gravel barrier morphology: Kakanui barrier.	47
Figure 3-17:	Calculated shoreline trends for the Waitaki District coast.	50
Figure 3-18:	Calculated shoreline trends for the Oamaru area.	51
Figure 3-19:	Calculated shoreline trends for the Kakanui area.	52
Figure 3-20:	Calculated shoreline trends for the Hampden and Moeraki area.	53
Figure 3-21:	Calculated shoreline trends for the Shag Point and Shag River mouth area.	54
Figure 3-22:	Calculated shoreline trends along Beach Road.	55
Figure 3-23:	95 th percentile of the short-term retreat for beach and cliff shores.	56
Figure 3-24:	Difference in elevation between 2004 and 2016 near Oamaru based on LiDAR surveys.	58
Figure 3-25:	Elevation profiles near Weaver Road.	59
Figure 3-26:	Elevation profile near Usk Street.	59
Figure 3-27:	Elevation profile north of Oamaru Creek.	60
Figure 3-28:	Difference in elevation between 2004 and 2016 near Kakanui based on LiDAR surveys.	61
Figure 3-29:	Elevation profile at Kakanui through a recent slump that removed part of the road.	62
Figure 3-30:	Elevation profile of the gravel barrier at Kakanui.	62
Figure 3-31:	Difference in elevation between 2004 and 2016 on Katiki Beach based on LiDAR surveys.	63
Figure 3-32:	Elevation profile on Katiki Beach.	63
Figure 3-33:	Elevation profile in Katiki Beach.	64
Figure 3-34:	Result of the cliff erosion simulation for the shore north of Oamaru.	65
Figure 3-35:	Histogram of predicted 100-year erosion hazard zone width for the most likely realisation (50 th percentile).	66
Figure 3-36:	Histogram of predicted 100-year erosion hazard zone width for the 95 th percentile realisation.	66
Figure 3-37:	Coastal hazard zone width for 95 th percentile (CHZ95) and for 50 th percentile (CHZ50) for 100-year prediction for the entire Waitaki District coastline.	68
Figure 3-38:	Coastal hazard zone width for 95 th percentile (CHZ95) and for 50 th percentile (CHZ50) for 100-year prediction for Oamaru.	69
Figure 3-39:	Coastal hazard zone width for 95 th percentile (CHZ95) and for 50 th percentile (CHZ50) for 100-year prediction for Beach Road.	70
Figure 3-40:	Coastal hazard zone width for 95 th percentile (CHZ95) and for 50 th percentile (CHZ50) for 100-year prediction for Kakanui.	71
Figure 3-41:	Coastal hazard zone width for 95 th percentile (CHZ95) and for 50 th percentile (CHZ50) for 100-year prediction for Hampden and Moeraki.	72
Figure 3-42:	Coastal hazard zone width for 95 th percentile (CHZ95) and for 50 th percentile (CHZ50) for 100-year prediction for Shag Point / Matakaea.	73
Figure 4-1:	Riprap section on Beach Road viewed on satellite imagery of 02/09/2006.	76
Figure 4-2:	Riprap section on Beach Road viewed on satellite imagery of 03/10/2012.	77

Executive summary

This study analysed the inundation and erosion hazards along the Waitaki District coast. The study, conducted by NIWA for the Otago Regional Council (ORC), found that while the erosion hazard is widespread, the inundation hazard only applies to relatively small parts of the populated area of the district (mostly Kakanui Estuary and Oamaru Port foreshore).

Coastal hazard zones were mapped for both the inundation and erosion hazards considering a 100-year planning time frame.

Inundation hazard zones are based on inundation extent across the populated area of the district and were adapted from previous work. Critical limitations in the available analysis, in particular with the estimates of extreme water levels and wave runup, constrained the use of the inundation hazard zone to low lying inland areas and does not allow the evaluation of the coastal inundation hazard in areas where wave impact is likely to be significant (e.g., Kaika, Karita, Katiki Road and Beach Road). Further study is recommended to refine the extreme water levels and wave runup and revise the inundation hazard zones.

The coastal erosion hazard zone was calculated for the entire length of the Waitaki District coast. This was based on extrapolation of historical erosion rates derived from analysis of aerial and satellite imagery and an allowance for short-term shoreline retreat due to storm erosion or cliff slumping/collapse. In areas where sufficient information was available, the erosion due to the future acceleration of sea-level rise was also taken into account. Separate simulation of the evolution of the cliffs north of Oamaru was undertaken using a numerical morphological model, and this showed that acceleration in sea-level rise should have little impact on the cliff retreat rate on that part of the coast.

The coastal erosion hazard zone was mapped for two outlook periods (50 and 100 years) and two risk levels: the CHZ95 zone mapped the line where there should only be a 5% chance that the erosion hazards could extend up to or landward of the line; and the less conservative CHZ50 zone mapped the line where there is a 50% chance that erosion hazards could extend up to or landward of the line. Decision makers should select the most suitable line depending on the planning horizon, value, and vulnerability of the assets potentially impacted by the predicted erosion.

The coastal erosion hazard zone width proposed for the 100-year outlook at 95-percentile confidence (CHZ95) is 65 m wide just north of Oamaru near Waitaki Boys High School. The CHZ95 width further north is close to 100 m which is similar to the 100 m width of the hazard zone previously proposed for the Waitaki District Council.

Much infrastructure (mostly roads) and many assets are within the CHZ95 zone. No new erosion hotspots were identified, with continued erosion expected at the current hotspots of Katiki Beach, Beach Road, Kakanui, and North Oamaru. Any plans to stabilise these shores with protective structures would need to ensure that the structures are properly built and maintained. Monitoring at these hotspots will help to refine estimates of the hazard zone widths and to better plan the nature and timing of hazard mitigation/adaptation.

The hazard zone estimates provided herein are based on a hybrid-probabilistic approach that can be reproduced and refined as new data become available.

1 Introduction

The Waitaki District is experiencing long-term retreat of its coastline. In particular, the coast north of Oamaru is experiencing a rapid recession of the soft sediment cliffs with reported retreat of 0.5 m/year (Gibb 1978). Coastal erosion in the District threatens communities, infrastructure, and assets. The Otago Regional Council is committed to better understanding of coastal hazards in the Otago Region. This focus in coastal hazards has come about through several recent drivers:

- Recent storm-related erosion events in Oamaru.
- The high cost associated with the repair and movement of coastal roads and breakwaters near Oamaru.
- The required update of the Waitaki District Plan.
- The need to address the effects of sea-level rise on coastal hazards as required by the NZ Coastal Policy Statement (NZCPS, 2010).
- A limited understanding of erosion rates along the coastline.

To address these concerns there is a need to understand and predict future coastal hazards and incorporate this understanding into future planning of development in the Waitaki District.

1.1 Project overview

The aims of this project are to:

1. Assess and update the existing coastal inundation information, including:
 - Provide feedback regarding the suitability of Lane et al. (2008) study
 - Advise the Otago Regional Council where additional information and studies are required
 - Update the inundation map with the new sea-level rise scenarios.
 - Convert the inundation information into hazard zoning for the 100-year average recurrence interval and two sea-level rise scenarios.
2. Evaluate the coastal erosion hazard for the Waitaki District including:
 - Map current shoreline position
 - Evaluate shoreline retreat rates using mapped shoreline position
 - Predict future shoreline position and construct hazard zones.

This project does not investigate the inundation related to tsunami, groundwater, river floods or urban flooding.

The study calculates the inundation hazard zone for a 100-year average recurrence interval (ARI) extreme water level. Coastal erosion hazard zones are calculated based on 50-year and 100-year projections of shoreline position following an adapted version of the shoreline recession approach proposed by Gibb (1982).

The study addresses coastal erosion for the entire Waitaki District and inundation hazards for Oamaru and the settlements of Kakanui, Hampden, Moeraki township and Boulders, and Shag Point/Matakaea (Figure 1-1).

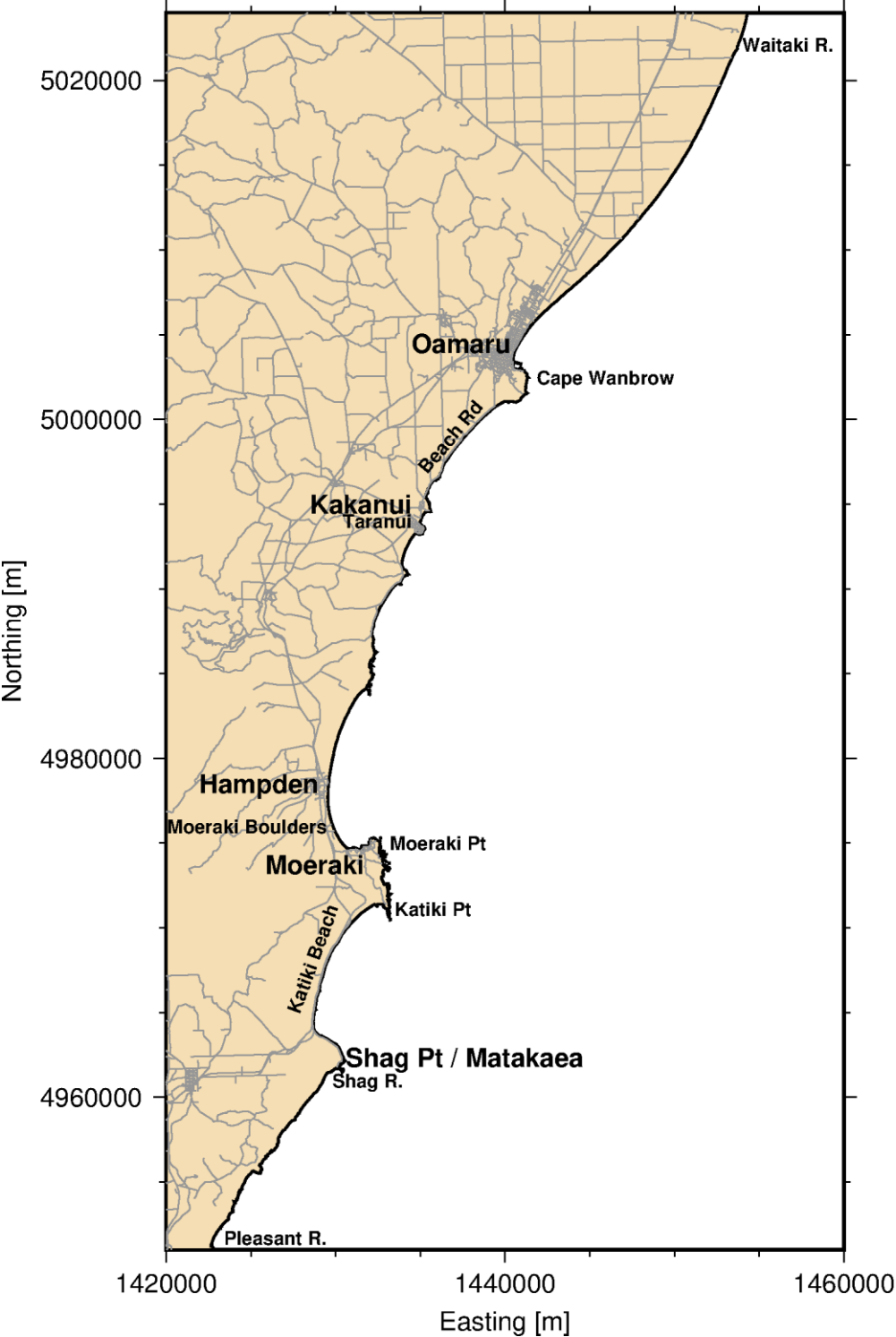


Figure 1-1: Location of the study area. Northing and easting are given in the New Zealand Transverse Mercator projection (NZTM).

Time constraints on the project did not allow for new field data collection nor even comprehensive field inspection of all the Waitaki District coast, but recommendations are made for future coastal hazard monitoring. This suggested monitoring is targeted to reduce the uncertainties where the coastal hazard risk is high and where communities and assets are more vulnerable.

The project outputs include:

- This report, which includes commentary on the methods and assumptions underpinning this hazard mapping.
- GIS files mapping the extents of the coastal inundation and erosion hazard zones.
- Four supplementary documents showing the different coastal inundation maps for storms with 20, 50, 100, and 500-year ARI and sea levels ranging from 0.0 to 1.3 m above present level.

Note that all the maps and all the northings and eastings in this report are given in the New Zealand Transverse Mercator projection (NZTM).

2 Coastal inundation hazard

Coastal inundation occurs when the elevation of the sea level exceeds that of the land, allowing water to flow inland and flood. Elevated sea levels are caused by a combination of normal tides (including neap and spring tides), storm surge due to the inverse barometer effect (i.e., lifting of the sea level by low atmospheric pressure) and wind, mean sea level anomalies (MSLA), and the release of wave energy at the coast causing wave setup and wave runup. The effects of future climate change, predominantly sea-level rise, will add to these factors.

For this project, the coastal inundation hazard due to storm tide (combined storm surge and tide), waves, and rising sea level was assessed in three steps:

- Review of Lane et al. (2008) for the prediction of coastal inundation extent from extreme water levels and waves in the Otago region. This step evaluated the suitability of the previous work for use in hazard zoning and advised on possible improvements.
- Updating the extents of the inundation hazard in Waitaki District by applying the results from Lane et al. (2008) to future sea-level rise scenarios that are in-line with guidance from the Ministry for the Environment.
- Convert the inundation extent into hazards zoning for the 100-year ARI extreme water level and two sea-level rise (SLR) scenarios.

2.1 Review of Lane et al. (2008)

Lane et al. (2008) used historical and hindcast data to describe the probability of extreme water levels from storm surge, tide, mean sea level anomaly and waves. Based on these probability distributions they calculated the 20, 50, 100 and 500-year ARI inundation events for the populated coastal areas of Oamaru, Kakanui, Hampden and Moeraki. Using the extreme water level and an estimate of wave runup, the report then shows inundation extent and inundation depths using a “bathtub”-type analysis applied over a coastal digital elevation model derived from the 2004 LiDAR survey gridded at a 10 m resolution. The report shows the impact of sea-level rise by applying sea-level rises of 0.3 m and 0.5 m to the bathtub analysis of the storm tide and wave runup.

The main finding of Lane et al. (2008) is that, in the Waitaki District, only the Kakanui River mouth area is at high risk of coastal inundation from storm tide in the 100-year ARI storm event. Most other populated coastal areas (Oamaru, Hampden, Moeraki and Shag Point) are located sufficiently above the present mean sea-level to avoid storm surge flooding.

The general methodology used in Lane et al. (2008) is sound but contains significant limitations in the analysis of wave runup, analysis of extreme water level and in the inundation mapping. The wave setup included in the extreme water levels is non-conservative, the analysis of wave runup is non-conservative (i.e., low), and the inundation mapping method (bathtub) is conservative. So, the results from Lane et al. (2008) potentially underestimate inundation depth along the coastline where wave runup occurs but overestimate the inland extend of inundation. The main other limitations are the short historical record, a simplistic approach to combining wave setup and storm surge, and lack of process-based simulation of storm surge and wave propagation over the bathymetry. Despite these limitations, improving the accuracy of the methodology used in Lane et al. (2008) is unlikely to significantly change the inundation mapping in the most populated locations in the Waitaki District because most populated coastal areas are located high above the storm surge levels. Kakanui and

Oamaru Port are the only areas where improvement to the extreme analysis and inundation simulation would refine the predicted inundation extent. This is because Kakanui is near the river mouth, is relatively low lying, and is only protected from elevated sea levels by a 20 m wide gravel/shingle barrier. The results from Lane et al. (2008) do not apply to rural parts of the Waitaki coast, thus the available information about topography and extreme water levels is insufficient to evaluate the coastal inundation hazard along these parts of the coast.

For the purposes of this work, we have used Lane et al. results, but as requested by ORC a detailed review of four aspects of the methodology (historical data, statistical model, inundation simulation and climate change impact) used by Lane et al. (2008) to assess the coastal inundation hazard is provided below. In addition, we note the potential improvements to the work that could be considered in the future.

2.1.1 Historical data

The validity of extreme water level estimates depends on the initial data used to produce the probability density function (PDF) which is then used in the extreme statistical model. The data used in the 2008 analysis were derived from a combination of wind, tide record and hindcast model results.

The historical storm surge (1961 – 2005) was reconstructed by combining the inverse barometer and wind setup component following Wild et al. (2005) using atmospheric pressure and wind data from Taiaroa Head (75 km south from Oamaru). Tidal information was extracted from the tidal model of Walters et al. (2001). The wave height was extracted from the wave model from Gorman et al. (2003).

Potential improvements to the work that could be considered in the future: improving the reconstruction approach and extending the hindcast to include recent storms would improve the extreme statistical model. This would better constrain the empirical PDF of the storm surge and reduce the uncertainty for the estimated 100-year ARI extreme water level and wave height. Developing and implementing improved methods is out of scope for this project but could be considered in future studies.

2.1.2 Statistical model used to evaluate extreme water levels

The statistical model used in Lane et al. (2008) is a type of stationary bivariate analysis which assumes that storm surge and large waves do not occur independently. This is used to describe co-occurrence of extreme storm surge and wave setup. The joint probability of storm surge and wave setup are calculated for set return intervals and then combined with tide level and mean level of the sea to obtain extreme water levels. This method for estimating extreme water levels corresponds to the present standard methodology but more recent methodologies may be more robust (e.g., Stephens and Robinson 2016). However, these more robust approaches require more data and analysis beyond the scope of this report.

The extreme water levels calculated from Lane et al. (2008) appear to be consistent with those predicted with more robust analysis. For example, they estimated the 100-year ARI extreme water level (storm surge + tide + mean sea level anomaly + wave setup) south of Dunedin at 2.05 m (relative to Dunedin Vertical Datum 1958, DVD58). If we remove from this value the estimate of the wave setup component of 0.5 m for south of Dunedin (Figure 3.8 in Lane et al. 2008), the predicted storm tide from Lane et al. (2008) is comparable to the 1.58 m (above DVD58) storm tide estimates reported by Stephens and Robinson (2016) using a more modern extreme analysis.

Beyond the approach used in the 2008 study, recent developments in the analysis of extremes may improve the statistical robustness and reduce the uncertainty of the derived storm surge distribution. Recent methods use multivariate analysis (e.g., following Gouldby et al. 2014 or Rueda et al. 2016) that account for multiple wave parameters (wave height, period and direction), separate components of the storm surge (wind setup and inverse barometer) and mean sea level anomaly.

Recent developments in coastal inundation research also aim to include seasonal and inter-annual variability in extreme distributions, with the aim of better understanding how a changing climate affects extreme events. This methodology often relies on weather pattern analysis and the non-linear relationship between the weather pattern and the interdependent components that contribute to the total water level and wave parameters. Although the necessary data is available in the Waitaki region through weather, wave and storm surge hindcasts, this type of analysis is laborious and generally applicable to large regions. Preliminary work by Rueda et al. (in review) applied this methodology to analyse the wave climate of New Zealand’s South Island and found strong inter-annual variability of large wave events.

Potential improvements to the work that could be considered in the future: Improvements to the method used in the 2008 report should better reflect the actual joint-occurrence of waves, storm surges and mean sea level anomaly along the Waitaki coastline. In addition, these modern methods are less conservative in predicting extreme events and would likely reduce the predicted extreme water levels. Developing and implementing improved methods is out of scope for this project but should be considered in future studies.

2.1.3 Wave runup calculations

The wave runup estimates from Lane et al. (2008) were calculated based on the empirical formula from Stockdon et al. (2006) using hindcasted wave conditions for the Waitaki coastline from Gorman et al. (2003). While the wave hindcast and empirical formula are robust, the values presented for runup in Lane et al. (2008) appear lower than expected when compared to nearby observations of beach morphology and runup estimates from South Canterbury. For example, the value for the maximum runup presented for the 100-year ARI event at Oamaru is 1.38 m (excluding wave setup), which is far smaller than the 6.0 m wave runup presented by Stephens et al. (2015) for Wainono Lagoon. It is likely that Lane et al. (2008) underestimated the beach slope or miscalculated how the extreme waves were determined, and therefore underestimated their runup predictions.

Table 2-1: Wave runup prediction. *Source:* Lane et al. (2008).

Location	Averaged predicted wave runup (m)	Maximum predicted wave runup (m)
Moeraki	0.28	0.85
Hampden	0.36	1.09
Kakanui	0.44	1.33
Oamaru	0.46	1.38

Potential improvements to the work that could be considered in the future: The wave runup results presented by Lane et al. (2008) are not realistic and require new calculations. This analysis is beyond the scope of this project but is critical for inundation hazard assessments.

2.1.4 Inundation simulation

The total water level calculated at the coast is extrapolated over land using a bathtub analysis where the total water level is assumed to reach a uniform elevation, and depth of inundation is then the difference in elevation between the water level and the land. This methodology cannot take into account how the storm surge flows over the land and underestimates attenuation of the propagating storm surge as it spreads inland over vegetation (Sheng et al. 2012), around obstructions (e.g., buildings) or interacts with permeable surfaces (e.g., gravel barriers), nor does it account for morphodynamic changes during such a storm. These two factors result in conservative estimates of inundation extent and depth, particularly at greater distances inland.

In addition, the analysis in Lane et al. (2008) applies a single value of wave setup and runup to each DEM grid, underestimating (or overestimating) the runup where wave focusing locally produces higher (or lower) runup and overestimating (or underestimating) runup for areas locally sheltered (or exposed) to waves.

Another process that is not explicitly considered in the 2008 analysis is the contribution of infragravity waves on the runup. These low frequency waves are generated from the breaking of wave groups in the surf zone, and they can further raise the water level at the shore for several minutes. Although their behaviour is tied to swell dissipation, they can excite resonant modes in bays and harbours and locally cause a significant amplification of the maximum water level. Infragravity waves also play a significant role in triggering overtopping and landward “rollover” of gravel barrier beaches and overtopping of coastal structures (McCall et al. 2015).

The limitations of the methodology used in Lane et al. (2008) can be evaluated by comparing the inundation extent predicted by the report with the extensive inundation observed at Kakanui from the recent storm of July 2017. Drone footage by Robertson (2017) collected immediately following the storm on 21st July 2017 was used to identify the maximum extent of inundation as indicated by debris (driftwood, seaweed etc.). The July 2017 event was a “compound” event, with coincident high storm surge (equivalent to the 1-year ARI storm tide in Timaru based on the Stephens et al. (2015) analysis) and river flooding stemming from heavy rainfall (largest recorded 24-hour rainfall accumulation in Oamaru since the record began in 1950), which renders the contribution of storm surge hard to separate from that due to river flooding. However, the extent of the inundation observed, in particular on the left bank of the river, appears to align best with the 20-year ARI inundation prediction with present day sea level (Figure 2-1). This result suggests that the inundation extent is more strongly controlled by topographical features on the floodplain than by the elevation of the storm surge.

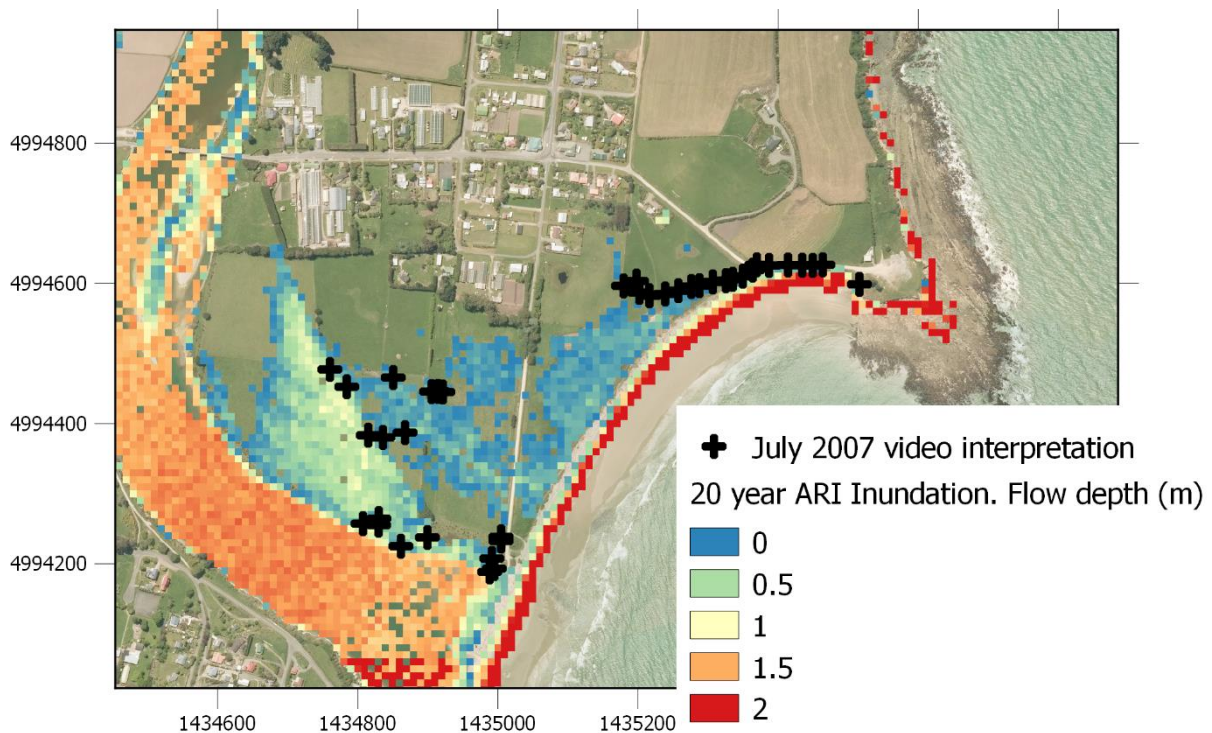


Figure 2-1: Comparison of measured and predicted inundation extent in Kakanui. Comparison of the predicted 20-year ARI inundation depths on present-day sea level (shading) with the observed July 2017 inundation extent (black crosses) at Kakanui. [Sources: modelled inundation extent Lane et al. (2008), inundation extent: Robertson 2017].

Potential improvements to the work that could be considered in the future: Improvement from using process-based simulations of the inundation is likely to lead to a somewhat smaller inundation extent for Kakanui, but the improvement may only be minor as the inundation extent is predominantly controlled by topographical features on the floodplain.

2.1.5 Climate change impacts

Lane et al. (2008) assume that the extreme distribution of storm surge would be stationary; that is, they assume (for lack of better information) that climate change is not going to significantly affect the distribution of waves, wind and storm surge. Challenging such an assumption is difficult because no regional scale climate model to date achieves a level of precision and accuracy that would allow an analysis of how climate change is going to affect these parameters. One solution to this issue is to analyse the relationship of the weather patterns and the distribution of processes that contribute to the water level and waves such as discussed above and apply these relationships to future weather patterns predicted from climate models. Ministry for the Environment (MfE 2017) recommends to “undertake sensitivity testing for coastal engineering projects and for defining coastal hazard exposure areas out to 2100, using:

- A range of possible future increases across New Zealand of 0–10 per cent for storm surge out to 2100.
- A range of possible future increases across New Zealand of 0–10 per cent for extreme waves and swell out to 2100.

- *Changes in 99th percentile wind speeds by 2100 and incorporating these for the relevant RCP scenario from MfE (2017) on climate change projections, to assess waves in limited-fetch situations, such as semi-enclosed harbours, sounds, fjords and estuaries.”*

Although Lane et al. (2008) do not consider the effect of climate change on storm surge and waves, they do consider the effect of sea-level rise. Their report presents inundation hazard maps for three sea-level rise scenarios including a present day and two future scenarios:

1. Present mean level of the sea (MLOS).
2. MLOS + 0.3 m.
3. MLOS + 0.5 m.

However, no justification was given in the report for how the sea-level rise scenarios were selected.

Implications for this project: Further assessments of climate change effects is out of scope for this project but should be considered in future analysis and may be completed with a reanalysis of the predicted runoff in a more detailed study of the extreme inundation hazards in the Waitaki district.

The future sea level scenarios are no longer in line with Ministry for the Environment recommendations. Updating the sea-level rise scenarios and the impact of sea-level rise on the coastal inundation extent is part of the scope of this report and is described in section 2.2 below.

2.1.6 Final remarks on Lane et al. (2008)

The general methodology used in Lane et al. (2008) is sound but contains significant limitations in the analysis of wave runoff, analysis of extreme water level and in the inundation mapping. Addressing many of these limitations is beyond the scope of this report but should be considered in future analysis.

Improved sea-level rise estimates for New Zealand and guidance for councils of what sea-level rise scenarios to consider have been published since Lane et al. (2008). The present study uses up-to-date sea-level rise scenarios and updates the coastal inundation extent using the results of storm surge and wave runoff from Lane et al. (2008).

2.2 Updated sea-level rise scenarios

The most recent national guidance on coastal hazards from the Ministry for the Environment (MfE 2017) recommends that different sea-level rise scenarios be used in an adaptive planning framework. This means that for different assets near the coast a different future timeframe and sea-level scenario may be used, with the timeframe and sea-level rise values proportional to the risk profile. For example, for the most high-risk assets, MfE (2017) suggest that: “Councils considering coastal subdivision, greenfield developments and major new infrastructure (Category A) should avoid hazard risk by using sea-level rise over more than 100 years and the H+ scenario¹”. For lower risk profiles (Category B, C and D), a shorter time frame and hazard outlook can be used.

To provide the Otago Regional Council with a range of options fit for the full range of assets, this study simulated additional sea-level rise scenarios, ranging from 0.3 m to 1.3 m above the present mean level of the sea, in increments of 0.2 m. Each of these scenarios corresponds to a different

¹ The H+ scenario is based on the RCP8.5 (83rd percentile) projection from Kopp et al. (2014)

timeframe for different IPCC emission scenarios (IPCC 2013) instead of simulating sea-level rise values directly tied to a single emission scenario and timeframe. The approximate timeframes for each simulated sea-level rise occurring under the different IPCC emissions scenarios are listed in Table 2-2.

Thus, in this study we consider sea-level rise up to 1.3 m above the present mean level of the sea, corresponding to the upper bound of the likely range of sea-level rise by 2115 under the RCP8.5 emission scenario, as well as intermediate sea-level rise values corresponding to earlier outlooks and/or lower emission scenarios.

Table 2-2: Sea level scenarios for coastal inundation prediction. Outlooks are based on emission scenarios from IPCC (2013). RCP2.6 is a low emissions, effective mitigation scenario; RCP8.5 is a high emissions, no mitigation scenario; the upper bound of the likely range of the estimate for RCP8.5 scenario is similar to the higher, more extreme scenario projection from Kopp et al. (2014) also referred to as H+ by MfE (2017).

Relative sea-level above present mean level of the sea (m)	Outlook for RCP2.6 Maximum likelihood	Outlook for RCP4.5 Maximum likelihood	Outlook for RCP8.5 Maximum likelihood	Outlook for RCP8.5 upper bound of likely range
+ 0.3	2070	2060	2055	2050
+ 0.5	2115	2095	2080	2070
+ 0.7	--	2125	2100	2085
+ 0.9	--	--	2115	2095
+ 1.1	--	--	2125	2105
+ 1.3	--	--	--	2115

2.3 Methodology for updated mapping of inundation hazard zones

In this study, we updated the coastal inundation prediction of Lane et al. (2008) by combining their results on extreme water level and wave runup (Table 2-3 and Table 2-1) with updated sea-level rise scenarios (Table 2-2). This was performed for the most populated areas of the coast (Moeraki, Hampden, Kakanui and Oamaru). Other areas of the Waitaki district may experience coastal inundation but the wave and storm surge information have not been calculated with sufficient details to assess inundation extent in these areas.

As with the study from Lane et al. (2008), the inundation was calculated on a 10-m resolution Digital Elevation Model (DEM) created from the 2004 Lidar survey, with the vertical datum set to the mean level of the sea (2008), 0.11 m above the Dunedin Vertical Datum 1958.

In Moeraki, Hampden, Kakanui and Oamaru, the inundation depth was calculated as:

$$Inundation = ExtWL + Wrup \times ShoreFlag + SLR - Z_s \quad (2.1)$$

where *Inundation* is the inundation depth (i.e., the maximum depth of inundation). *ExtWL* is the combined storm surge height, mean sea level anomaly, tide, and wave setup (Table 2-3), as calculated by Lane et al. (2008). *Wrup* is the maximum wave runup as calculated by Lane et al. (2008) and is only applied where *ShoreFlag* is 1. *ShoreFlag* is a flag which includes or excludes the contribution of wave runup, and is only applied to those parts of the DEM grids that are located on the shoreface (i.e., beach, coastal defences, cliffs); it is excluded in parts of the DEM that are on land, in estuaries or inside marinas/ports. *SLR* is the sea-level rise, and *Z_s* is the ground elevation.

While LiDAR data provide high resolution topography information, it is important to consider the overall limitations of the Lane et al. (2008) analysis. Lane et al. wrote: *“The high resolution of the LIDAR allows the correct representation of smaller features such as sand-dunes which contain rises in sea level and protect the land behind. However, an important caveat to note is that due to the high resolution of the LIDAR data, very precise maps of inundation will be produced. The precision of these maps does not, however, imply an equivalent level of accuracy in the predictions, which may be affected by imprecise knowledge of sea-level phenomena. The simplifying assumptions involved in making the sea-level estimates, and the consequent limitations of the values produced, should be kept in mind when examining and interpreting the maps.”*

Furthermore, the inundation is calculated as a “bathtub” model which only maps constant levels of water. It does not account for the propagation of the flood water, momentum and head loss due to the roughness of the environment, nor does it contain any information about the duration of the inundation. The model also does not account for any rainfall or river flow that may contribute to the inundation. Although the simulation includes allowance for future sea-level rise, it does not account for any change in the wave climate that may occur in the future. This type of simulation is a first order assessment that is well suited for identifying vulnerable areas, but more detailed assessments are required for risk assessment of assets and values in those areas.

Table 2-3: Predicted extreme water levels (m above MSL) for four average recurrence interval (ARI). Extreme water level here is a combination of storm surge height, mean level of the sea, tide, and wave setup. These values are given relative to the mean level of the sea (2008). [Source: Lane et al. 2008].

Location	20-year ARI	50-year ARI	100-year ARI	500-year ARI
Moeraki	1.60	1.67	1.71	1.83
Hampden	1.84	1.91	1.96	2.07
Kakanui	1.96	2.03	2.08	2.20
Oamaru	2.01	2.08	2.14	2.26

Maps of the modelled inundation depth were created for each of the four ARIs of extreme water level and seven sea-level scenarios at each site. Based on these maps, three coastal inundation hazard zones were created using the 100-year ARI extreme water level and three sea-level rise scenarios:

1. An intermediate emission scenario (RCP 4.5) sea-level rise for 2125 of 0.7 m;
2. A high emission scenario (RCP 8.5) sea-level rise for 2125 of 1.1 m; and
3. Extreme scenario of 1.3 m sea-level rise for 2125 based on the RCP 8.5 (upper bound of likely range) similar to the H+ scenario suggested by MfE (2017).

The results of the inundation modelling follow.

2.4 Results

For each area of interest (Oamaru, Kakanui, Hampden, Moeraki), we present below the maps of the predicted inundation for the 100-year ARI extreme water level at the 2008 mean sea level

(referenced to Dunedin Vertical Datum 1958 + 0.11 m.) (+0.0 m SLR) and for the 100-year ARI extreme water level at future sea-level rise of 1.3 m (+1.3 m SLR) (forecast for 2115 for the RCP8.5 upper bound of likely range). The inundation for 20, 50 and 500-year ARI at present MLOS, +0.3 m, +0.5 m, +0.7m, +0.9 m, +1.1 m and +1.3 m SLR are presented in a supplementary document.

2.4.1 Oamaru

The inundation extent for the 100-year ARI event at present MLOS along Oamaru is limited to the coastal beach and extends up Oamaru Creek by approximately 300 m (Figure 2-2). The intermediate sea-level rise scenarios show a gradual increase to the inundation extent, with the areas landward from Esplanade Road only predicted to be inundated with the highest sea-level rise scenario of +1.3 m SLR (Figure 2-3).

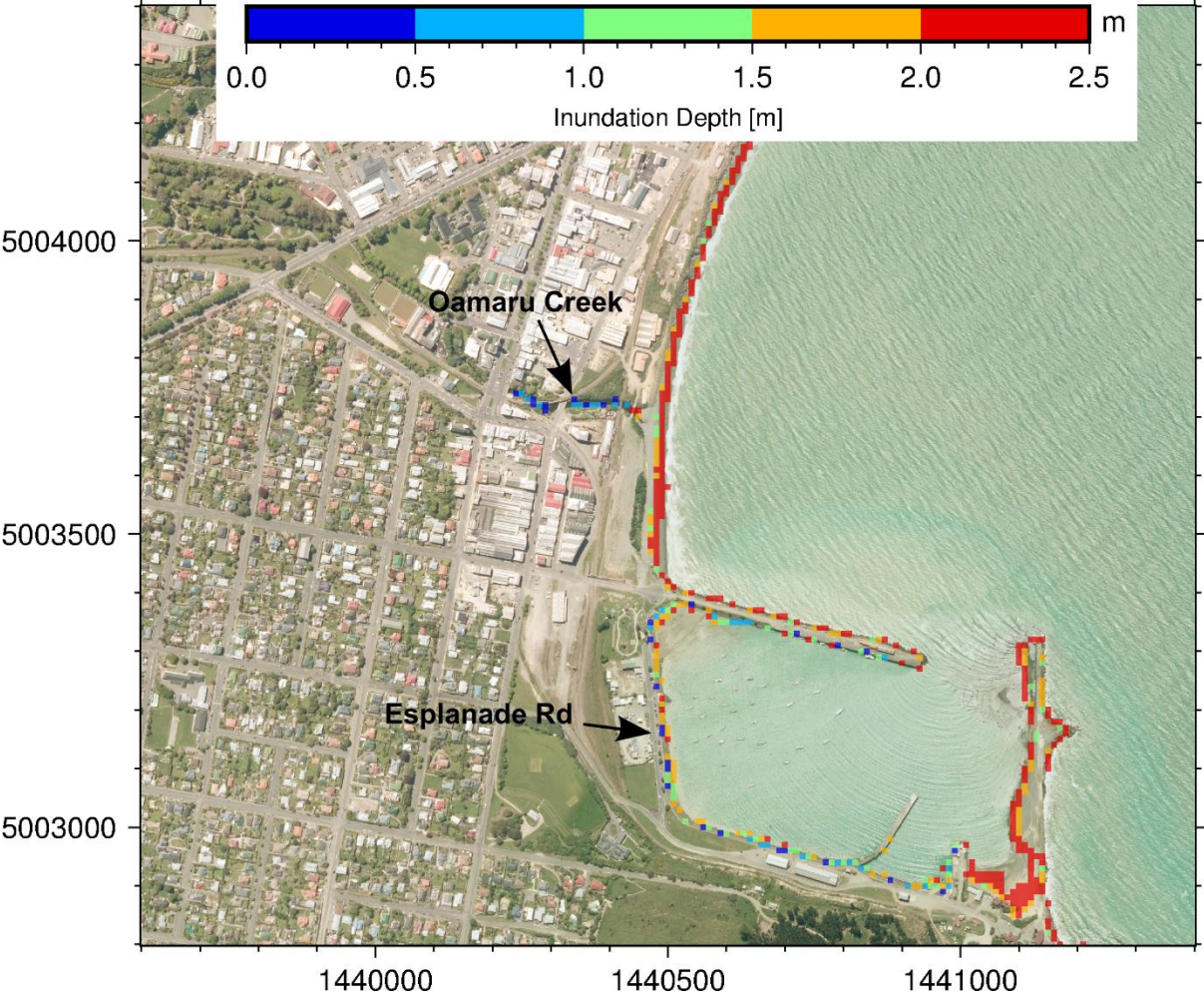


Figure 2-2: Predicted inundation depth for the 100-year ARI storm and +0.0 m SLR for Oamaru.

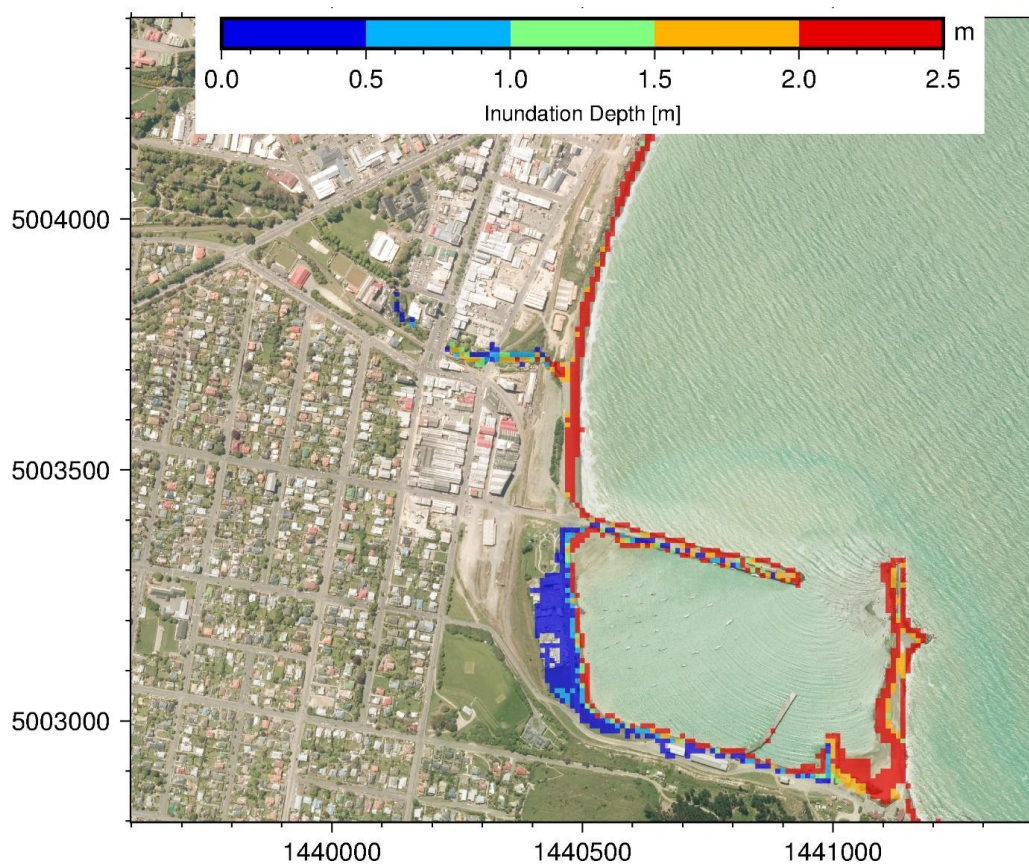


Figure 2-3: Predicted inundation depth for the 100-year ARI storm and +1.3 m SLR for Oamaru.

Sea-level rise increases the coastal inundation risk in Esplanade Road and the area of the port behind that road. However, the model shows inundation of Esplanade Road only for the higher sea-level rise scenario for the most extreme events (Table 2-4).

Table 2-4: Inundation depth for different extreme water level scenarios and sea-level rise scenarios at Esplanade Road. Double dash means no inundation. These values were extracted from a single point located near the center of Esplanade Road (E1440470, N5003200).

Sea-level rise (m)	20-year ARI (2.01 m) Extreme water level	50-year ARI (2.08 m) Extreme water level	100-year ARI (2.14 m) Extreme water level	500-year ARI (2.26 m) Extreme water level
+0.0	--	--	--	--
+0.3	--	--	--	--
+0.5	--	--	--	--
+0.7	--	--	--	--
+0.9	--	--	--	0.11
+1.1	0.06	0.13	0.20	0.32
+1.3	0.26	0.33	0.40	0.52

2.4.2 Kakanui

The inundation extent at Kakanui for the predicted 20-year ARI event closely matches the inundation extent of the recent 2017 storm (**Error! Reference source not found.**Figure 2-4). In both cases, the waves overtop the gravel barrier and gravel spit and significantly inundate the backshore, while inundation flows will also enter via the Kakanui River mouth. Sea-level rise increases the inundation extent, covering all the fields on the north side of the estuary and reaching the properties at the south end of Cobblestone Road. On the south side of the estuary, inundation is predicted near the bridge and in the area encircled by River Road (Figure 2-5).

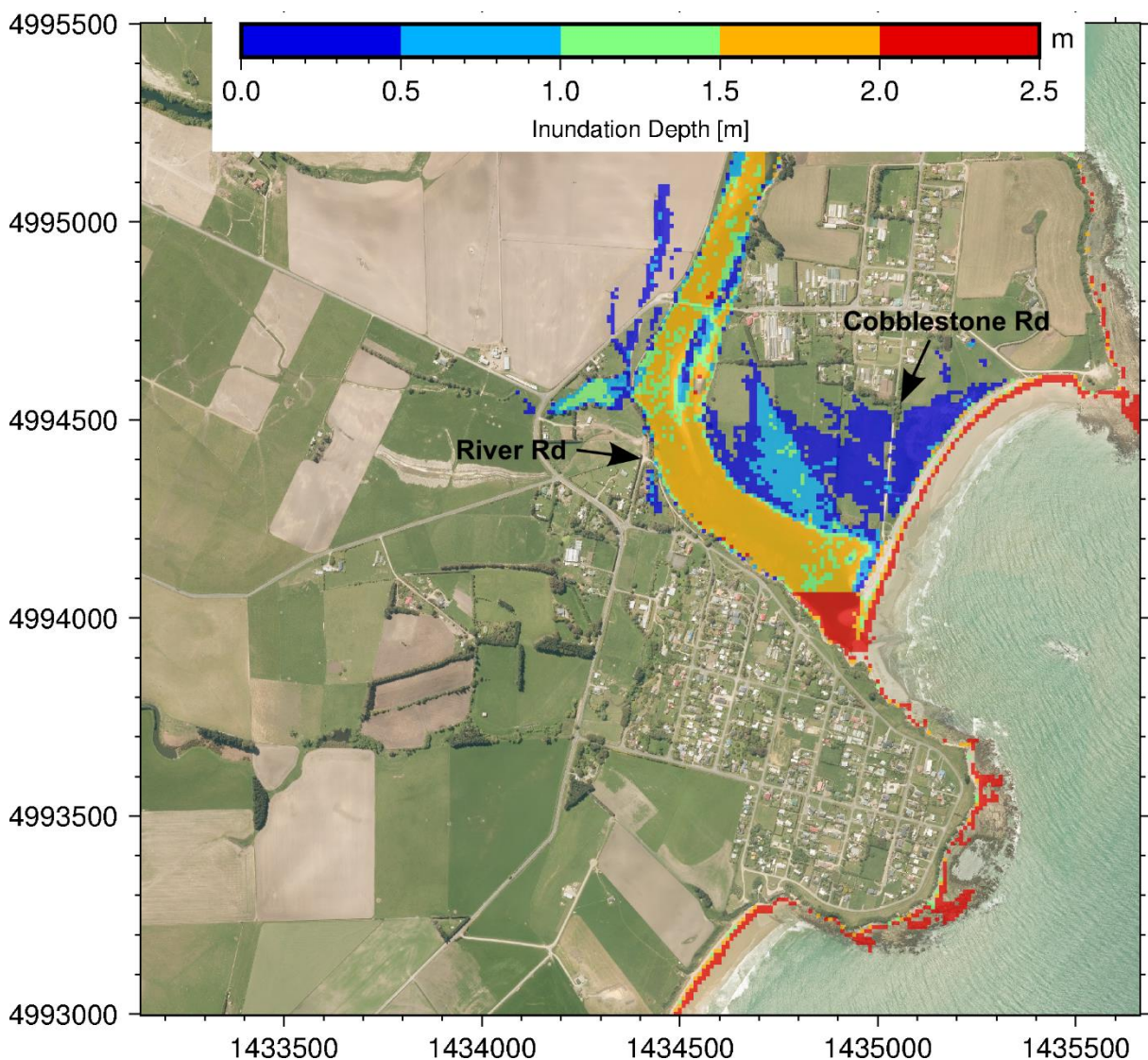


Figure 2-4: Predicted inundation depth for the 100-year ARI storm and +0.0 m SLR for Kakanui.

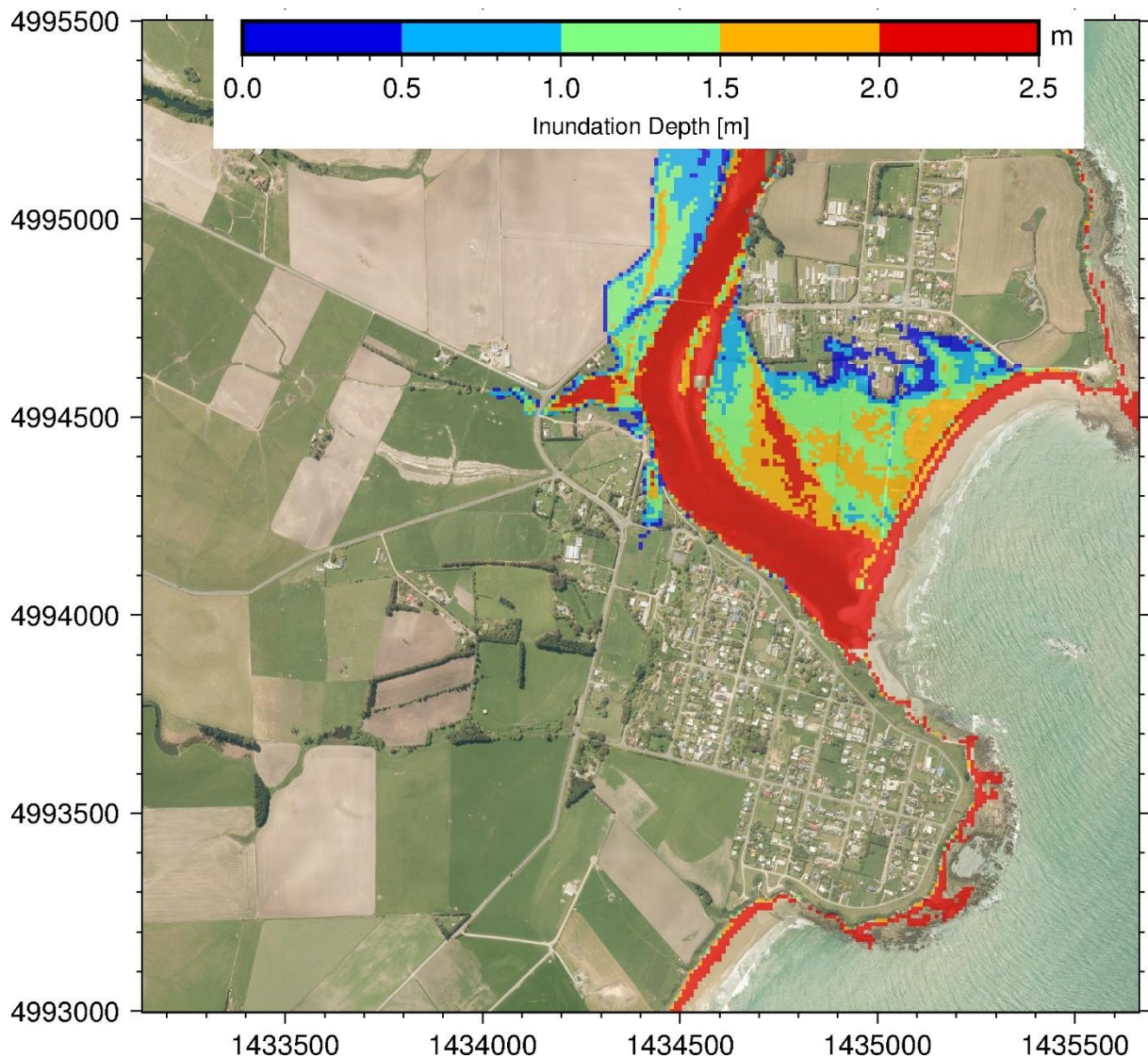


Figure 2-5: Predicted inundation depth for the 100-year ARI storm and +1.3 m SLR for Kakanui.

2.4.3 Hampden

The inundation extent in Hampden for a 100-year ARI storm at present day sea-level is limited to the coastal fringe and areas adjacent to and 200 m upstream from the mouths of Kurinui Creek and Kuriiti Creek (Figure 2-6). For the highest sea-level rise scenario (+1.3 m SLR) the inundation extends further inland to Carlisle Street and covers the wetlands located on the landward side of Carlisle Street and between the creek mouths (Figure 2-7). The intermediate sea-level rise scenarios are included in supplementary material and show a gradual increase of wetland inundation between the present day and the +1.3 m sea-level rise scenario.

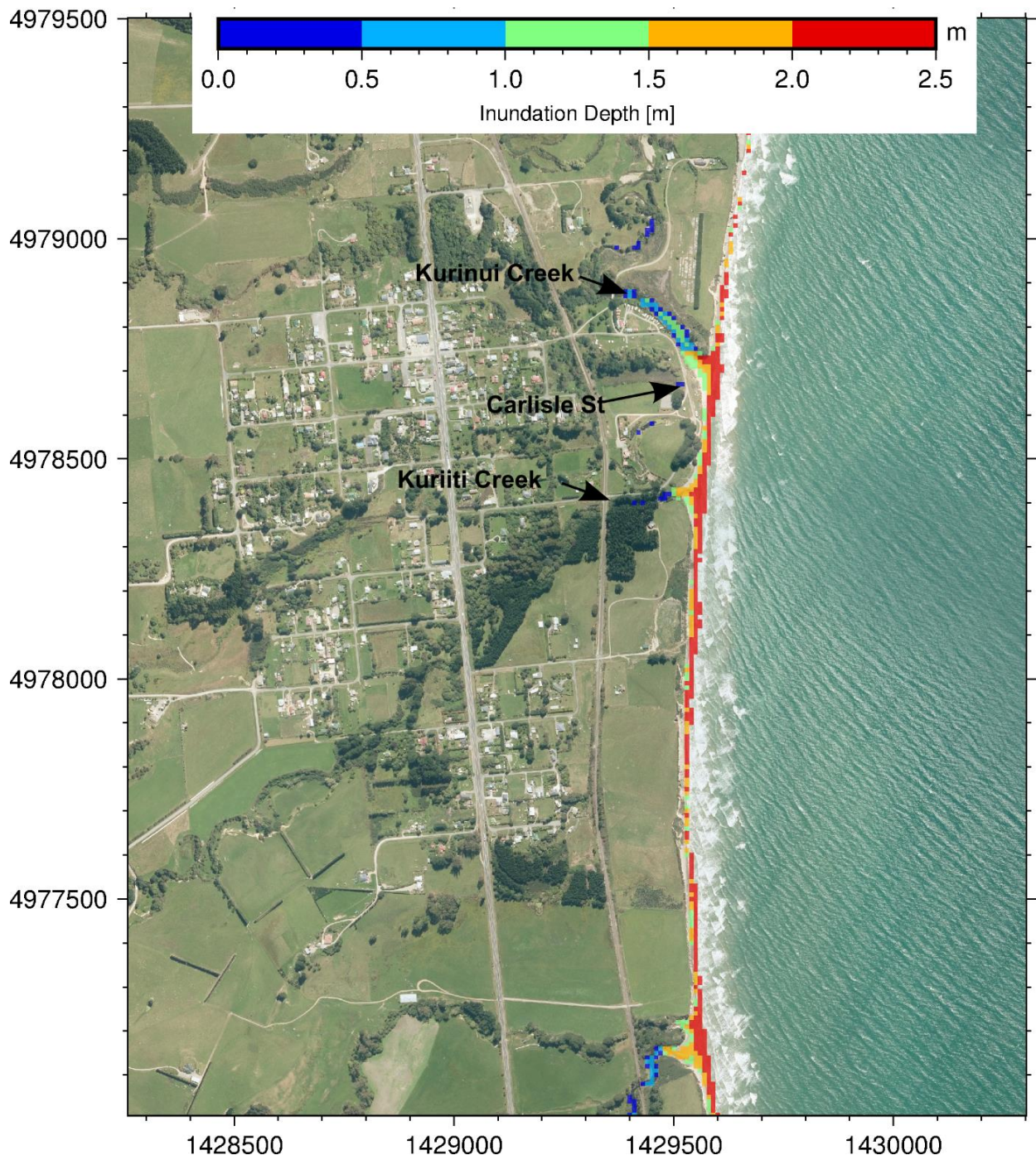


Figure 2-6: Inundation depth for the 100-year ARI storm and +0.0 m SLR for Hampden.

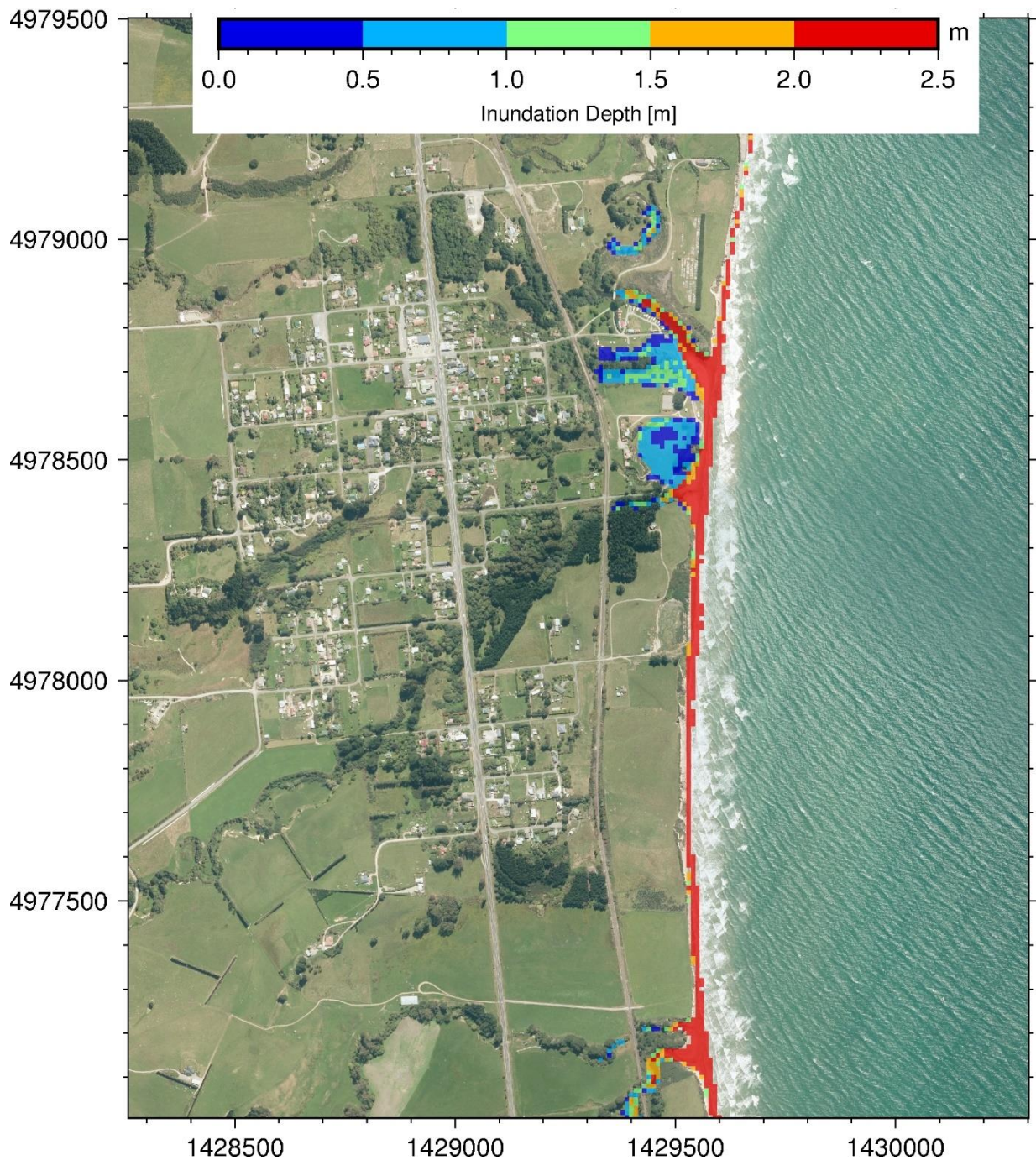


Figure 2-7: Inundation depth for the 100-year ARI storm and +1.3 m SLR for Hampden.

2.4.4 Moeraki

The predicted inundation extent at Moeraki for a 100-year ARI storm under the present-day sea level scenario is confined to the coastal fringe (Figure 2-8). The inundation extent for the highest sea-level rise scenario (+ 1.3 m SLR) increases slightly to cover the area between the old and new jetty (Figure 2-9).

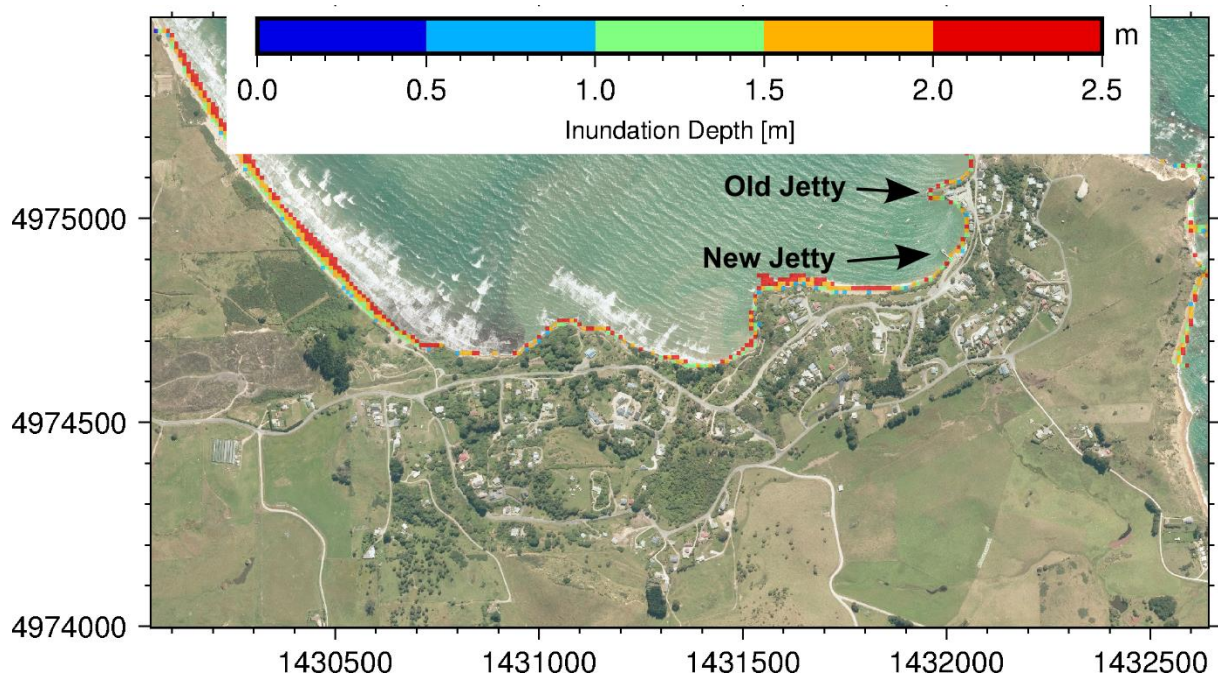


Figure 2-8: Inundation depth for the 100-year ARI storm and +0.0 m SLR for Moeraki.

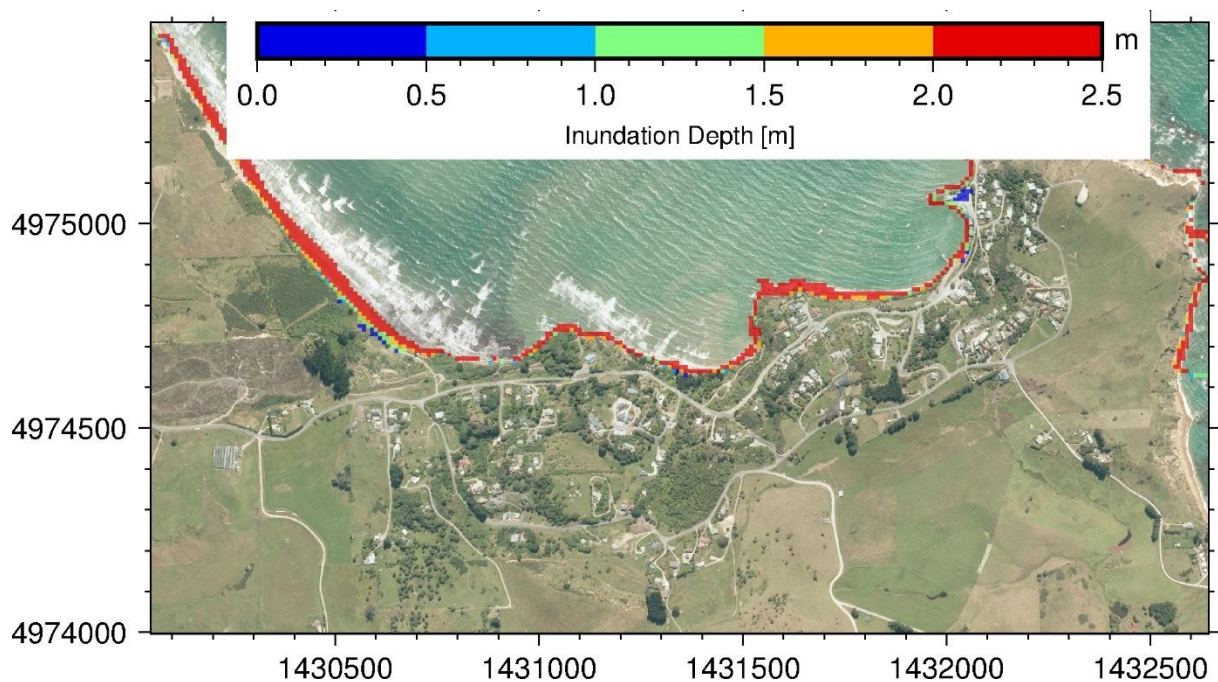


Figure 2-9: Inundation depth for the 100-year ARI storm and +1.3 m SLR for Moeraki.

2.4.5 Coastal inundation hazard zones

Coastal inundation hazard zones were developed using the predicted inundation depth for the 100-year ARI extreme water level event and considering three sea-level rise scenarios:

1. Sea-level rise of 0.7 m above present MLOS.
2. Sea-level rise of 1.1 m above present MLOS.
3. Sea-level rise of 1.3 m above present MLOS.

Note that the contributions to inundation from terrestrial (river and urban) and groundwater flooding are not included.

The hazard zones for each scenario are presented in Figure 2-10 to Figure 2-13. Showing the varying degree of area exposed to coastal inundation hazard when accounting for sea-level rise. Note only red areas are flooded under scenario 1; red and orange areas are flooded under scenario 2; red, orange and yellow areas are flooded under scenario 3; where only red is visible, all three zones coincide.

For the Ministry for the Environment’s guidance to coastal hazards and climate change, Scenario 3 corresponds to the transitional response for development planning category A (Coastal subdivision, greenfield developments and major new infrastructure) whereas Scenario 1 and 2 are part of the information that can be used to define the transitional response for Category B and C of the development planning (MfE 2017).



Figure 2-10: Coastal inundation hazard zone extents for Oamaru. Zones are based on the 100-year ARI inundation event and a SLR of +0.7 m (Scenario 1), +1.1 m (Scenario 2) and +1.3 m (Scenario 3).

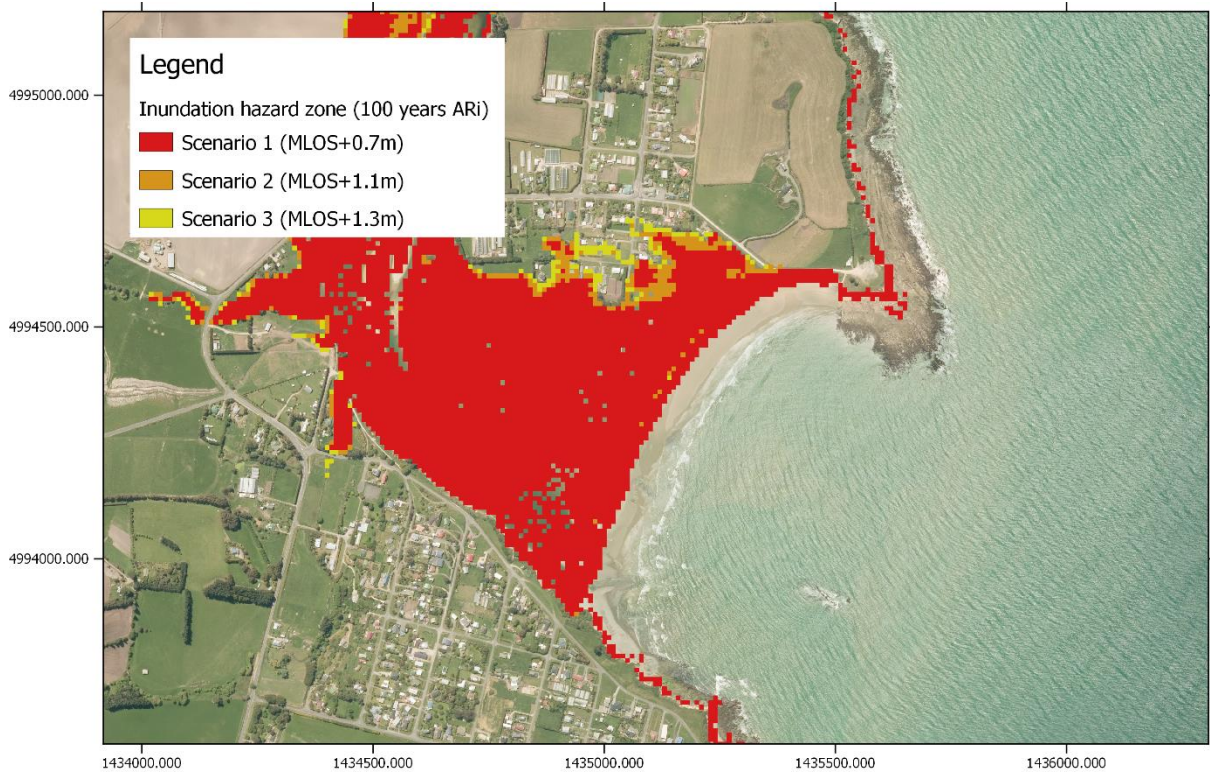


Figure 2-11: Coastal inundation hazard zone extents for Kakanui. Zones are based on the 100-year ARI event and a SLR of +0.7 m (Scenario 1), +1.1 m (Scenario 2) and +1.3 m (Scenario 3) above present day MLOS.

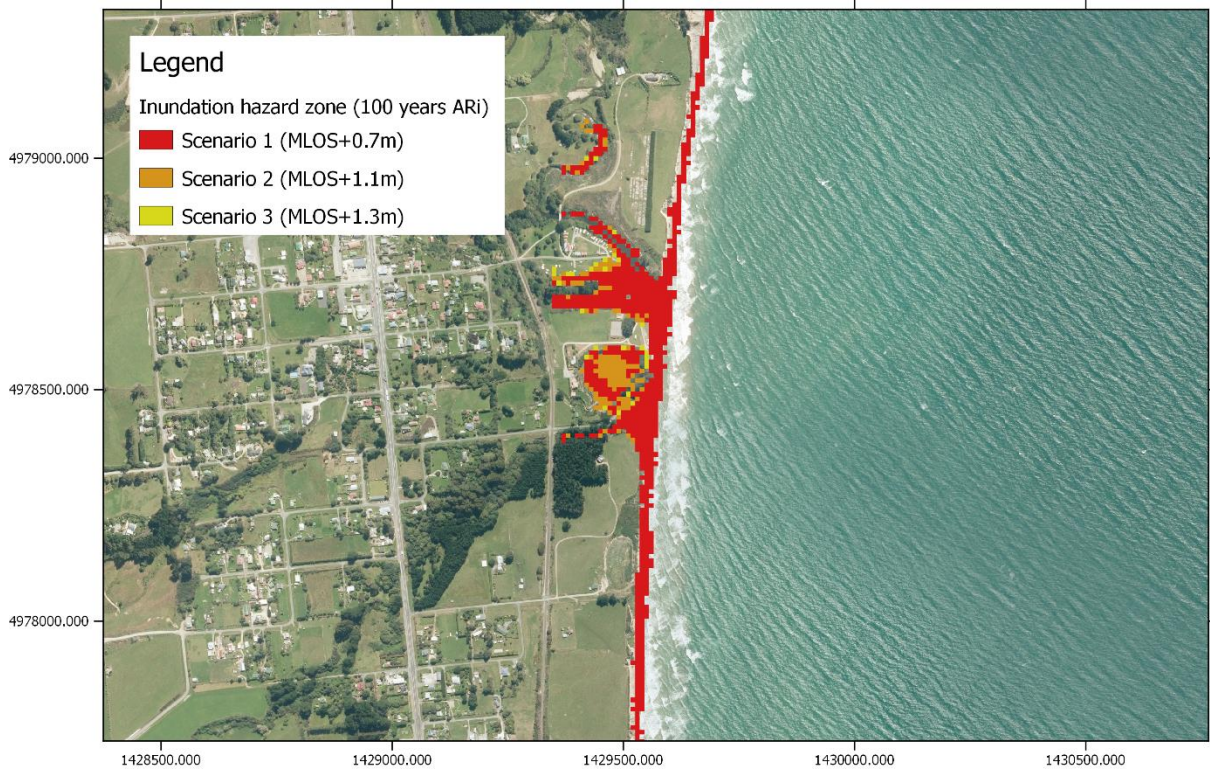


Figure 2-12: Coastal inundation hazard zone extents for Hampden. Zones are based on the 100-year ARI event and a SLR of +0.7 m (Scenario 1), +1.1 m (Scenario 2) and +1.3 m (Scenario 3) above present day MLOS.

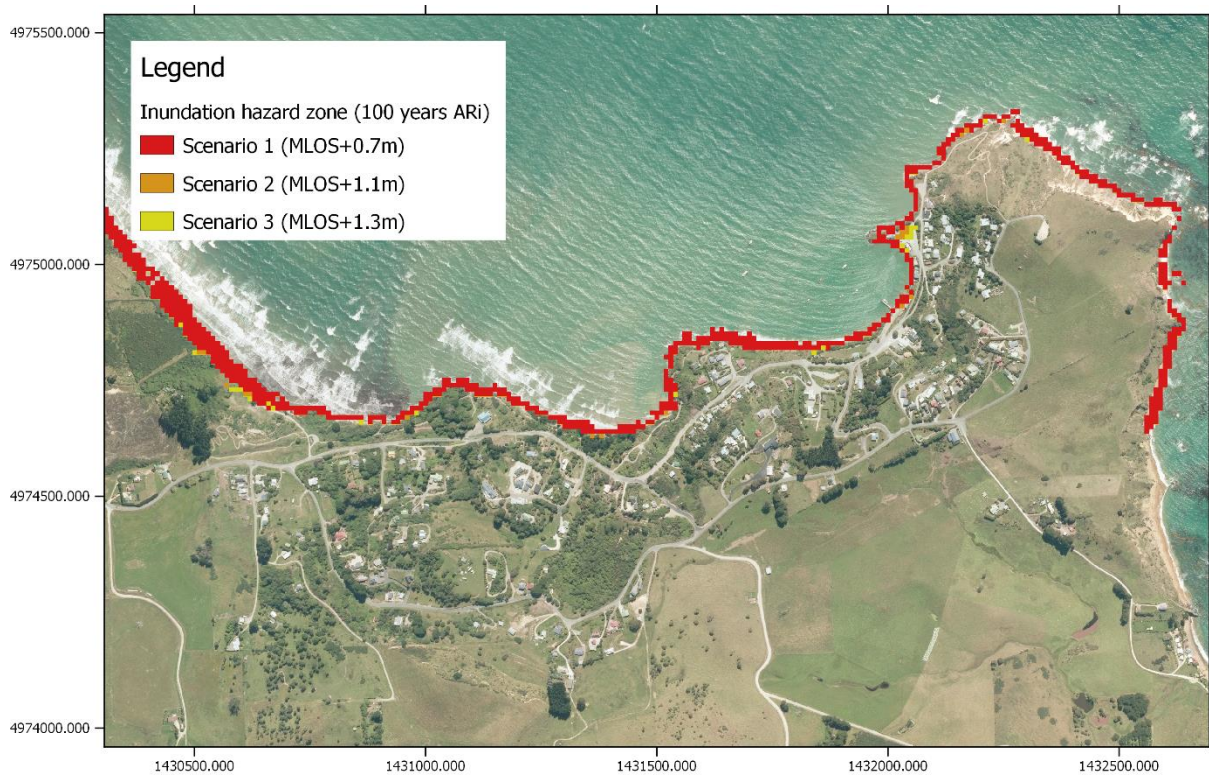


Figure 2-13: Coastal inundation hazard zone extents for Moeraki. Zones are based on the 100-year ARI event and a SLR of +0.7 m (Scenario 1), +1.1 m (Scenario 2) and +1.3 m (Scenario 3) above present day MLOS.

3 Coastal erosion hazard

3.1 Introduction

The shore of Waitaki District is very diverse, alternating between cliffs and beaches. High cliffs with hard bedrock dominate the landscape of Cape Wanbrow, Moeraki Point to Katiki Point, Shag Point, and most of the coast south of the Shag River. Cliffs formed in softer, sedimentary material (loess, gravel, or mudstone) occur between the Waitaki River mouth and Oamaru and along much of the shore between Moeraki and Beach Road, south of Cape Wanbrow. Sand, gravel, or mixed-sand-and-gravel beaches are present in most bays, often backed by low cliffs and sometimes fronted by reef platforms. The main estuaries are fronted with gravel or sand spits.

Waitaki District has historically experienced dramatic shoreline retreat. This has been focussed in several “hotspots”:

- Oamaru to the Waitaki River.
- Beach Road.
- Kakanui.
- Hampden.
- Katiki Beach.

The area north of Oamaru was reported to be eroding as early as the 1870s when port development was begun at Oamaru (Carruther 1871). The reported erosion rates there have proven variable (1.4 m/y – 0.1 m/y), averaging around 0.5 m/y (Gibb 1978). Over decadal time scales, the erosion rates north of Oamaru vary alongshore and with time – in response to the occurrence of storms and localised cliff collapse. Over longer time scales, the rates would appear to be more uniform, as evident from the straight coastline.

South from Oamaru, the road to Kakanui (Beach Road) has experienced severe erosion events in recent years, with a retreat of 12 m between 2006 and 2014 and the closure of a section of the coastal road despite the protective armouring. Along this road, the erosion is cutting back into a low alluvial backshore flat, composed of interbedded lenses of fine rounded gravel with shelly coarse sand (estuarine/beach depositional-environment) and clay/silt lenses in places (swale deposits), with a loess cap topped by soil/peat, sometimes with a thin sand-dune cap. The beach material is coarse and of similar composition to the material within the cliff, suggesting that the beach is formed exclusively of the eroded material.

At Kakanui, the gravel barrier at the river mouth has been retreating landward, with rates of 5 m/y reported by Gibb (1978). This particularly high rate may be the result of both the removal/destruction of the pier in the bay in the 1970s and particularly severe storms in 1974 (Pattle 1974). More recent rates of erosion have lowered to 1 m/y (Johnstone 2001).

North of Hampden, a calcareous muddy sandstone and greensand capped by clay-rich gravelly sand is producing many slumps, with the top of the cliff retreating rapidly. The coast south of Hampden is formed in the same lithology and is also eroding (as evident by the Moeraki boulders being left on the beach) but no report has been made of the rates of erosion observed there.

Katiki beach is showing multiple spans of erosion, several reaching close to State Highway 1 (SH1). There, patches of riprap have been under construction (Figure 3-1). Older riprap was observed to be in a poor state (i.e., settled in the beach or partially dismantled by waves with scattered rock visible on the beach), implying that these are not performing as a long-term shoreline control.



Figure 3-1: Armouring of the backshore cliff on Katiki Road (7/12/2017).

The purpose of our study was to compile information on historical erosion rates and to develop coastal erosion hazard zones, with emphasis on these hotspots.

3.2 Methodology

Although existing reports of erosion provide information on erosion rates in the Waitaki District, they are insufficient for predicting future shoreline position and defining coastal erosion hazard zones. The prediction of future shoreline position requires up-to-date and systematic analysis of the time-trend in the shoreline position and a consistent analysis of the associated errors. The shoreline trend analysis undertaken here is based solely on the shoreline positions detected from aerial and satellite imagery. While this produced a consistent, uniform-alongshore dataset suitable to analyse shoreline trend for the whole coast of Waitaki District it does not account for site specific backshore geologies. Other estimates of shoreline evolution based on repeat LiDAR surveys, beach profiles and morphological model simulation are also used here to validate and complement the information calculated from the imagery-based shoreline detection.

3.2.1 Shoreline detection

Shoreline positions were manually extracted from historical aerial photography and satellite imagery (Table 3-1). The features extracted were the vegetation line along beach environments (often corresponds to the toe of dunes) or the cliff top along cliff-backed shores/beaches, following Boak and Turner (2005). In areas where coastal defence structures are present (e.g., rock wall in Oamaru) the rear-facing toe of the structure was used to define the shoreline.

More sets of historical imagery were found apart from those listed in Table 3-1, but these other sets were not used, either because the resolution of the imagery was too low or because distortion of the image would not allow for suitable geo-referencing.

For each set of imagery, the shoreline position was digitized at a scale of 1:600, with points digitised at a spacing that averaged 6.75 m (e.g., Figure 3-2). In each set of imagery, the error in the shoreline position was calculated as the sum of a shoreline-digitising error (typically 3 pixels width) and a geo-referencing error (measured as the offset of permanent features between georeferenced imagery and the LINZ 2014 baseline imagery). The error for each shoreline position was variable, ranging from 1.2 m to 7 m. The historical shorelines were archived as ArcGIS shapefiles.

For the span of shore between Oamaru and the Waitaki River, a valuable early historical shoreline fix from 1871 was also available. This was derived from photogrammetric analysis of cadastral maps (as reported by Hicks and Bind 2013).

Table 3-1: Imagery data source used in the shoreline detection.

Date	Area	Estimated error (m)	Source
1860s-1870s	Waitaki River mouth to Oamaru	20	Cadastral map
30 Aug 1955	Waitaki River mouth to Oamaru, Beach Road	6 – 8	Retrolens
12-13 Mar 1979	Waitaki River mouth to Oamaru, Katiki Rd, Hampden	5 – 8	Retrolens
Jan-Feb 2000	Waitaki River mouth to Oamaru	7 – 8	LINZ
Jan-Feb 2006	All of Waitaki	2	LINZ
02 Sep 2006	Moeraki, Hampden, Cape Wanbrow	7	DigitalGlobe
04 Dec 2007	Shag Point, Stony Creek	8	DigitalGlobe
19 Jan 2012	North Oamaru	6 – 8	DigitalGlobe
24 Mar 2012	Waitaki River mouth to North Oamaru	6 – 8	DigitalGlobe
03 Oct 2012	Beach Road, Kakanui, All Day Bay	6 – 8	DigitalGlobe
28 Oct 2012	Pleasant River to Waianakarua River	7	DigitalGlobe
26 Nov 2012	Te Hapapureirei Beach, Kakanui Point, Oamaru Port, North Oamaru	6 – 8	DigitalGlobe
22 Mar 2013	Oamaru	7	DigitalGlobe
Jan – Feb 2014	All of Waitaki	1	LINZ
14 Mar 2015	North Oamaru to Waitaki River	7	DigitalGlobe
09 Jun 2015	North Hampden	7	DigitalGlobe
27 Feb 2016	North Hampden to Beach Road	6	DigitalGlobe
20 Oct 2016	Beach Road to North Oamaru	6	DigitalGlobe

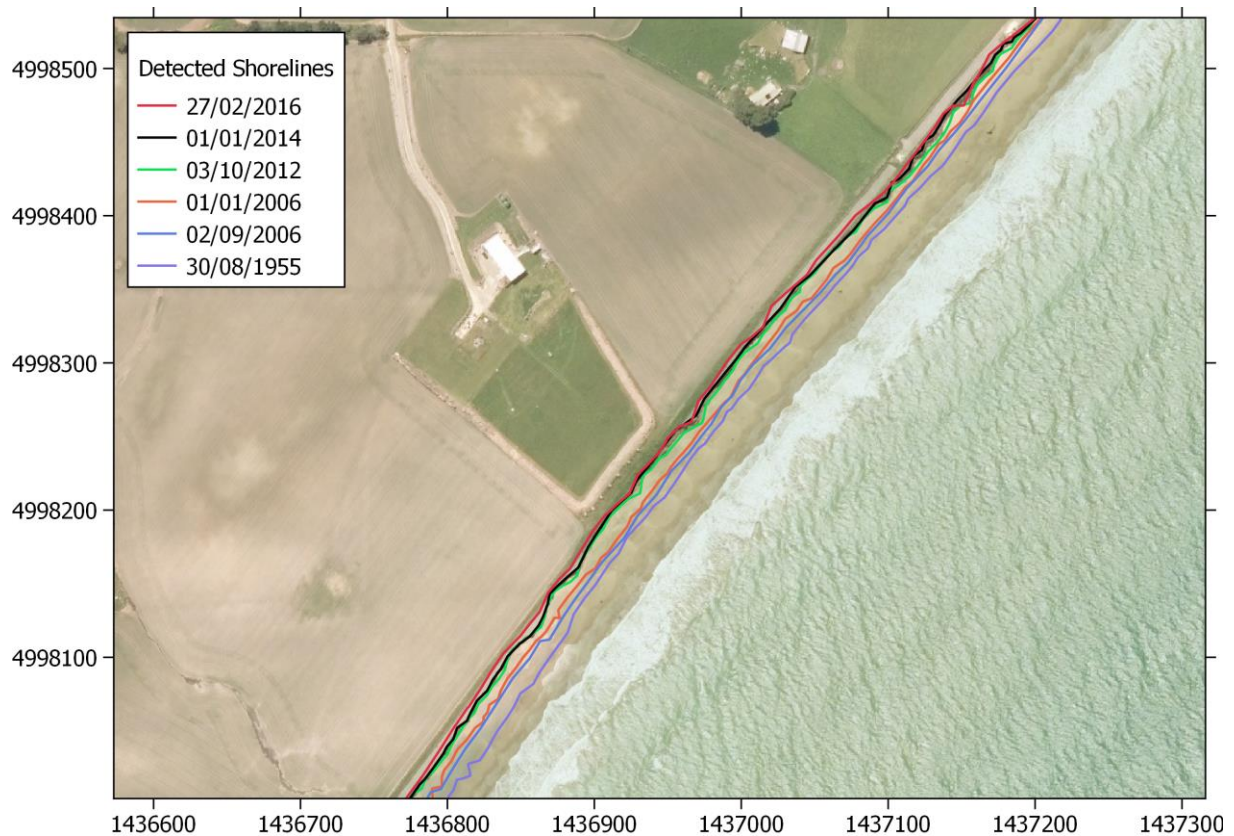


Figure 3-2: Example of shoreline detection along Beach Road, south of Oamaru. Black line shows the detected shoreline corresponding to the background image (Jan - 2014) [Image source: LINZ].

3.2.2 Shoreline analysis

The dataset of historical shoreline positions was used to calculate historical average retreat rates at stations every 5 m along the entire Waitaki District coast (19,408 stations in total). Transects perpendicular to the coast were constructed at each station using the AMBUR software (Jackson et al. 2012) (Figure 3-3). Then, the intersections between the mapped shorelines and each of the transects were captured and their offset from an arbitrary reference offshore was calculated (Figure 3-4).



Figure 3-3: Example of transects perpendicular to the coast. The distance alongshore between each transect is 5 m. [Image source: LINZ].

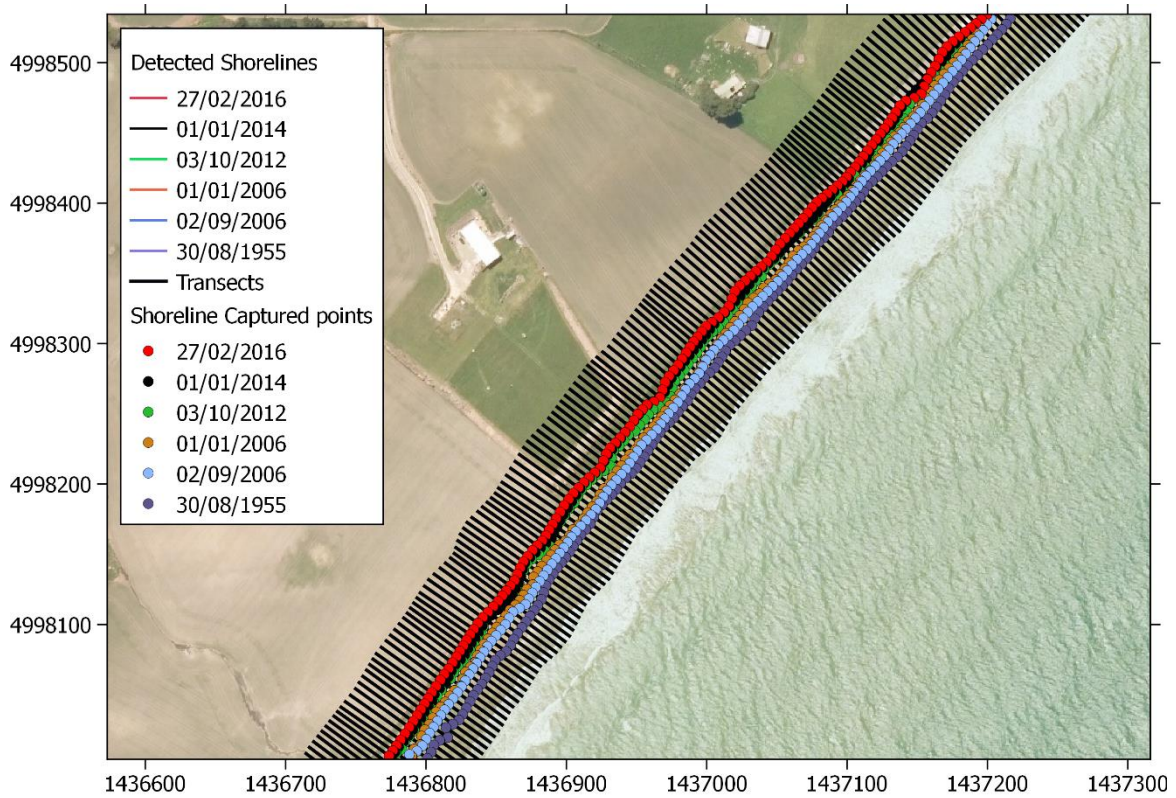


Figure 3-4: Example of intersection point between the transects and detected shorelines. The coloured points represent the intersection between shorelines and the transects. [Image source: LINZ].

For each of the transects, a weighted least square fit was used to calculate a linear time-trend in shoreline position, using the inverse of the shoreline position error estimate as the weighting factor (e.g., Figure 3-5). The trend rate and its standard error contained large alongshore variability which was smoothed using a moving-average filter with a width of 30 points along sections of uniform morphology (i.e., 15 points covering 75 m either side of the target point were averaged). The filtered shoreline trend and its standard error were recorded to be used in defining the coastal erosion hazard zones. In addition, for each transect, the residuals of the trend (distance between the trend and historical shoreline position) were also calculated for use in the coastal hazard zone calculations.

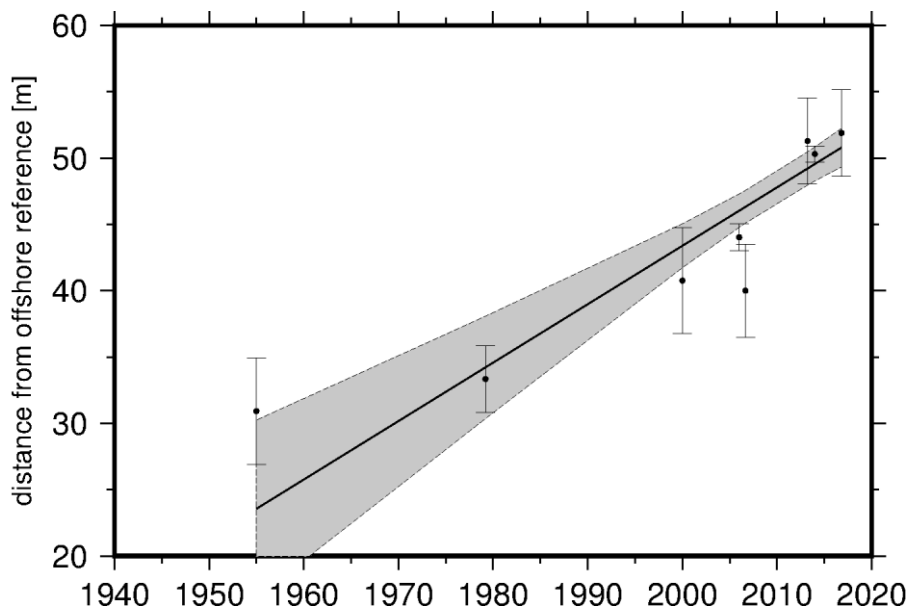


Figure 3-5: Example of shoreline trend analysis. The black line is the linear trend. The grey area represents the 95th percentile confidence interval around where the true trend-line could be. The black dots are the shoreline distance from the offshore edge of the transect, with associated error bars.

3.2.3 LiDAR volume change

For a number of areas along the coast, a recent LiDAR survey from 2016 existed in addition to an older LiDAR survey from 2004, which covered the entire Otago shoreline. The data of both surveys were used to create Digital Elevation Models (DEMs) with a ground resolution of 2 m. These DEMs were analysed in areas of particular interest (Oamaru township, Kakanui and Katiki Beach). This provided elevation changes to show a 2-dimensional overview of areas of erosion and accretion between the 2004 and 2016 surveys.

Results of the LiDAR volume change analysis are presented in section 3.3.3.

3.2.4 Beach profiles

Profile survey data for 12 sites north of Oamaru were provided by Otago Regional Council. Repeat surveys were available for some of these profiles which enabled independent analysis of the top-of-cliff retreat rates. The data from these profiles were also valuable for setting-up the shoreline simulation model. However, the limited number of repeat surveys meant that the profiles could not be used to assess the cliff erosion rate or the modes of erosion.

The surveyed beach profiles for Oamaru central are shown in Figure 3-6, with the top of cliff illustrated to show measured retreat rates.

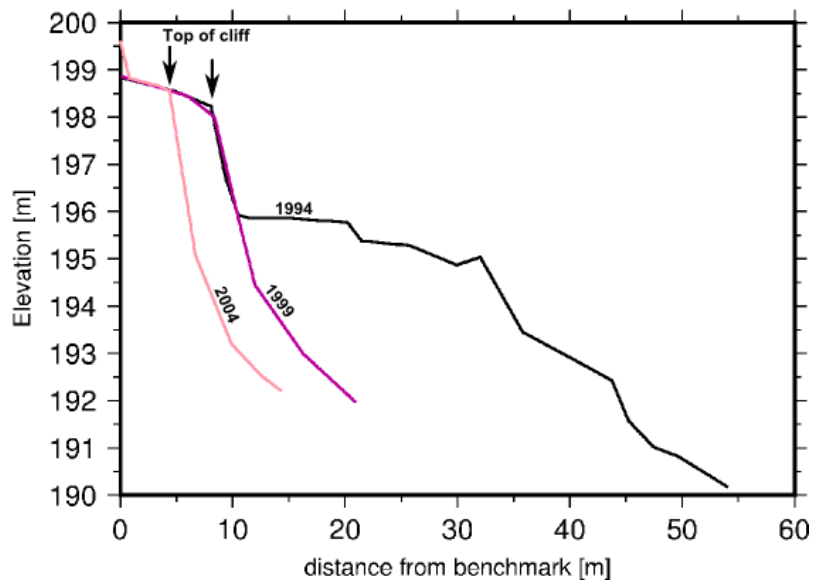


Figure 3-6: Oamaru (central) beach profiles surveyed by Otago Regional Council. Note: The vertical elevation is referenced to an arbitrary datum.

3.2.5 Shoreline simulations

SCAPE (Soft Cliff and Platform Erosion) is a coastal model designed to represent the mesoscale evolution of cliff-lined coasts (Walkden and Hall 2005). The SCAPE model was designed and thoroughly tested on the cliff/barrier coasts in Suffolk to assess the response of the cliff and barrier system there to accelerated sea-level rise (Walkden et al. 2015).

The SCAPE model is tested here to evaluate the response of the cliff-backed coast north of Oamaru to projected sea-level rise. While SCAPE allows for the simulation of a complex coastal system, the model implemented here remains simplistic as little environmental information is available to force and validate the model.

The model was set up for a 5 km-long span of shore, represented by 10 parallel and cross-shore transects spaced 500 m apart. The model shore trended 40 degrees east of north (i.e., transects are facing 130 degrees east of north). The model cliff heights were set to 12 m above present mean sea level (12.11 m DVD58). The beach crest level was set at 2.8 m above mean sea level. The daily tidal range and forcing variables (including storm surge and wave statistics) were taken from Gorman et al. (2002). The daily tidal range and forcing variables only spanned 20 years so it was repeated 505 times for duration of the simulation (1100 years).

The profile shape of the steep gravel beaches north of Oamaru was approximated using a 'Bruun constant' (Bruun 1962) of 0.8.

The SCAPE model has no option for specifying the rates of loss of material due to abrasion, which was previously shown to be significant (Hicks 2011). However, this can be approximated by reducing the proportion of material from the eroding cliff that can be retained on the shore (10 per cent). The alongshore flux of sediment was not allowed to exceed 150 m³/tide, which is consistent with previous estimates of longshore transport rates for this shore (Hicks 2011).

The model assumed uniform cliff lithology both in the vertical (i.e., up the cliff height) and alongshore. This is in contrast with sporadic field observations that suggest that the loess layer (4-

5 m thick in Oamaru) thins towards the north. The data available are insufficient to directly evaluate how the lithology of the cliff affects the cliff recession and the development of the gravel beach.

The model was initially run for 1,000 years to allow it to reach an equilibrium. The rate of sea-level rise for this “running-in” period was set to 0.002 m/y, in keeping with the historical rates observed on the South Island east coast (Hannah and Bell 2012).

Model validation was achieved mainly by comparing the shore retreat rates over the last 100 years of the running-in period with those observed historically for this shore away from the armoured structures protecting the Oamaru port and town centre. The modelled rate for this period of 0.33 m/y compared well with the observed rates between 0.3 m/y and 0.4 m/y (see section 3.3.1). The SCAPE simulation also reproduced a variability of erosion rates driven by the occurrence of storms and cliff collapse which is similar to historical observation (Figure 3-7). The model also produced an equilibrium beach width similar to that observed by Dickson et al. (2009), providing additional validation.

Multiple simulations were run to assess the sensitivity of the results to the selected model parameters. The model was found to be very sensitive to the ‘Bruun constant’, slump period, talus slope, maximum longshore sediment flux and beach return ratio, but quite insensitive to the berm slope. This suggests that while the model produced valid results, more information about the dynamics of the cliff erosion are required to confirm the validity of the parameter selection.

We concluded from these validation results that simulation of the future shoreline position using SCAPE is reasonable and reproduced the dominant erosive trend, therefore giving confidence for use in the forecasting of future shoreline trends. However, the model is sensitive to parameters that are not well known, thus more data would be required to improve confidence in the model.

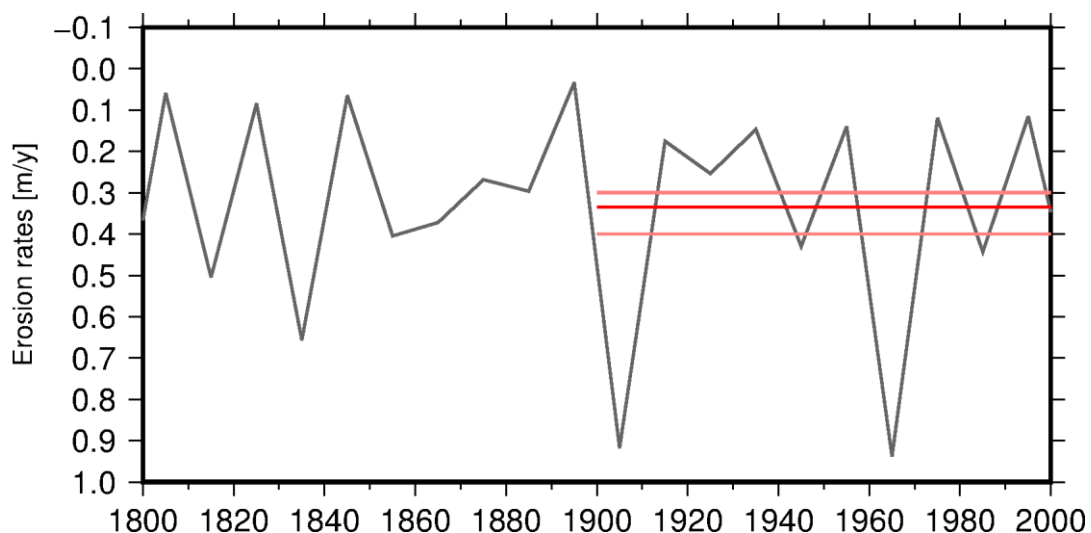


Figure 3-7: Erosion rates simulated for Oamaru using SCAPE+. The grey line shows the annual erosion rates, the light red lines the range of observed historical long-term rates for this section of the coast, and the bold red line is the averaged simulated rate.

The model simulation was then repeated (including the run-in period) and extended to 2115 using two sea-level rise scenarios: (1) the historical rate of sea-level rise of 0.002 m/y was applied from start to finish (1015 to 2115) with mean sea level reaching 0.22 m above present day mean sea level

by 2115; (2) the historical rate of 0.002 m/y is applied from 1015 to 2015 and from 2015 the predicted sea-level rise associated with IPCC scenario RCP8.5 upper bound of likely range (+1.3 m by 2115 based on the IPCC 5-yearly sea level prediction) is applied. These two scenarios cover the range of expected shoreline responses over this timeframe.

3.2.6 Coastal erosion hazard zone mapping

Overview of approach

The coastal erosion hazard zone was created from estimates of the future shoreline position combined with an allowance for processes that cause short term shoreline fluctuations and/or backshore slope failure.

The base formula used to calculate the coastal hazard zone width (CHZ) was adapted from Gibb (1982):

$$CHZ = R \times T + S \quad (3.1)$$

where *CHZ* is the hazard zone width, *R* is the long-term average rate of shoreline retreat which is based on the observed historical rate of shore retreat that, in some cases, can be adjusted to account for accelerated future sea-level rise, *T* is the time span for the hazard zone planning period (50 or 100 years in this case), and *S* is a factor to account for short term shoreline change due to storm erosion/accretion cycles or for slumps in cliffs in the backshore. The formula is applied at each shore station (every 5 m alongshore for this study), and the actual hazard zone is set back by the CHZ width from the 2014 shoreline position, which serves as a reference line.

A hybrid-probabilistic approach was used to manage uncertainty in the *R* and *S* terms in Equation 3.1. With a conventional probabilistic approach, both *R* and *S* in Equation 3.1 are represented by probabilistic distributions and (using what is termed a Monte Carlo approach) 10,000 realisations of the CHZ width are made by drawing values of *R* and *S* at random from their respective distributions. The resulting distribution of CHZ realisations (e.g., Figure 3-8) shows what the range in projected hazard zone width is, which width is most likely, and what the risk is that erosion could extend beyond any given width within the range. For example, if the CHZ line was drawn based on the 50th percentile of the realisations, which is the most likely outcome, then there would be a 50% chance that the erosion hazard would extend beyond that line by the end of the planning period. On the other hand, if the CHZ line was drawn based on the 95th percentile of the realisations, then there would only be a small (5%) chance that the actual future erosion hazard would extend beyond the line. It follows that for planning purposes, different percentiles may be chosen to match the value of assets and the level of risk. For example, if the land in the possible hazard zone range was farmland, then a reasonable risk of erosion could be accepted and a 50th percentile CHZ line might be used. However, in a township (with higher-valued assets), then only a small risk of those assets being eroded could be tolerated and so a 95th percentile CHZ line might best be used.

We term our approach “hybrid-probabilistic” for two reasons. First, while in an ideal case the type of probabilistic distribution function selected should be the one that best fits the available data, in the Waitaki coast case, because of the limited amount of historical data available, a normal distribution was assumed for all terms. A normal distribution is reasonably justified to account for error in digitization and shoreline detection that affect the estimation of historical shoreline retreat rates, but for short term shoreline fluctuations such as storm cut and slope failure, an extreme-value type of

distribution is likely better suited but requires data on past extreme storm cut /slope failure that are not available.

Second, in the ideal case the procedures for determining the R and S terms in Equation 3.1 are well specified, so that the probability distributions assigned to them relate only to the uncertainties in the parameters used to derive them. This is the case, for example, with sandy beaches backed by dunes, where the effect of accelerated sea-level rise in the R term can be calculated from foreshore slope using the “Bruun rule”, and the magnitude of short-term erosion “bites” can be assessed from repeated surveys of beach profiles. However, for other shore morphologies (e.g., rocky cliffs, perched beaches) for which neither the response to sea-level rise or the magnitude of shore erosion events are well formulated, the distributions associated with the R and S terms need to be estimated based on expert knowledge and approximation. Significant spans of the Waitaki District shore fall into this latter category because of the nature of the shore morphology and the availability of data.

The upshot is that these hybrid modifications introduce additional uncertainty in the hazard zone width that is not captured in the Monte Carlo probabilistic approach used herein. This additional uncertainty is difficult to quantify but can be managed in part at least by making a qualitative assessment of the reliability of the hazard zone width for each shore morphology type.

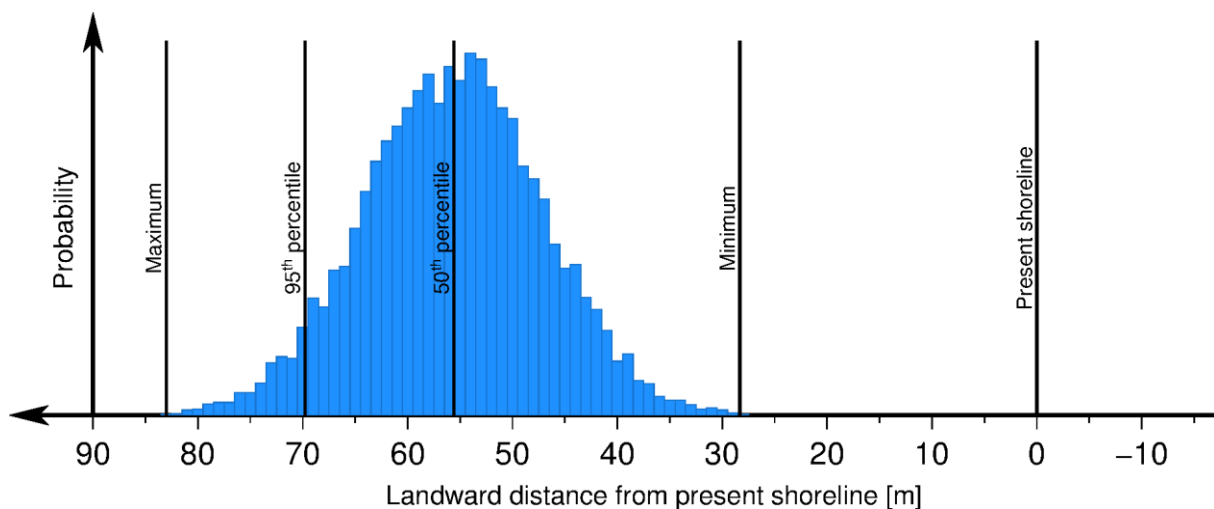


Figure 3-8: Example of probabilistic coastal hazard zone prediction. The vertical blue bars show the histogram of 10,000 realisations of the CHZ width made by drawing values of R and S at random from their respective distributions. The black bars represent statistical measures of the distribution. This distribution was calculated for a transect located on Beach Road.

Morphological diversity

The morphology of the coast in the Waitaki District is diverse and the base formula (Eq. 3.1) is not well suited for all morphologies because the data available and uncertainties around processes vary with morphology. To account for this diversity of coastal morphology, the base formula was adapted to account for six major types of morphology along the coast (mapped in Figure 3-9):

- Bedrock cliffs
- Unconsolidated cliffs
- Geologically controlled beaches (perched beaches)

- Wide gravel barriers
- Dune-backed beaches and thin sand/gravel barriers
- Major coastal structures (e.g., rock armouring, seawalls).

The approach used for each morphology type, and the modifications made to the base erosion hazard zone width formula, are detailed in the following sections.

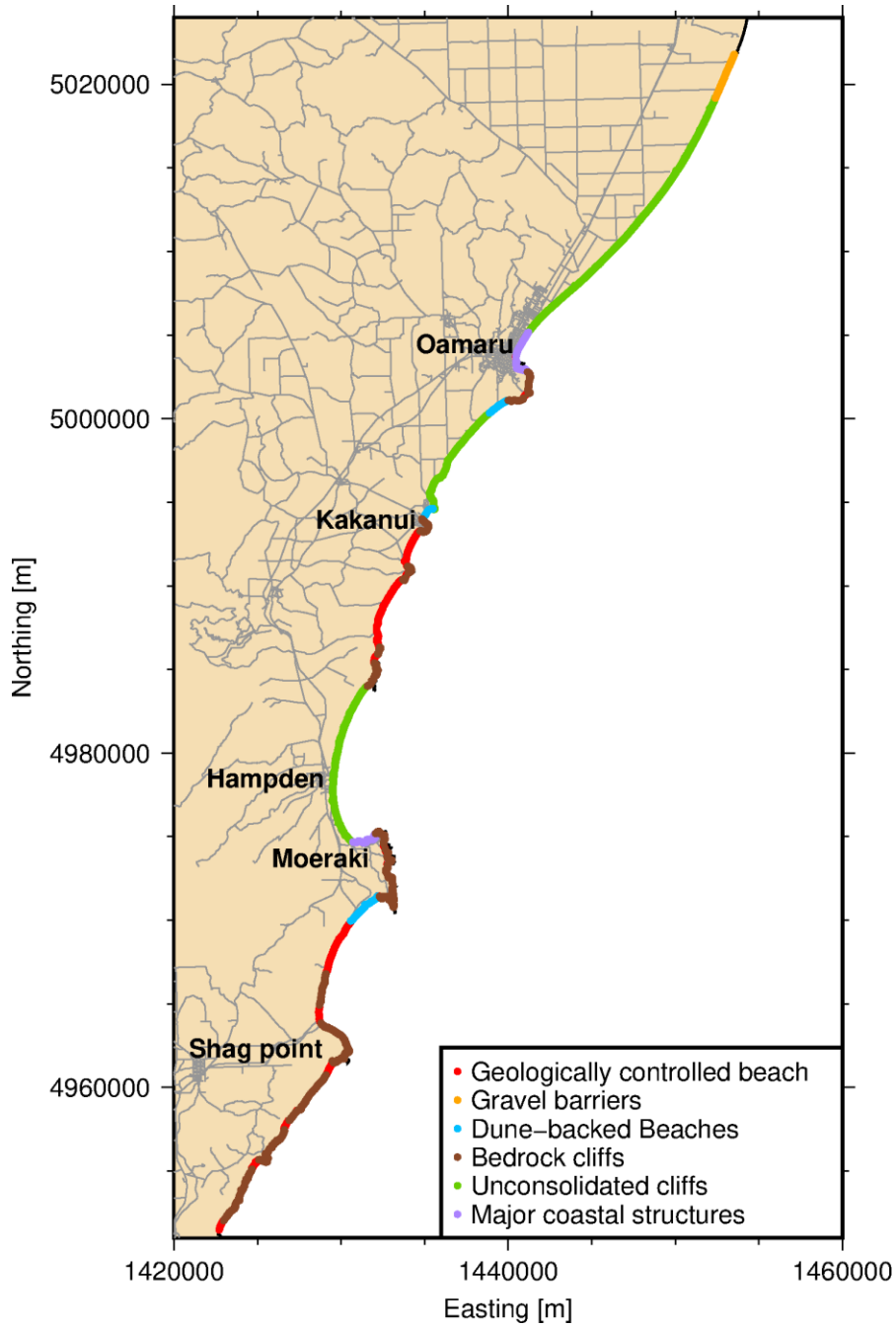


Figure 3-9: Coastal morphology types along the Waitaki District coast.

Bedrock cliffs

Bedrock cliffs describes the consolidated/hard-rock cliffs of high competency (HC) found at Cape Wanbrow, between Moeraki Point and Katiki Point, and between Pleasant River and Shag River (Figure 3-10). For these cliffs, future retreat is expected to be dominated by mass failures (e.g., slumps) and rock fall that are not directly affected by waves and sea level. The rate of retreat would therefore be dominated by the accumulation of all the slumps that occur within a given period. The geology and slope of these cliff must play a significant role in their retreat, but no information about their competence is explicitly taken into account in this study. Thus, their future shore positions are based only on projections of the observed historical trends.

The formula used to assess the coastal erosion hazard is:

$$CHZ = R_{HC} \times T + S_{HC} \quad (3.2)$$

R_{HC} is the bedrock cliff erosion rate based on the calculated historical rates but using a running mean value smoothed over a 300 m span of shore. The shoreline detection on these high cliffs can be very unclear (e.g., Figure 3-10) and subject to errors in georeferencing and by misinterpretation of shadows and slumps. This results in the historical shoreline positions showing a high variability alongshore that is not representative of the variation in the position of the top of the cliff. To prevent these errors inducing erroneous coastal hazard zones, the historical shoreline trends were smoothed alongshore and 'clamped' to discard rates showing progradation (i.e., cliffs advancing into the sea). Uncertainties in the historical rate were accounted for by producing a normal probability distribution centred on the smoothed historical rate (clamped to remove any value less than 0.05 m/y) and with a standard error derived by similarly smoothing alongshore the standard error of the erosion trends. These smoothed standard errors ranged between 0.001 m/y and 0.003 m/y.

S_{HC} was originally conceived (in the Gibb, 1982 model) to represent the largest slump or slope failure observed in the field. However, without an adequate record of cliff failure or field mapping in Waitaki District, S_{HC} was selected as the average value of the maximum absolute shoreline position change for all the cliff profiles located within 150 m of the profile being analysed. This was represented by a normal distribution centred on the averaged value and with a standard deviation calculated as $1/3^{\text{rd}}$ of the range of the absolute shoreline position change recorded off all the cliff profiles located within 150 m of the profile being analysed. This allows for a distribution of slump width that is representative of the cliff and is constructed independently for each transect. This approach was developed to avoid potential bias in just selecting the maximum between-survey change, since the number of historical shorelines captured at each profile is small (3–6 per profile) and a slow but steady retreat of the cliff occurring during a period when no aerial images are available will be mistaken for a single large slump, overestimating the largest slump during that period. In addition, S_{HC} and R_{HC} are not independent variable in our analysis, and in some cases S_{HC} may duplicate the retreat captured in R_{HC} .

While these estimates of coastal hazard zone for bedrock cliffs are conservative (mainly due to the S_{HC} distribution being conservatively wide), a conservative approach is warranted given that the data available do not allow account to be taken of all the cliff recession processes (e.g., drainage concentration factor). It is also recommended for this shore type that a minimum width of erosion hazard zone is adopted. This safety width would allow for cases where S_{HC} was mapped to be small because no significant slump could be observed from the imagery analysis but where slumps are known to occur based on geological evidence.

Note that for hard cliffs, accelerated sea-level rise is not expected to lead to acceleration of coastal erosion or slumping and is not taken into account.



Figure 3-10: Example of bedrock cliff morphology. Shag Point cliffs.

Unconsolidated cliffs

Cliffs formed in unconsolidated sediments (gravel, loess, clay, old sand dunes) have a low competency (LC) and their retreat is directly correlated to wave and sea-level actions. The sediment that falls off the cliff is reworked by waves and forms a beach at the foot of the cliffs, which, in turn, protects the cliff from waves. This morphology can be seen at the cliffs north of Oamaru (Figure 3-11), at Beach Road (Figure 3-12), and along most of the coast near Hampden (Figure 3-13). For these cliffs, which typically front old alluvial fans or coastal terraces, the location of the cliff top is typically more obvious than for bedrock cliffs with a rising backshore, leading to smaller shoreline detection errors. However, they also show a greater alongshore variability of erosion rate due to small slumps, which can mask or confuse the long-term erosion rate.

The formula used to assess the erosion hazard on low competency cliffs is:

$$CHZ = R_{LC} \times T + S_{LC} \quad (3.3)$$

As with bedrock cliffs, R_{LC} is the erosion rate sampled from a normal distribution constructed using the historical erosion rates and their associated standard errors, both smoothed alongshore on a 300 m wide window to remove the contribution of short-term slumps to the long-term retreat. The normal distribution is justified when considering that the errors are due to digitization (for which a normal distribution is expected) and fitting the linear trends.

Unconsolidated cliffs could be affected by an acceleration of sea-level rise, especially if their elevation is comparable to the predicted rise of sea-level or if the rise of sea-level is affecting a new, less competent, geological layer. In this study the data necessary to properly account for cliff height

and geology with acceleration of sea-level rise is not available throughout the district. However, the effect of the acceleration of sea-level rise was tested for the cliffs north of Oamaru using the shoreline dynamics model SCAPE (see Section 3.2.5). That simulation found that for those cliffs the acceleration of sea-level rise had little to no effect on the cliff erosion rates. Since this may not be true for lower cliffs or cliffs with a less competent geology, further study is recommended of the retreat mechanism of the unconsolidated cliffs elsewhere in the district and their sensitivity to an acceleration of sea-level rise.

S_{LC} was calculated the same way as for S_{HC} , with S_{LC} selected as a normal distribution centred on the averaged value of the maximum absolute shoreline position change for all the cliff profiles located within 150 m of the profile being analysed. The normal distribution standard deviation is calculated as $1/3^{rd}$ of the range of the absolute shoreline position change recorded at all the cliff profiles located within 150 m of the profile being analysed. Again, with the approach we used S_{LC} and R_{LC} are not independent variables and in some cases S_{LC} may duplicate retreat captured in R_{LC} but is showing the sudden retreat that should be expected at any time.

The formulation here attempts at combining the effect of complex processes of cliff retreat into a normal distribution. While this is the most that can be achieved with available data, important processes of retreat may be ignored or underestimated. Therefore, it is also recommended to include a minimum width of the hazard zone. Discussion and recommendation of the minimum width is provided in section 3.2.7.



Figure 3-11: Example of unconsolidated cliff morphology: north of Oamaru. Note mainly gravel cliffs with loess cap.



Figure 3-12: Example of unconsolidated cliff morphology: Beach Road. Note remnants of the old coastal road on the cliff top and scattered light-coloured blocks from a failed rip-rap wall in the distance (circled).



Figure 3-13: Example of unconsolidated cliff morphology: Hampden. Note cliffs formed in soft mudstone containing scattered concretions.

Geologically controlled beaches (perched beaches)

The Waitaki District beaches are predominantly perched beaches that are often backed with low cliffs. Perched beaches are beaches that are underlain and/or fronted seaward by hard substrate (reefs, pavements, shallow bedrock, etc) (e.g., Figure 3-15). The response of these types of beach to sea-level rise is poorly understood (Gallop et al. 2011) as the form and character of the nearshore substrate and backshore could either damp or amplify the effect of sea-level rise. In the case of the Waitaki District coast, there is not enough information to robustly assess the effect of an accelerated sea-level rise on these shorelines. Using the standard Bruun model or variations, developed for beaches with a sand-formed offshore profile and a sandy backshore, would lead to exaggerated shoreline retreat by predicting shoreline positions too far into the backshore. Therefore, for geologically controlled beaches, no acceleration of erosion due to sea-level rise was accounted for.

Thus, for perched beaches and beaches backed with low cliffs, the hazard zone formula used is:

$$CHZ = R_{PB} \times T + S_{PB} \quad (3.4)$$

As previously, R_{PB} is the erosion rate sampled from a normal distribution constructed using the historical erosion trends and the associated standard error, both smoothed alongshore.

In these cases, the shoreline is expected to experience cycles of storm erosion and post-storm recovery (accretion/revegetation of backshore) superimposed on a long-term retreat trend, and S_{PB} is the short-term shoreline retreat of the vegetation line due to storms rather than the extent of slumps (e.g., as used to define S_{HC} and S_{LC}). The methodology of cliff slump-width estimation used for the cliffed morphologies will tend to overestimate this storm cut. A better approach is to estimate S_{PB} from the residuals of the linear long-term shoreline trends – which index the magnitude of short-term cycles. The S_{PB} distribution at each station (defined by a mean and standard deviation) was sampled from the pooled absolute values of the residuals from the shoreline trend analyses of all the transects within 150 m of the target transect. Unlike S_{HC} and S_{LC} , S_{PB} does not duplicate the erosion rates. It is likely that S_{PB} follows an extreme value type distribution, but not enough data is available to construct an accurate extreme value distribution, so a normal distribution was assumed.

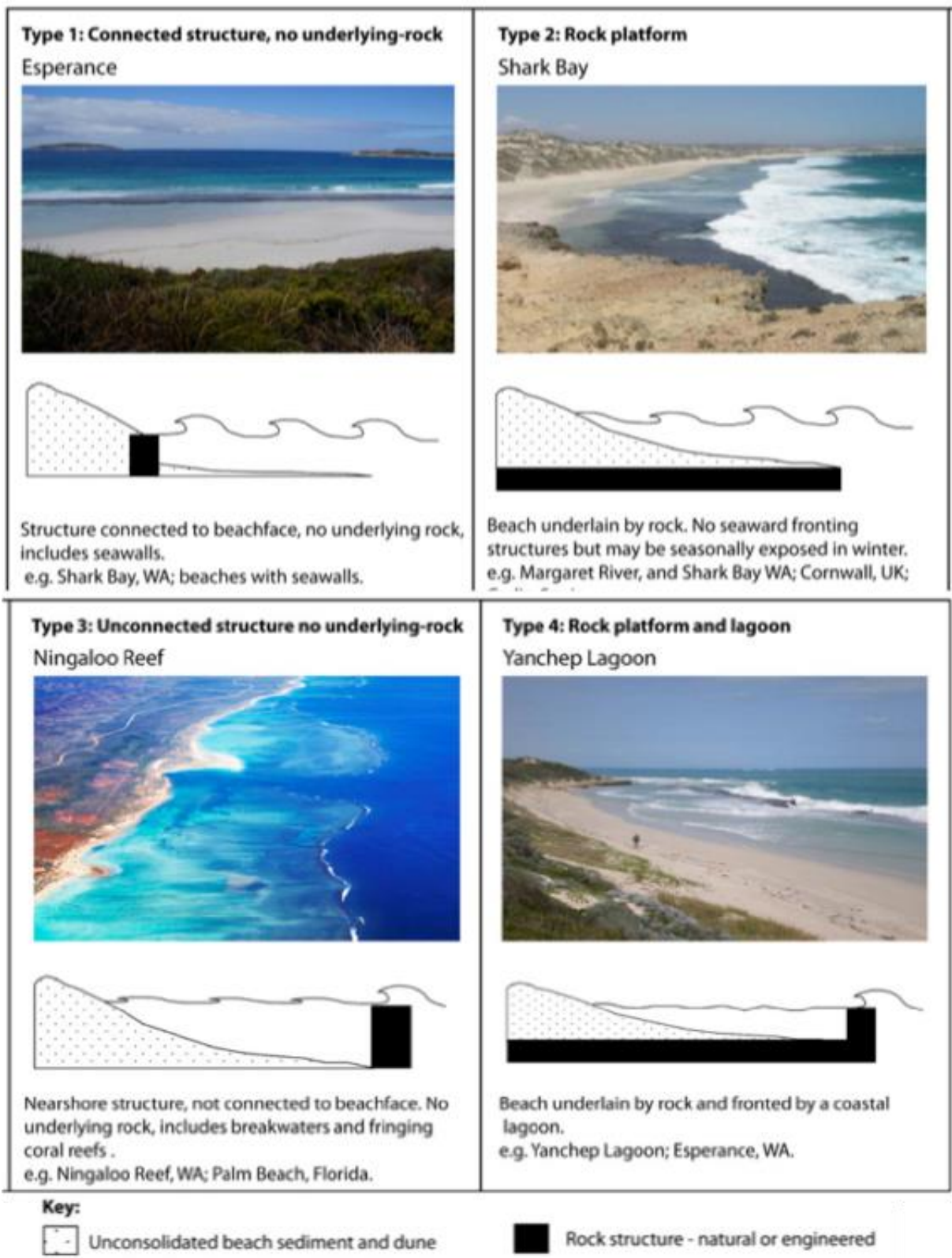


Figure 3-14: Four main types of perched beaches. The beaches of Waitaki District are often represented by Type 2 perched beaches but are generally a mix of the four main types. [Source: Gallop et al. (2011)].



Figure 3-15: Example of geologically controlled beach: South Katiki Beach. Note the outcropping reefs on the right and near the top of the beach.

Wide gravel barriers

The span of shore near the Waitaki River mouth is a wide gravel barrier. Gravel beach evolution in Canterbury and North Otago has been more extensively studied than the rest of the shoreline of Waitaki District. This allows us to use a more complex formulation than for most other beaches in the district. In this case the hazard zone formula is:

$$CHZ = (R_{Measures} + R_{Residual}) \times T + S_{RM} \quad (3.5)$$

where $R_{Measures}$ represents the retreat rate due to sea-level rise. The retreat due to sea-level rise is based on the approach of Measures et al. (2014) for Kaitorete Spit. This approach is transferable to the gravel barriers of Waitaki District because it is based on a geometric calculation, and although Kaitorete Spit has a different wave climate the morphologies of both sites are similar. $R_{Residual}$ is the difference between the historical shoreline retreat rate and the shoreline retreat rate predicted by using a similar method as $R_{Measures}$ using an historical rate of sea-level rise of 0.002 m/y. $R_{Measures}$ is calculated as:

$$R_{Measures} = 0.01 * \Delta S \left(\frac{\Delta S}{2} + H_{bs} \right) \left(\frac{1}{\tan \alpha} + \frac{1}{\tan \beta} \right) / H_{fs} \quad (3.6)$$

where ΔS is the expected sea-level rise over the period of 100 year, H_{bs} is the height of the backshore, α is the corresponding backshore slope, H_{fs} is the height of the foreshore using the toe of the gravel beach as a base, and β is the corresponding foreshore slope. This approach is equivalent to a Bruun-type response to sea level but bypasses the uncertainty of estimating the depth of closure. Lidar data of the Waitaki river mouth was used to measure the geometry

parameters used in equation (3.6) at a single profile and assumed constant for the length of shoreline considered (Table 3-2).

Table 3-2: Wide gravel barrier geometry parameters used in equation 3.6 for the Waitaki River mouth. Parameters measured from LiDAR data.

Geometry parameter	Value
H_{bs}	5.7 m
H_{fs}	12.3 m
α	2.8°
β	4.7°

Dune-backed beaches and thin sand-gravel barriers

Beaches backed by a dune field are seldom present in Waitaki District. The northern section of Katiki Beach and the northern section of beach fronting Beach Road are the largest sections that are not strongly geologically controlled by nearby cliffs. Dune backed beaches as well as the thin gravel barrier in Kakanui (e.g., Figure 3-16) are expected to show a Bruun-type of response to sea-level rise. However, the shoreline retreat may not be solely due to sea-level rise and other historical effects may be acting (e.g., change in wave climate or coastal sand supply or adjustment of the shoreline due to the removal of the pier at Kakanui). In this case, the background/residual shoreline retreat needs to be accounted for. In these cases, the coastal hazard zone formula is:

$$CHZ = (R_{Bruun} + R_{Residual}) \times T + S_{PB} \quad (3.7)$$

R_{Bruun} is the expected shoreline retreat rate based on future sea-level rise using the Bruun model. $R_{Residual}$ is the difference between the historical shoreline retreat rate and the shoreline retreat rate predicted by a Bruun model using an historical rate of sea-level rise of 0.002 m/y. S_{PB} is, as described above, the short-term shoreline retreat due to storms, and is sampled from a normal distribution based on the residuals of the shoreline trend analysis. R_{Bruun} was calculated as:

$$R_{Bruun} = \alpha_B \times R_{SLR} \quad (3.8)$$

where α_B is the inverse of the active beach slope and R_{SLR} is the future average rate of sea-level rise. The active beach slope is usually calculated over the distance from the dune/barrier crest to the closure depth (i.e., the offshore depth where waves stop influencing the seafloor morphology) on the offshore profile, and is more generally calculated as:

$$\alpha_B = \frac{L_d + L_b}{h_d - h_b}$$

where L_d is the offshore distance to the depth of closure, L_b is the distance of the dune/barrier crest to the backshore toe, h_d is the depth of closure, and h_b is the elevation of the backshore. While h_b and L_b can easily be calculated from Lidar data, the depth of closure is not trivial to define and the

offshore bathymetry in Waitaki is not well known. The closure point is likely located between 6 and 8 m depth which occurs between 500 to 800 m offshore for all three beaches of interest (Kakanui, north Katiki and north Beach Rd). Therefore, α_B was sampled from a normal distribution with a mean of 75 and a standard deviation of 7.3. A single scenario of accelerated sea-level rise rate (R_{SLR}) of 0.011 m/y was used. This corresponds to a sea-level rise of 1.3 m over the 100 years from 2015 to 2115 when the historical rate of sea-level rise (0.002 m/y) is included.

Kakanui gravel barrier is a thin barrier (as opposed to the wide, flat-topped barrier at the Waitaki River mouth) and is located on top of a sandy subtidal beach that may also show a Bruun-type response to sea-level rise. Therefore, the approach used for Kakanui Beach was similar to that used for a dune backed beach. In the Kakanui case, however, the Bruun-type response may overestimate the shoreline retreat due to sea-level rise because of the proximity of geological controls (i.e., nearshore substrate, adjacent rocky headlands) which are not taken account of by the Bruun model.



Figure 3-16: Example of thin sand/gravel barrier morphology: Kakanui barrier.

Major coastal structures

Near Oamaru Port, the coast has been protected by a seawall and heavy rock revetments since at least the 1920s, yet the reclamations and revetment are not perfectly stable, and small shoreline changes have occurred and need to be taken account of in the coastal hazard zone. These are calculated as:

$$CHZ = R_{hist} \times T \quad (3.9)$$

where R_{hist} is the historical shoreline trend rate sampled from a normal distribution constructed using the alongshore-smoothed shoreline trend rates and their longshore-smoothed standard errors. The shore protection here is designed to prevent any sudden retreat of the shoreline during a single

storm, but net shoreline retreat due to the cumulative effect of storms and successive repairs of the structure is captured by the R_{hist} term. Evidence from shoreline detection data and Lidar imagery in Oamaru confirm that the shore has crept inland slightly as the result of periodic damage and repair.

Note that this formula does not apply in the future if the coastal protection ceases to be maintained or is removed. It is assumed that the protective structures fronting Oamaru will be maintained at least for the next 100 years. However, short spans of small-scale/shallow-depth coastal protection, such as the riprap at Katiki Beach and along Beach Road and the seawalls at Kaika, were not considered in this analysis of hazard zones as we assume that in their present state they will not continue to hold the shoreline at its current position indefinitely as sea-level rises and erosion trends persist.

Also, note that the effect of acceleration of sea-level rise on the retreat rate has not been taken into account.

3.2.7 Caveat and limitations

The coastal erosion hazard zoning method outlined above attempts to define zones based on expected future shoreline retreat processes evaluated from shoreline detection from aerial imagery. As a consequence, many factors and processes (e.g., the geology of the backshore or foreshore, longshore sediment transport) locally important to driving or preventing shoreline retreat may be missed by the analysis or may be inaccurate. For example, apart from Waitaki River mouth, streams and estuaries are treated the same as the surrounding morphology (dune backed beach or perched beach) and sand/gravel spit retreat may be inaccurate because the influence of sediment supply by rivers is not explicitly accounted for.

There are large uncertainties associated with shoreline response to the acceleration of sea-level rise. The only established approaches are that soft sediment shorelines (beaches) and wide barriers are expected to respond following variations of the generalised Bruun model, but this study did not have available sufficient information on offshore profile geometry to implement this approach as robustly as it could have been. No such response model exists for beaches that are geologically controlled, such as perched beaches. Similarly, shoreline simulations using the SCAPE model suggest that the Bruun model would not be accurate for unconsolidated cliffs, so no estimate of the impact of acceleration of sea-level rise is taken into account on these morphologies.

Also, the dataset used to evaluate the historical shoreline and short-term erosion are based on a relatively few sets of imagery data. For most of the southern half of the coast (Kakanui and further South), the oldest imagery that could be used for shoreline capture (with low distortion of the georeferenced image and adequate resolution) is generally 2006 (with 1973 for Hampden). This means only about 10 years of shoreline record, which is unlikely to be adequate to isolate a long-term retreat trend from the signature of storm events. While some uncertainty is accounted for in the error estimate on the shoreline trend, it does not account for the short sampling period afforded by the data span. Therefore, the results of the analysis should be used with caution.

To account for these limitations, a minimum width should be set for the hazard zones. This minimum zone could follow practical landmarks (e.g., nearby road) or geomorphic limits (i.e., entire sand/gravel spit or coastal dune field). In a practical sense, the coastal hazard zone should not be narrower than the largest shoreline detection error of 8 m.

3.3 Results

3.3.1 Shoreline trends

Figure 3-17 shows the measured erosion rates for the wider Waitaki District. Figure 3-18 to Figure 3-22 show more detailed measurements of erosion rate for the urban areas. GIS data and digital files are available within the appended supplementary material.

The shoreline analysis off historical imagery shows that more than 60 % of the coast of Waitaki District is retreating at a rate of 0.15 m/y or more. The largest erosion rates of 2.0 m/y occur north of Hampden at the location of a large slump². north of Oamaru, the entire coastline is retreating at rates between 0.3 and 0.9 m/y. Small pockets of accretion have occurred at the north end of Beach Road (0.3 m/y accretion), north of All Day Bay (0.16 m/y accretion), and the Shag River mouth spit (0.9 m/y accretion). Since these accretion cases are typically located at the northern end of bays, it may be the result of inter-decadal variability in wave direction rather than a long-term trend.

In the built-up areas, Oamaru shows erosion rates of 0.4 m/y near Waitaki Boys High School, 0.35 m/y near Foyle Street, and 0.3 m/y near Weaver Street. Even the area with rock protection shows retreat rates of 0.2 m/y (Torr ridge Street) - despite the coastal protection. Some parts of the port show accretion because of refurbishment of the seawall (Figure 3-18). At Kakanui, the gravel barrier is showing retreat rates of around 0.7 m/y. Near the Kakanui spit tip, the rates increase to 1.3 m/y (Figure 3-19). At Hampden, the erosion rates are around 0.10 m/y, a rate considerably less than the erosion observed at the large slump feature north of the town (Figure 3-20). At Moeraki, the shoreline change analysis suggests accretion, but the error estimates associated with these rates are high suggesting that it is likely influenced by an inter-decadal cycle or simply measurement error. At Shag Point, the rates appear to be variable (likely reflecting measurement error) but predominantly show no overall changes in the shoreline (Figure 3-21).

Elsewhere, the southern portion of Beach Road is an erosion hotspot, eroding at an average rate of 0.38 m/y (Figure 3-22), while the shore along the southern portion of Katiki Beach, alongside SH1, is eroding at 0.4 – 0.6 m/y.

² Here the shoreline has been defined as the scarp of the cliff and although the scarp has retreated 2m/y, the toe of the slump may have retreated more slowly.

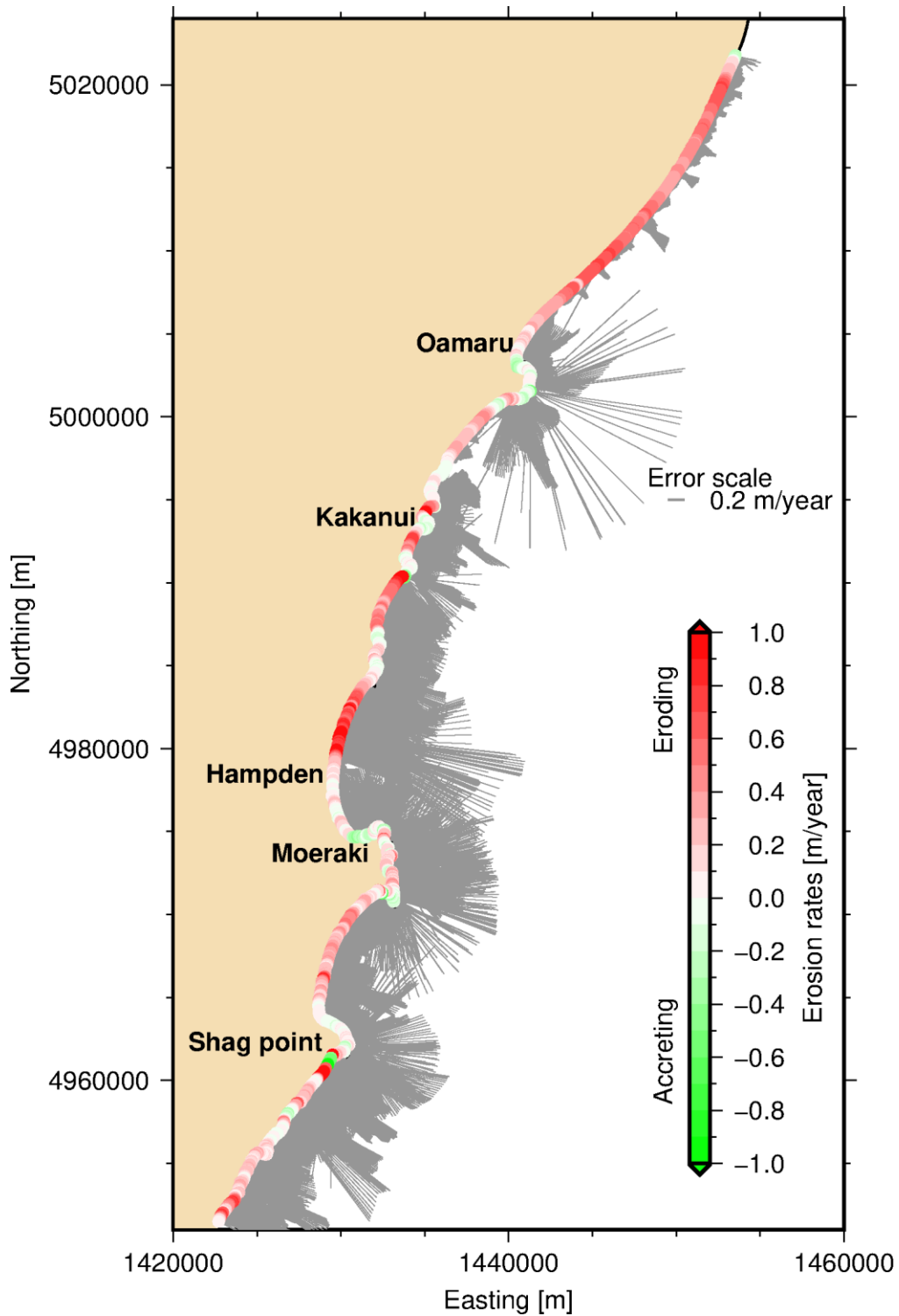


Figure 3-17: Calculated shoreline trends for the Waitaki District coast. Green and red shaded circles show the average erosion rate (m/year). The grey shaded lines show the standard error calculated for the erosion rate; their length scales as on the legend. High error may be due to lack of data or low resolution in shoreline fitting.

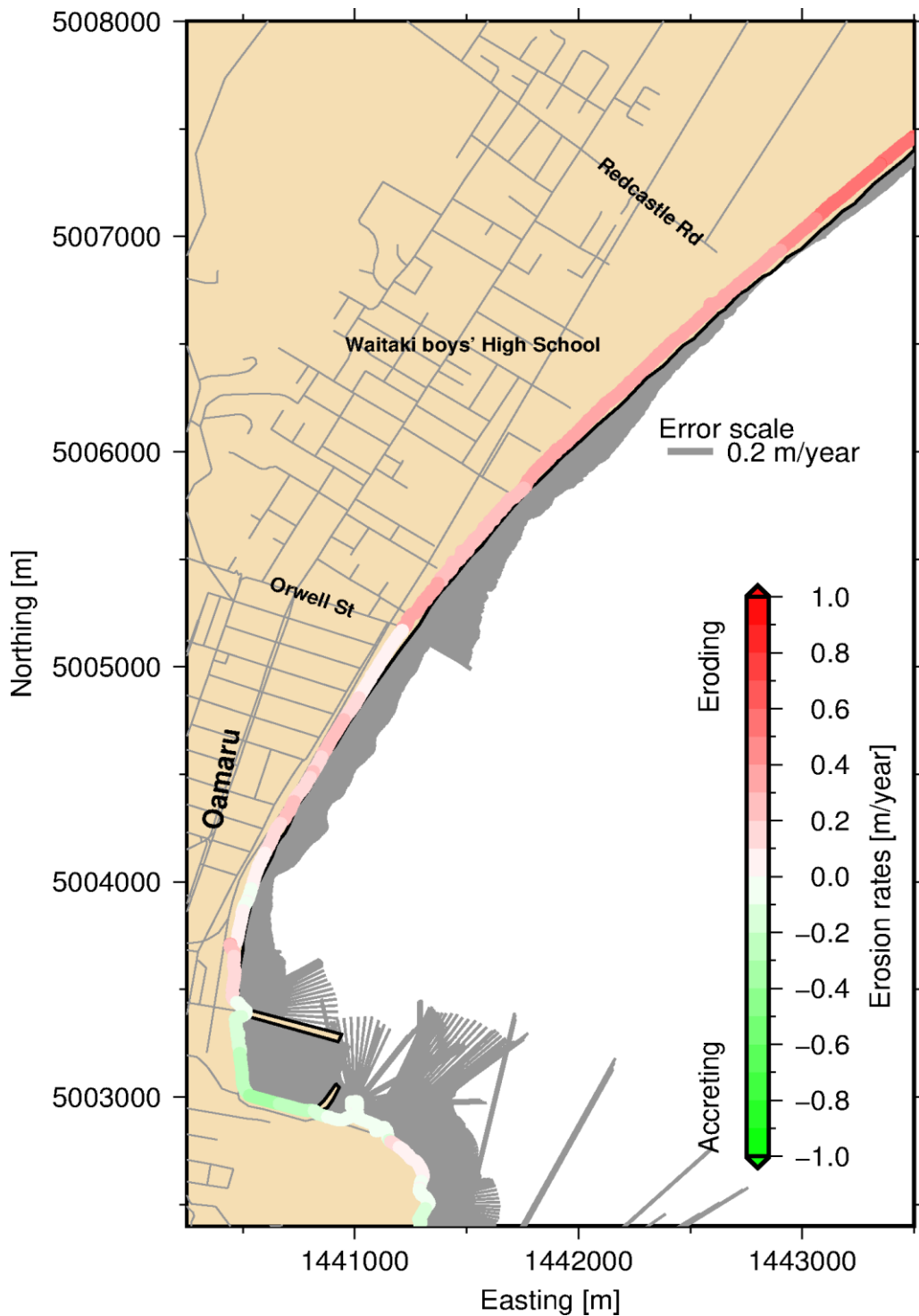


Figure 3-18: Calculated shoreline trends for the Oamaru area. Green and red shaded circles show the average erosion rate [m/year]. The grey lines show the standard error calculated for the erosion rate. High error may be due to lack of data or imprecise shoreline fixing.

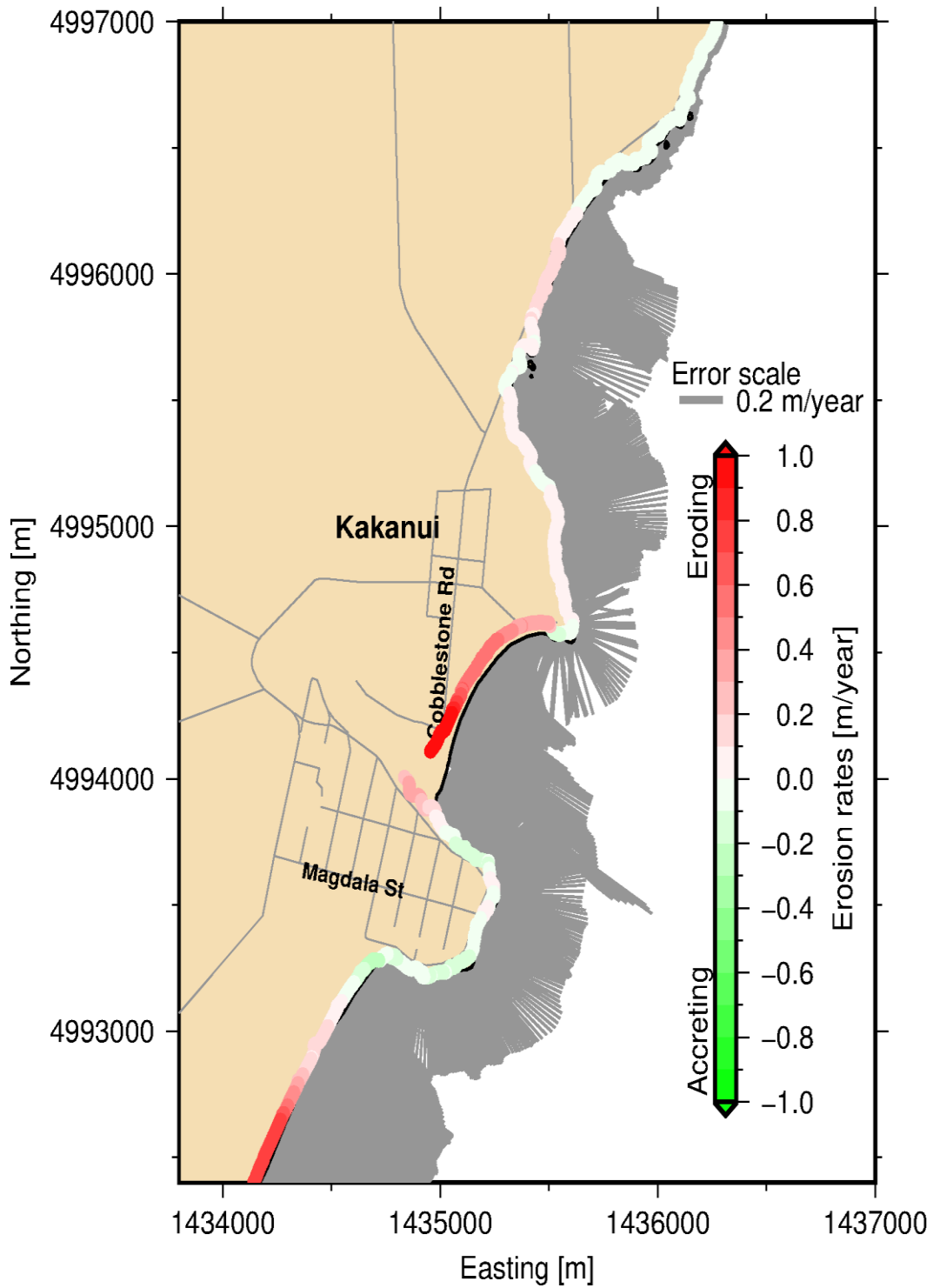


Figure 3-19: Calculated shoreline trends for the Kakanui area. Green and red shaded circles show the average erosion rate [m/year]. The grey lines show the standard error calculated for the erosion rate. High error may be due to lack of data or imprecise shoreline fixing.

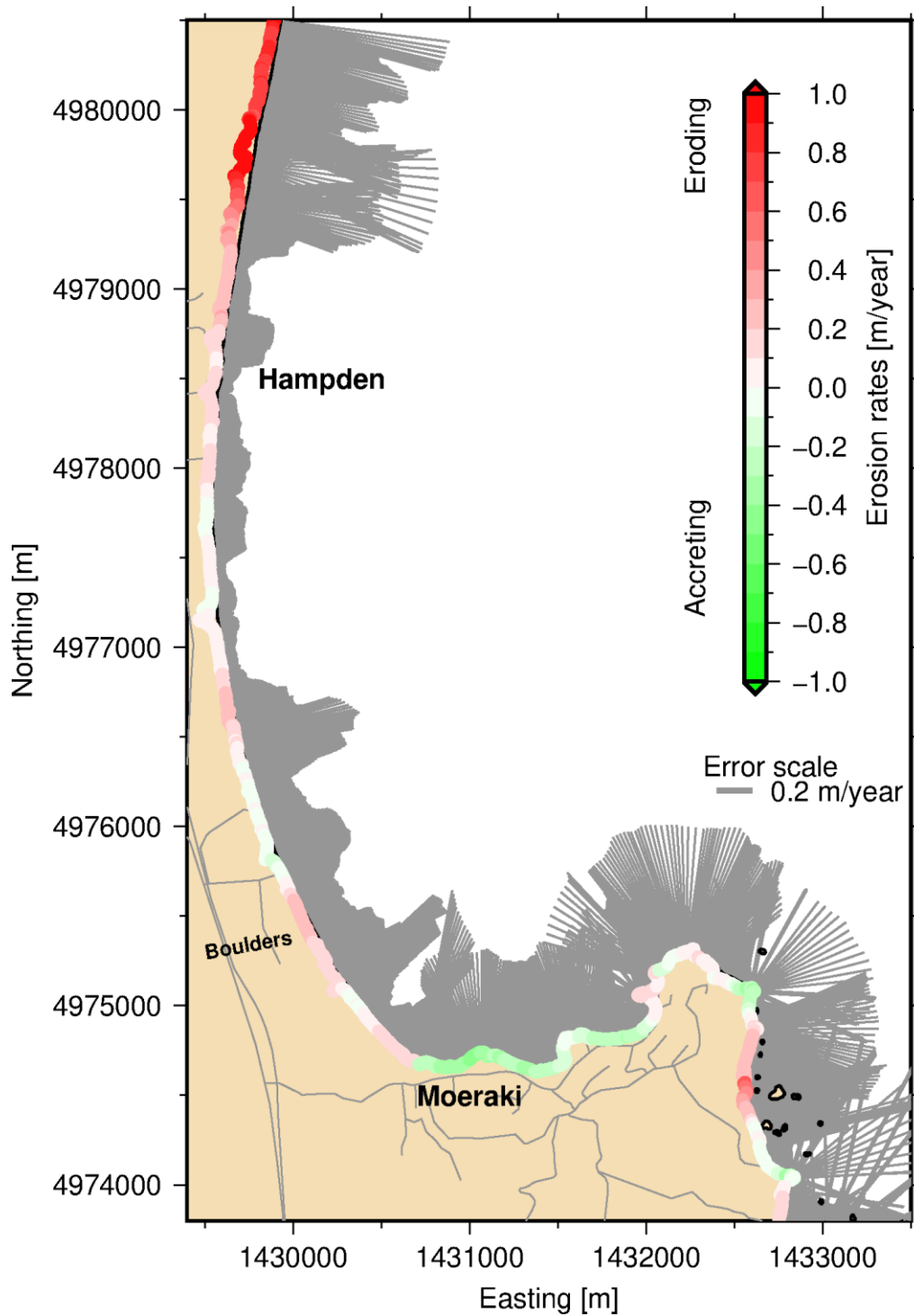


Figure 3-20: Calculated shoreline trends for the Hampden and Moeraki area. Green and red shaded circles show the average erosion rate [m/year]. The grey lines show the standard error calculated for the erosion rate. High error may be due to lack of data or imprecise shoreline fixing.

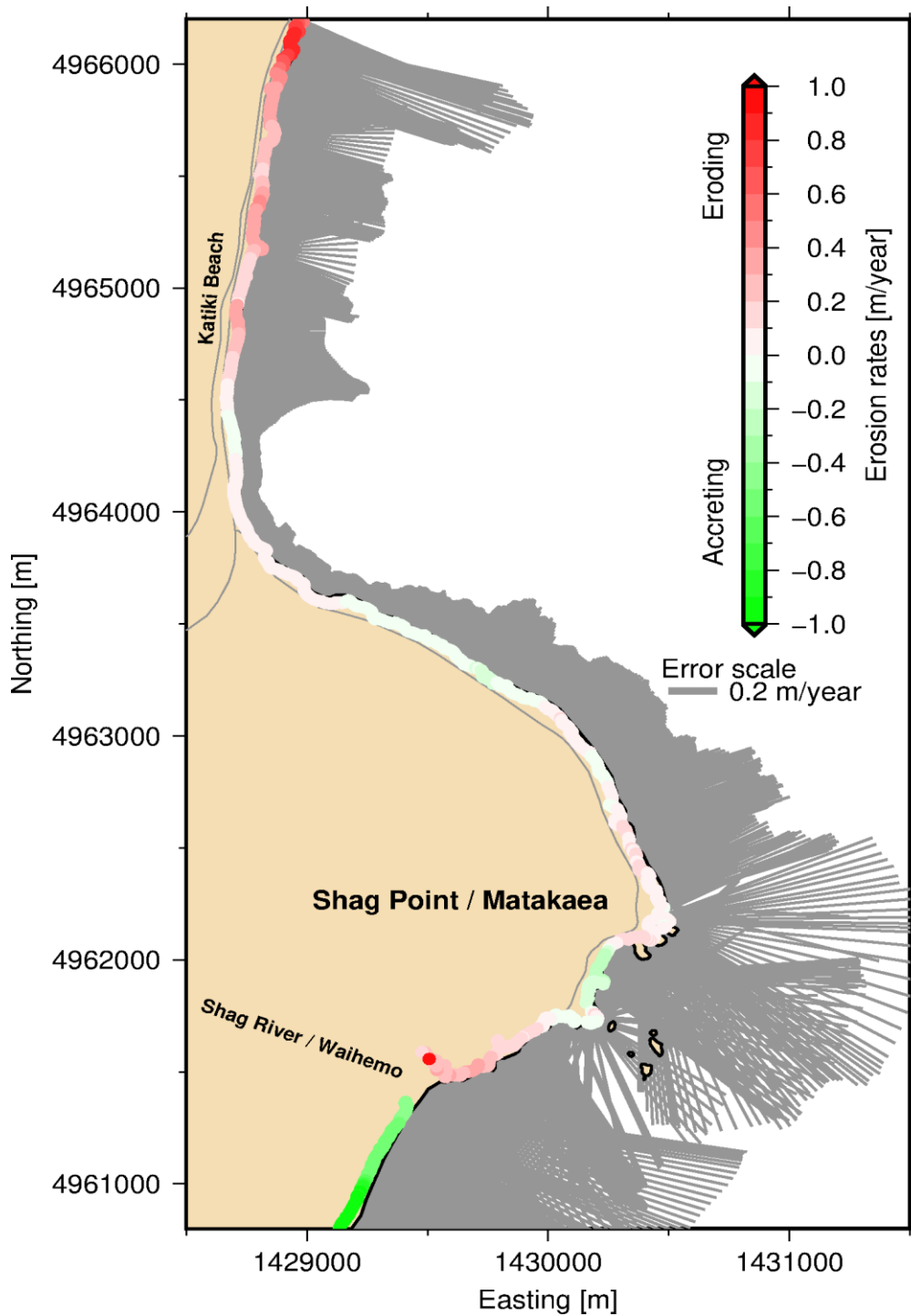


Figure 3-21: Calculated shoreline trends for the Shag Point and Shag River mouth area. Green and red shaded circles show the average erosion rate [m/year]. The grey lines show the standard error calculated for the erosion rate. High error may be due to lack of data or imprecise shoreline fixing.

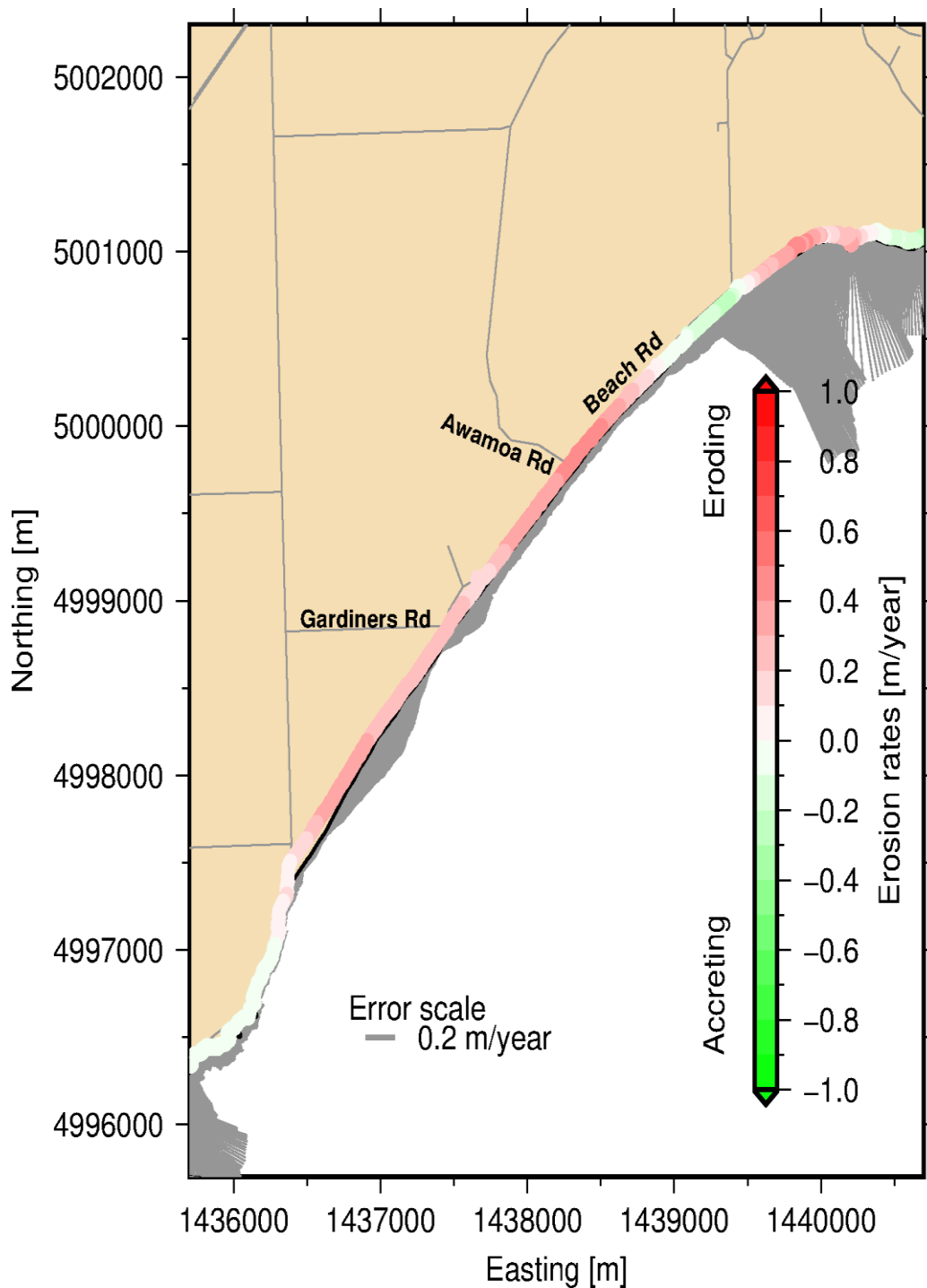


Figure 3-22: Calculated shoreline trends along Beach Road. Green and red shaded circles show the average erosion rate [m/year]. The grey lines show the standard error calculated for the erosion rate. High error may be due to lack of data or imprecise shoreline fixing.

3.3.2 Short term shoreline retreat

Short term retreat was estimated for different coastal morphology types as a component of the hazard zone. While a statistical distribution was used in the hazard zone definition, it is useful to evaluate the 95th percentile for short term retreat (Figure 3-23) to better understand the weight of this component in the overall hazard width. As with the rest of this report, the shoreline here refers to the vegetation line or cliff top line for cliffed shorelines. Short term retreat of the vegetation line

due to a storm is expected to be much less than the retreat of the water line on a sandy beach. The largest short-term shoreline retreat is predicted for soft cliffs and in particular for the section north of Oamaru and Beach Road, contributing up to 1/3rd of the historical erosion rate contribution over 100 years. Small (~1 m) short term retreat is expected on the dune-backed northern segment of Katiki Beach; this is negligible compared to the 20-40 m expected retreat from the historical rates applied over 100 years.

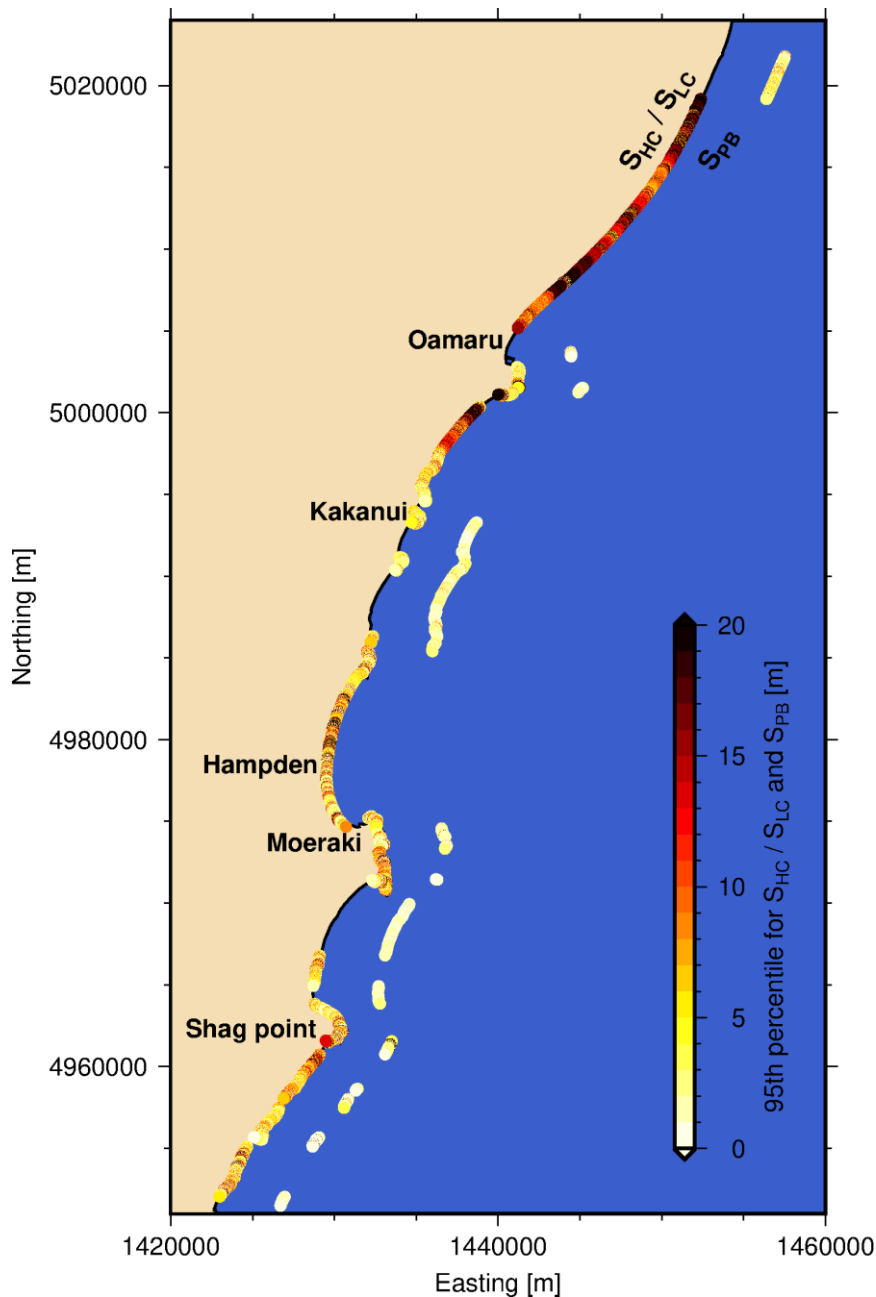


Figure 3-23: 95th percentile of the short-term retreat for beach and cliff shores. The hazard zone is defined using a statistical distribution of the morphology-dependent S (short term retreat) term. S_{HC} (bedrock cliffs) and S_{LC} (unconsolidated cliffs) are showed on the shoreline while S_{PB} (perched beaches) are showed intentionally shifted eastward of the shoreline for clarity.

3.3.3 LiDAR volume change

Shoreline topographical changes detected from the 2004 and 2016 LiDAR surveys provide another measure of rates of shoreline shift and may also show changes too subtle to detect from vertical imagery. In areas such as the eroding cliffs at the northern end of Oamaru (Figure 3-24, Figure 3-25), the cliff retreat rates indicated by the LiDAR are consistent with those from the shoreline analysis from aerial imagery. At central Oamaru, however, and surprisingly, the LiDAR analysis showed changes occurring on the rock protection beside the railway (Figure 3-24). In front of Eden Street, this rock protection lost up to 5.6 m in elevation between 2004 and 2016. The Lidar also shows the recent construction of the rock protection north of Oamaru Creek and accretion south of Oamaru Creek (Figure 3-24, Figure 3-27). This accretion was not reflected in the vegetation line observable on imagery.

At Kakanui, the LiDAR elevation changes clearly show the slump located at the end of Beach Road near the Coast Café restaurant (Figure 3-28 and Figure 3-29). The toe of the cliff retreated nearly 10 m at this feature between the 2004 and 2016 surveys. The LiDAR surveys also show the “rollover” process on the gravel barrier at Kakanui, where material on the front of the gravel beach is washed over onto the back of the barrier during storms, effecting a landward translation of the barrier (Figure 3-30). Despite this rollover, there appears to have been negligible net change in the volume of the gravel barrier between the two surveys (a 1 per cent net volume gain was detected).

The LiDAR elevation difference at Katiki Beach shows considerable variability alongshore (Figure 3-31). For example, Profile Katiki XS1 (Figure 3-32) shows a foreshore erosion/accretion pattern similar to that observed with storm-and-recovery cycles: with the high berm and narrow foreshore in 2004 typical of a post-storm profile, and the wider foreshore with a low berm in 2016 more typical of a recovered profile. In contrast, Profile Katiki XS2, backed by a cliff, shows cliff retreat since 2004 (Figure 3-33) but a slight net rise in the level of the beach fronting the cliff. This variable behaviour suggests that Katiki Beach may not behave like a simple sandy beach and that the nature of the backshore and the reefs outcropping in the nearshore and offshore play a significant role in the coastal processes there.



Figure 3-24: Difference in elevation between 2004 and 2016 near Oamaru based on LiDAR surveys.

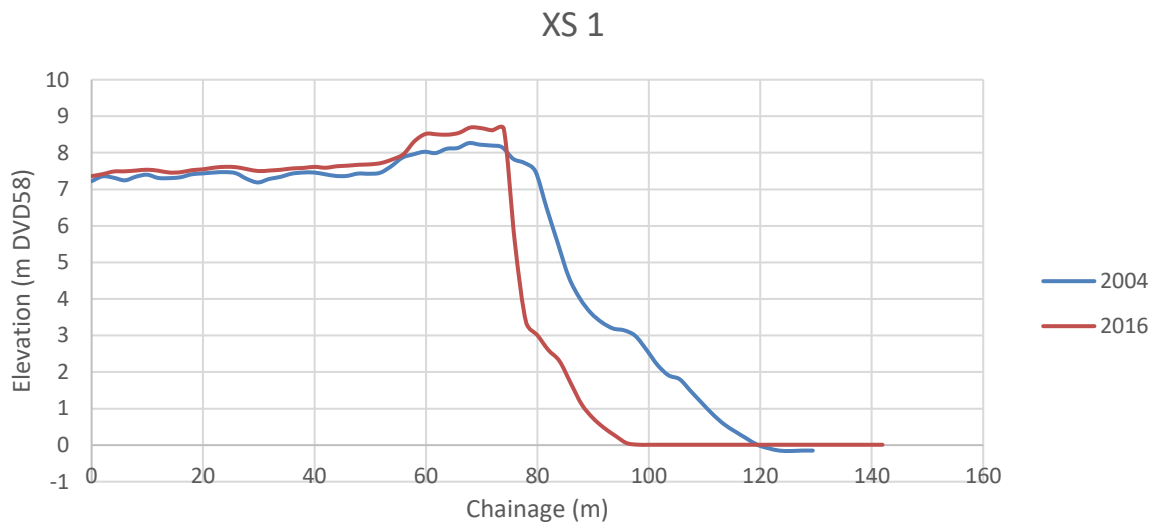


Figure 3-25: Elevation profiles near Weaver Road. Elevation was extracted from the 2004 and 2016 LiDAR survey. Profile location shown in Figure 3-24.

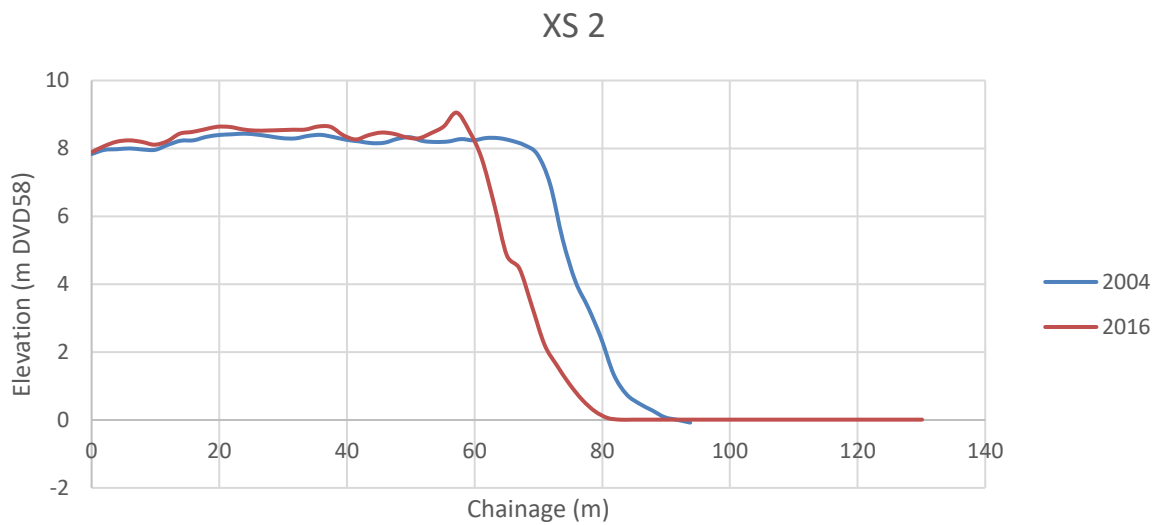


Figure 3-26: Elevation profile near Usk Street. Elevation was extracted from the 2004 and 2016 LiDAR surveys. Note that this profile is located on the armoured part of the coast and shows the degradation of the rock armouring between the two dates. Profile location shown in Figure 3-24.

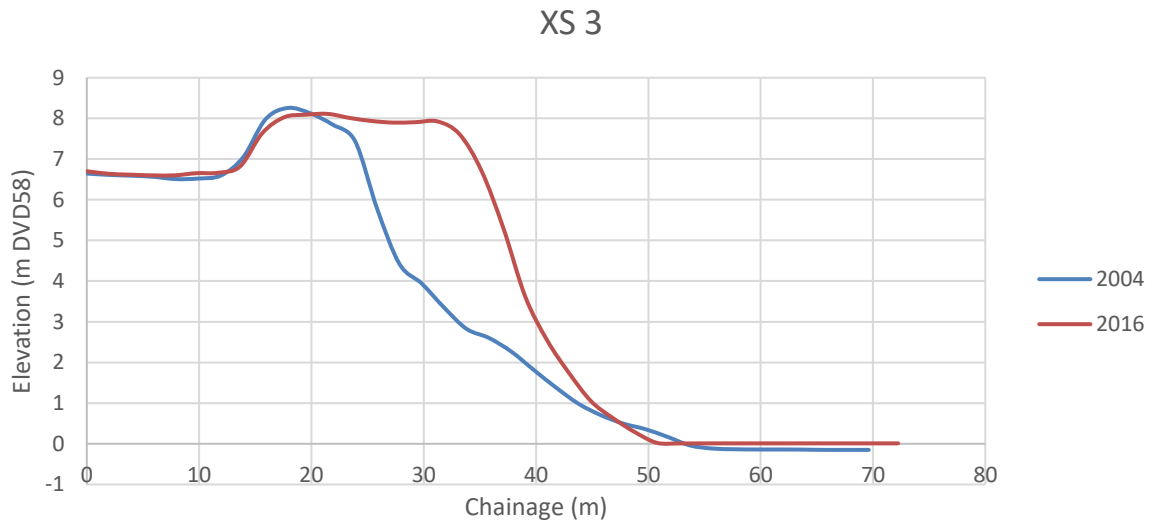


Figure 3-27: Elevation profile north of Oamaru Creek. Elevation was extracted from the 2004 and 2016 LiDAR surveys. Note the increased elevation here shows the recent placement of rock armouring. Profile location shown in Figure 3-24.

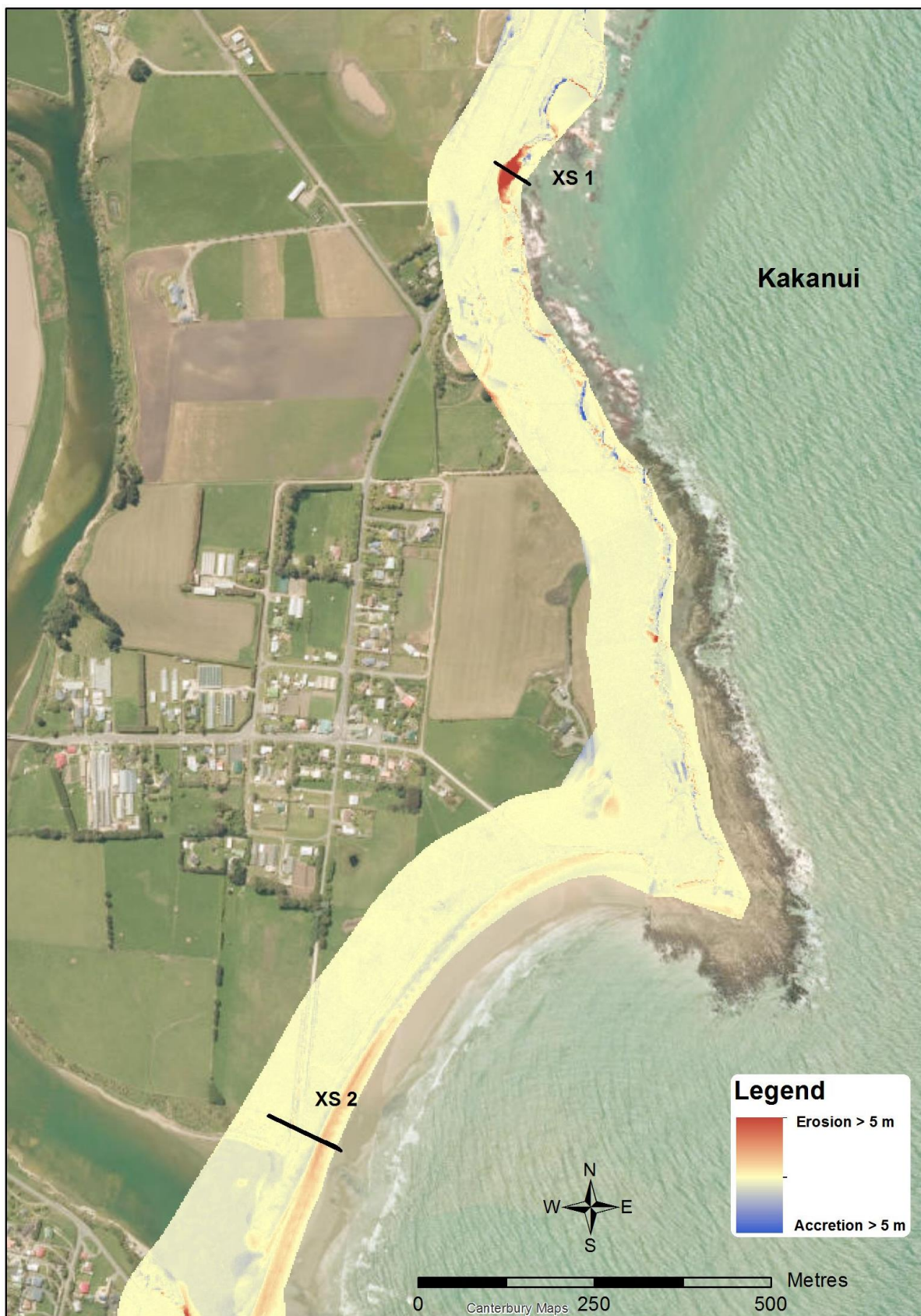


Figure 3-28: Difference in elevation between 2004 and 2016 near Kakanui based on LiDAR surveys.

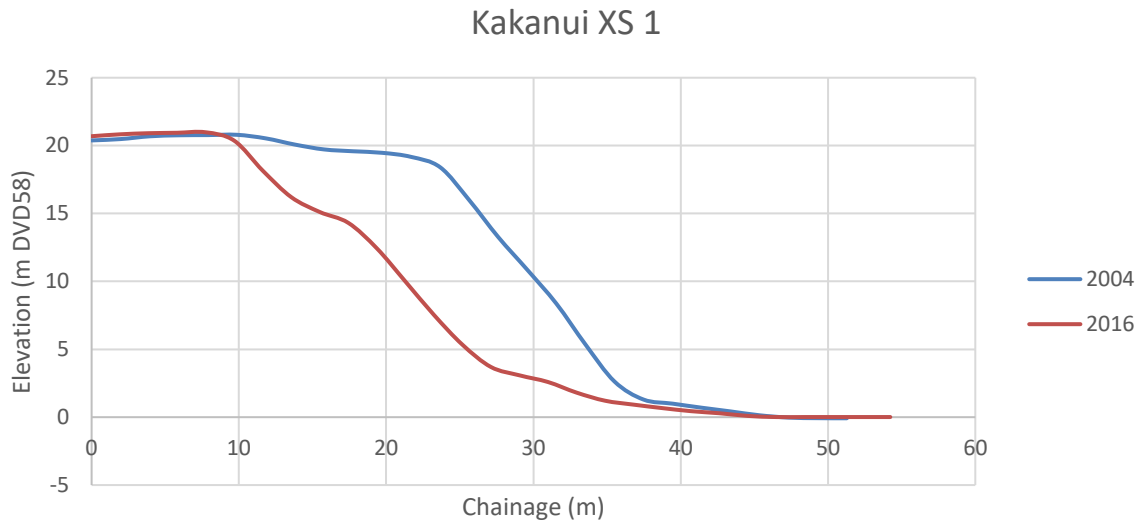


Figure 3-29: Elevation profile at Kakanui through a recent slump that removed part of the road. Elevation was extracted from the 2004 and 2016 LiDAR surveys. Profile located on Figure 3-28.

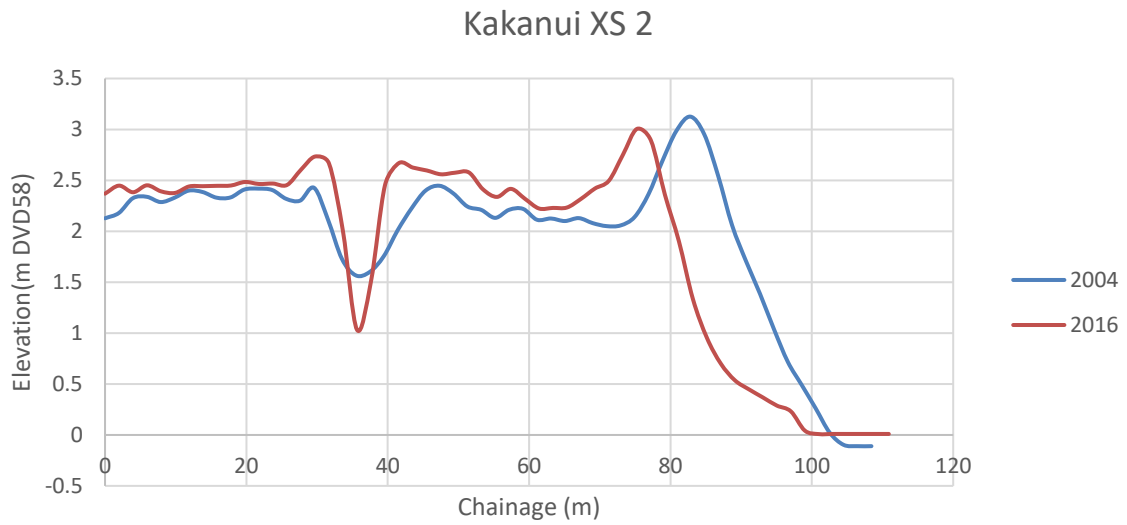


Figure 3-30: Elevation profile of the gravel barrier at Kakanui. Elevation was extracted from the 2004 and 2016 LiDAR surveys. Profile located on Figure 3-28.

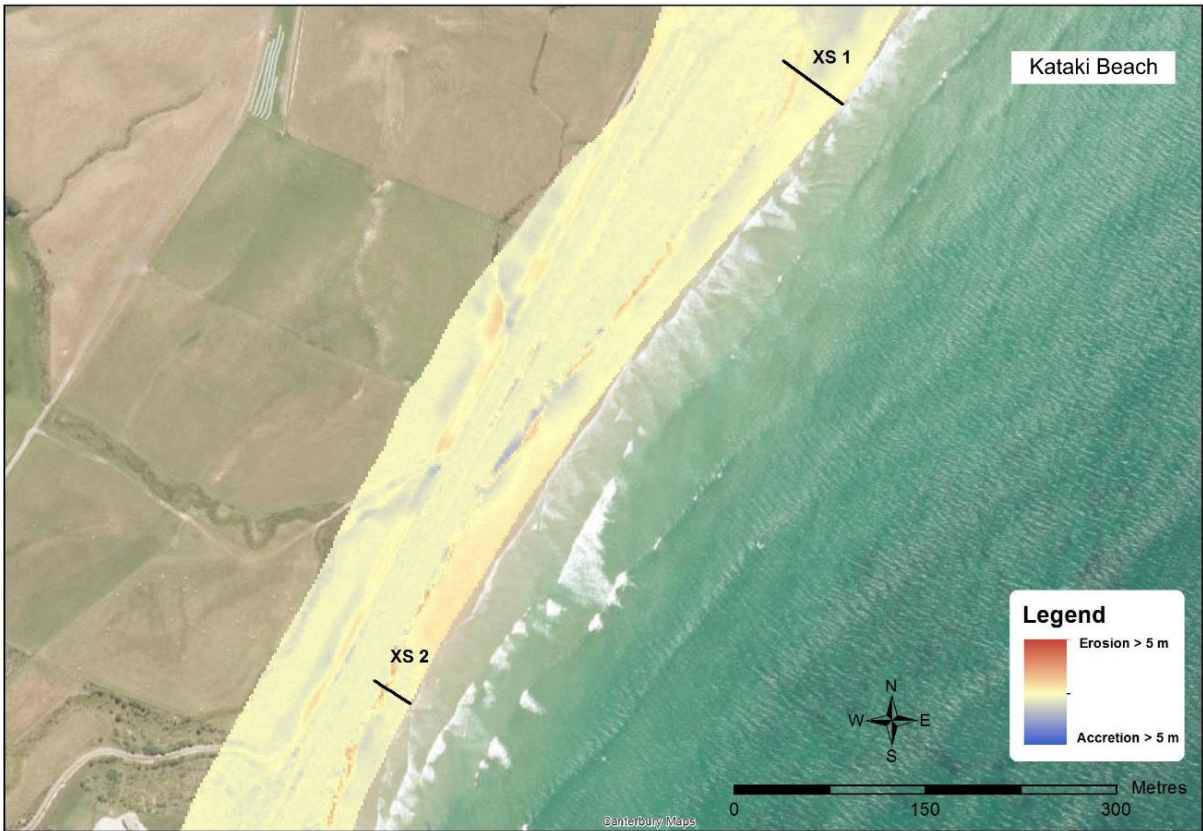


Figure 3-31: Difference in elevation between 2004 and 2016 on Katiki Beach based on LiDAR surveys.

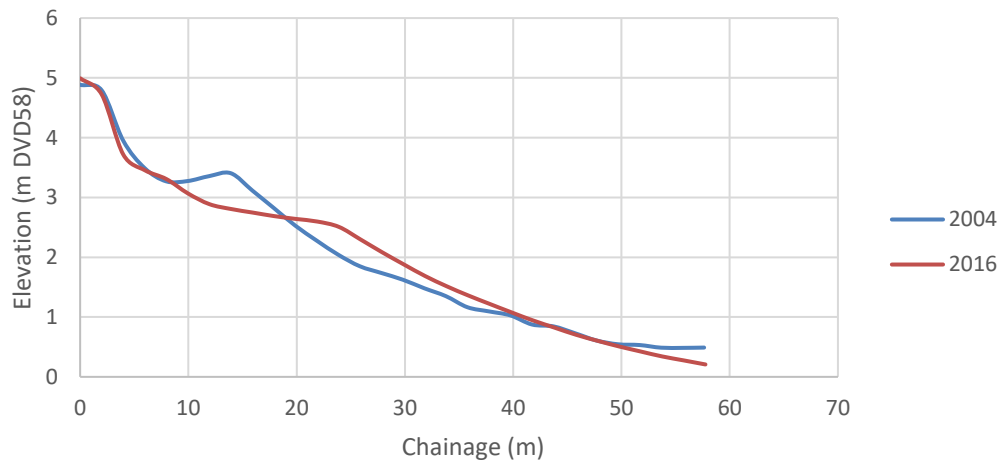


Figure 3-32: Elevation profile on Katiki Beach. Elevation was extracted from the 2004 and 2016 LiDAR surveys. Profile is located on Figure 3-31.

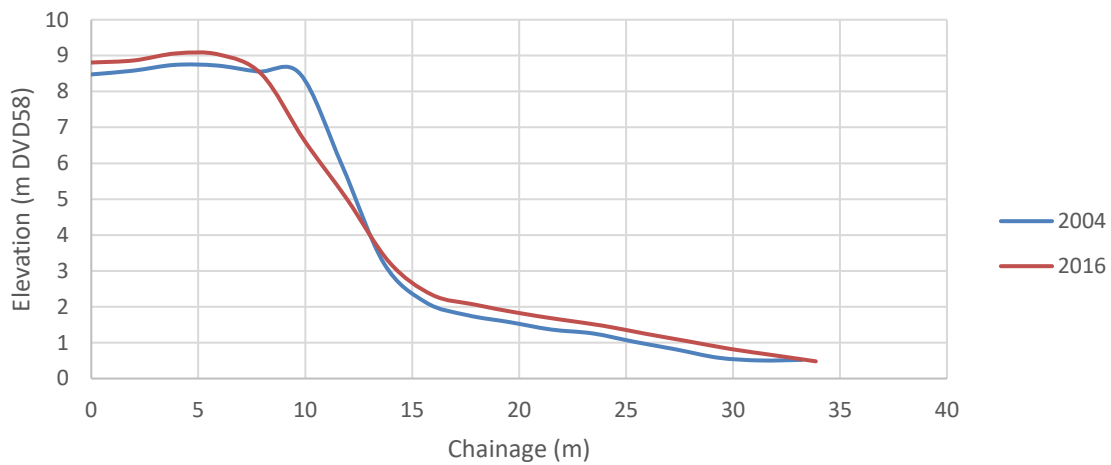


Figure 3-33: Elevation profile in Katiki Beach. Elevation was extracted from the 2004 and 2016 LiDAR surveys. Profile is located on Figure 3-31.

3.3.4 Profiles

Beach profiles monitored by Otago Regional Council only cover up to three dates (May 1994, March 1999 and March 2008) and 12 locations from Oamaru central to the Waitaki River mouth. The four profiles surveyed both in 1994 and 1999 show that the top of the cliff remained at the same location over that period (Table 3-2). The retreat of the cliff between 1994 and 2008, which varied between 3 m and 9 m, thus appears to have occurred during the period 1999-2008. This highlights that the cliff erosion is episodic and is driven almost entirely by storm events.

Table 3-3: Location of cliff top on profiles surveyed by Otago Regional Council.

Profile location	Distance seaward from benchmark 1994 (m)	Distance seaward from benchmark 1999 (m)	Distance seaward from benchmark 2008 (m)	Cliff retreat 1994-2008 (m)
Central	9.3	10.3	4.4	4.9
Foyle Street	6.7	6.4	1.7	5.0
Boys High School	6.6	6.5	2.9	3.7
Hedges Road	16.4		13.4	3.0
Bigg Road	34.1	34.2	27.4	6.7
Stewart Road	20.8		11.8	9.0
Corbet Road	25.8		21.9	3.9
Seacliff Road	20.5		11.9	8.6

3.3.5 SCAPE simulation

Simulation of the effect of accelerated sea-level rise on the cliff erosion near Oamaru using the SCAPE model was undertaken by first simulating the cliff erosion to 2115 using the historical sea-level rise rate of 0.002 m/y (0.2 m at 2115) and then repeating the simulation using the sea levels predicted by the RCP8.5 scenario (+1.3 m in 2115). The position of the cliff in both sea-level rise scenarios is very similar (Figure 3-34), suggesting that an acceleration of sea-level rise is not likely to

significantly increase the cliff erosion rate. This result is consistent with the concept that storms are the largest driver of the erosion. Storm changes associated with climate change were not considered in this simulation.

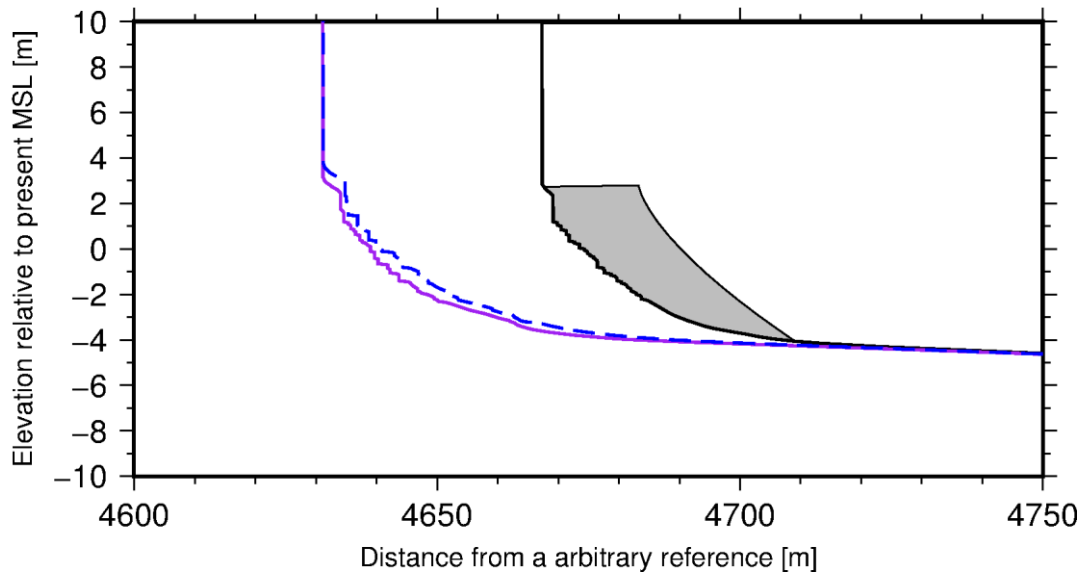


Figure 3-34: Result of the cliff erosion simulation for the shore north of Oamaru. The black line is the 2015 simulated bedrock profile. The grey area is the beach. The purple line is the simulated future bedrock profile for 2115 with a sea-level rise of 0.002 m/y, and the blue dotted line is the future bedrock profile for 2115 using the RCP8.5 upper bound of the likely range of sea-level rise.

3.3.6 Coastal erosion hazard zones

As detailed in Section 3.2, the coastal erosion hazard zones (CHZ) were mapped from shore-normal transects at 5 m intervals along the entire Waitaki District coastline, and its width was defined by different equations depending on the type of coastal morphology (section 3.2.6). The hazard zone includes predictions of shoreline position 50 and 100 years into the future, and to allow that these predictions are uncertain, 50th percentile and 95th percentile shoreline changes were calculated³. Overall for Waitaki District for the 100-year calculation, the 50th percentile predicted change in shoreline position varied between 6 m accretion and 213 m erosion, while the 95th percentile change varied between 11 m of erosion and 339 m of erosion.

The histogram of the coastal hazard zone widths shows that the CHZ50 width is mostly between 5 m and 95 m, with the most common width between 5 and 15 m (Figure 3-35). The CHZ95 widths were mostly between 5 m and 145 m with a most common value at 25-35 m (Figure 3-36), meaning that most of the coastal hazard zones calculated are wider than the minimum width suggested (8 m).

³ With the 50th percentile prediction, there is a 50% chance that the actual future shoreline retreat would be larger (or less) than predicted, whereas with the 95th percentile prediction there would only be a 5% chance that the actual retreat would exceed the prediction. Thus the 95th percentile prediction is a conservative one, with a high likelihood that the actual retreat will be less.

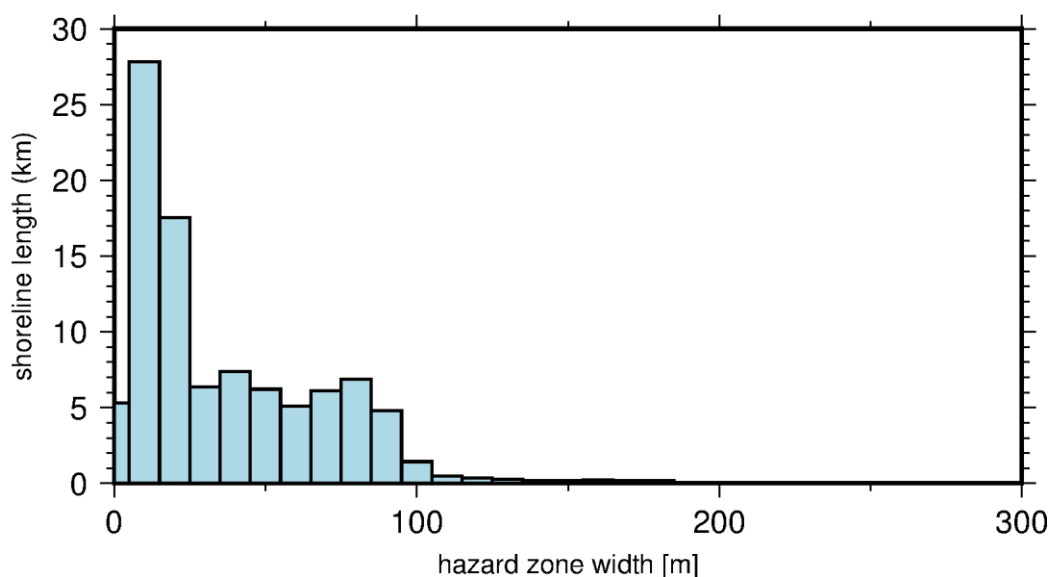


Figure 3-35: Histogram of predicted 100-year erosion hazard zone width for the most likely realisation (50th percentile).

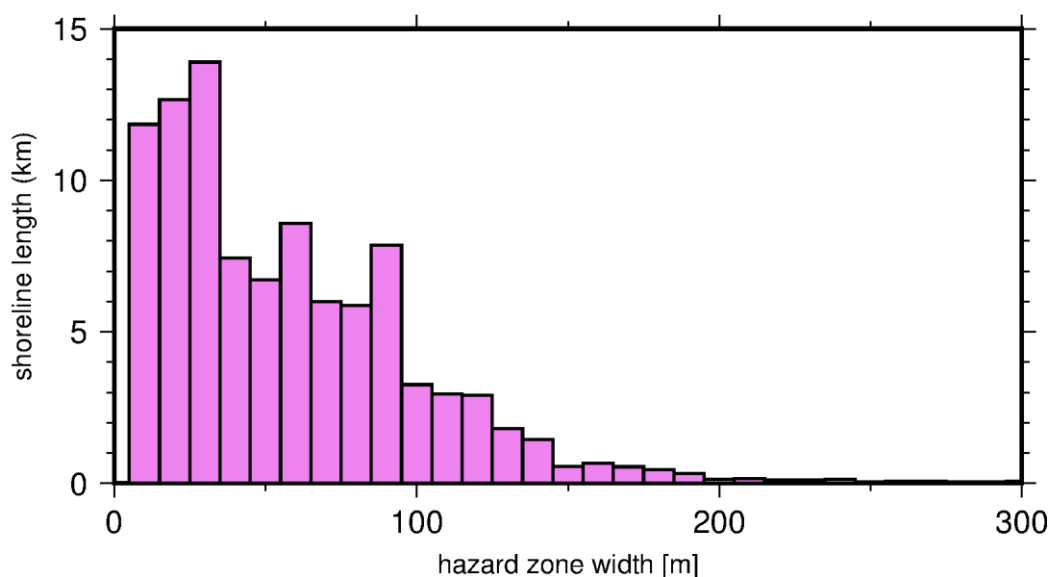


Figure 3-36: Histogram of predicted 100-year erosion hazard zone width for the 95th percentile realisation.

The hazard zone widths are mapped in Figure 3-37 whilst the hazard zone lines are included in the GIS supplementary material.

The description below outlines the general CHZ behaviour sequentially from north to south (Figure 3-37 to Figure 3-42).

The CHZ95 is less than 20 m wide at the Waitaki River mouth but it widens to 100 m at Seacliff Road. Further south the CHZ95 remains around 100 m until Simpson Road, where it starts to decrease to 60 m near Richmond Road. South of Richmond Road, the CHZ95 widens again to 120 m near McEneaney Road. Further south, the CHZ95 remains close to 100 m wide until it starts to decrease south of Hedges Road. The CHZ95 width is 65 m at Waitaki Boys High School, 77 m at Foyle Street,

and 60 m at Orwell Street. Behind the armoured coast at Oamaru, the CHZ95 narrows to less than 20 m by Oamaru central and 30 m at Oamaru Creek. In the inner harbour, the hazard zone width is less than 10 m.

At Beach Road, a current hotspot for coastal erosion south of Oamaru, the CHZ95 is close to 200 m wide on the northern section and 40 m wide along the southern section. Despite recent accretion trends (Figure 3-22) at the north end of the beach, the wide hazard zone there reflects the uncertainty of how the backshore dunes and cliffs respond in the short term. This section of the beach is also likely to erode in response to the acceleration of sea-level rise. The cliff section at the south end of Beach Road appears more stable but the extent of potential slumps is unclear. The slump that occurred in 2016 just north of the Coast Café was taken into account in the analysis but it is not clear whether other large slumps are likely on this stretch of coast.

Further south, at Kakanui, the rapid shoreline retreat and the expected vulnerability of the gravel barrier to sea-level rise creates a wide hazard zone for the whole beach, becoming wider southward toward the spit where the expected retreat is most uncertain. This is likely an overestimate of the shoreline retreat, but the estimated erosion hazard zone corresponds well to the estimates of the coastal inundation hazard zone there.

The coast north of Hampden is affected by a major slump. The slump appears to affect the entire hillside, while the toe of the slump is being washed away by the waves. The hazard is more of a geological hazard that is being kept active by coastal processes. The analysis used in this study is, however, not adequate to assess the hazard for such large slumps and the hazard zone is likely a conservative overestimate.

The slump does not affect Hampden town. In Hampden, the CHZ50 is 30 m wide and the CHZ95 is 55 m wide. These values remain similar most of the way south towards the Moeraki boulders, where the CHZ95 is extended to 80 m due to the presence of slumps in the cliff.

Moeraki town has experienced little historical changes in its shoreline and thus the CHZ95 is relatively narrow (35 m). The promontory to the old jetty may not be stable so the hazard zone was increased in this area. The town shoreline is currently stable because of the coastal defence structure preventing shoreline retreat, and it is assumed that it will be maintained in the future thus keeping the shoreline stable.

The coastal settlements of Te Karita and Kaika are located right on the beach edge and ad-hoc seawalls have been installed. This suggests that coastal erosion is a prominent problem for the two settlements. However, the presence of the seawall is hiding the natural movement of the shore, and the estimates of potential shoreline retreat are likely underestimated. There is, therefore, uncertainty in the future position of the shoreline at these locations - which is reflected in the CHZ95 widths of 70 m for Te Karita and 40 m at Kaika.

The northern end of Katiki Beach appears to be behaving similarly to an equilibrium sandy beach, and Bruun model predictions there of the impact of accelerated sea-level rise are considered reasonable. There, the CHZ95 extends between 100 m and 120 m. Further south, Katiki Beach is subject to greater geological control and the retreat rates become more variable but less overall - the CHZ95 width is typically 50 m to 60 m. At the southern end of Katiki Beach the beach transitions into a cliff and the CHZ95 width is reduced to less than 20 m. It is worth noting that of the 7 km span of SH1 along Katiki Beach, only 1.2 km is *not* in CHZ95 (and only 1.5 km is *not* in CHZ50).

The cliffs at Shag Point appear stable, with only slight changes detected in the shoreline analysis. This results in a CHZ95 of 15 m to 20 m from the existing cliff-line.

The cliffs south of the Shag River appear to have been stable with only small slumps detected, leading to a CHZ95 width of 30 m.

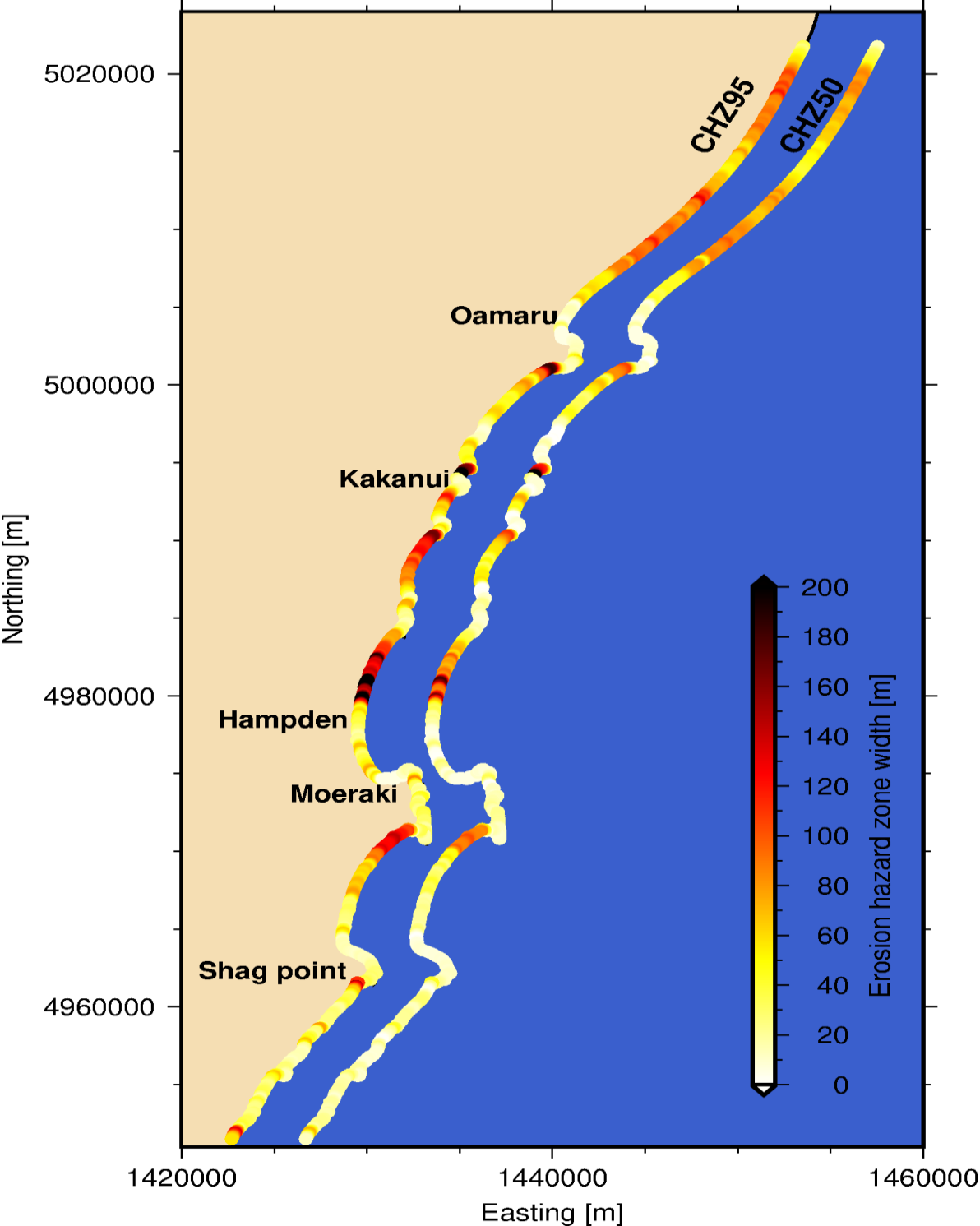


Figure 3-37: Coastal hazard zone width for 95th percentile (CHZ95) and for 50th percentile (CHZ50) for 100-year prediction for the entire Waitaki District coastline. Note the CHZ50 points are offset to the east.

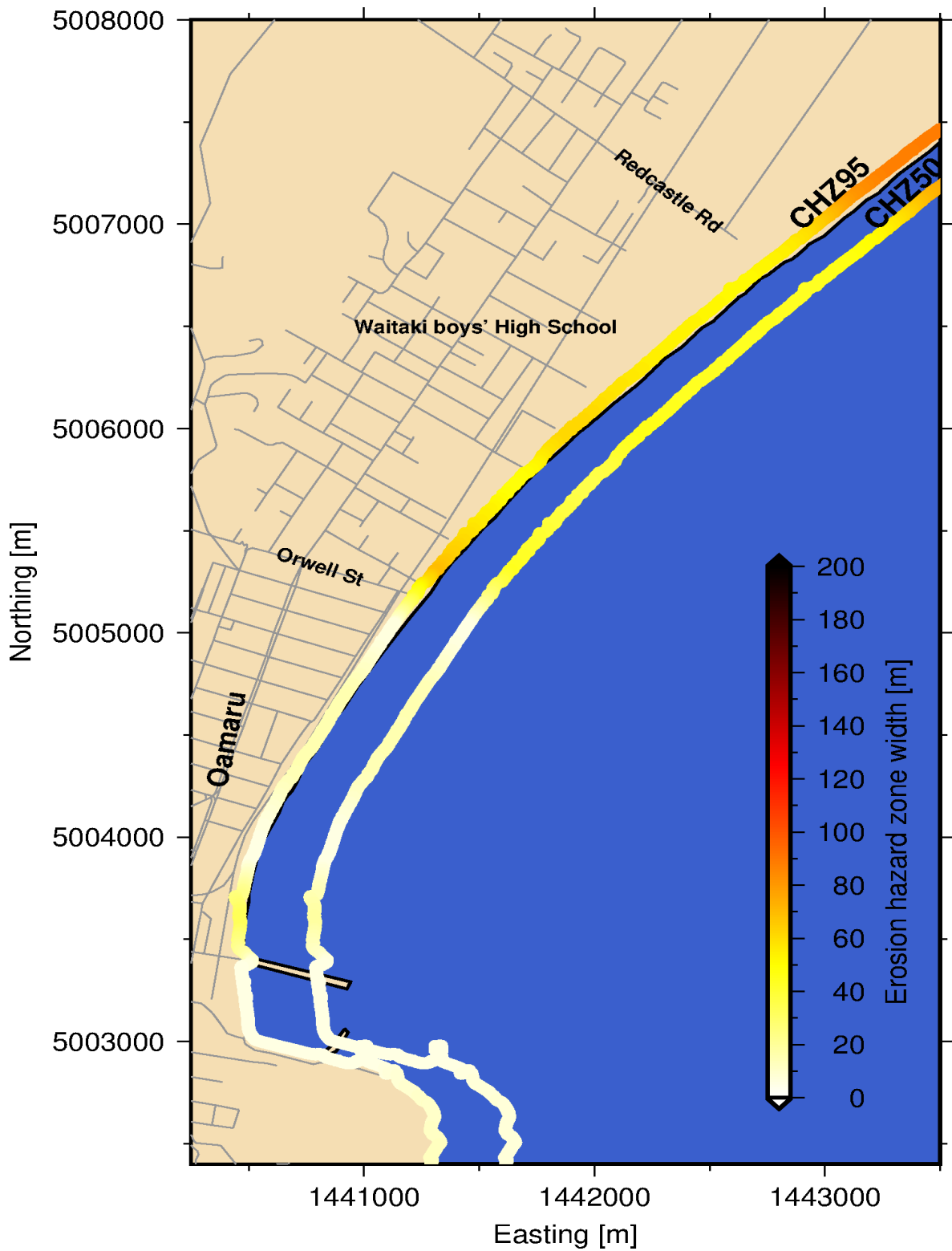


Figure 3-38: Coastal hazard zone width for 95th percentile (CHZ95) and for 50th percentile (CHZ50) for 100-year prediction for Oamaru. Note the CHZ50 points are offset to the east.

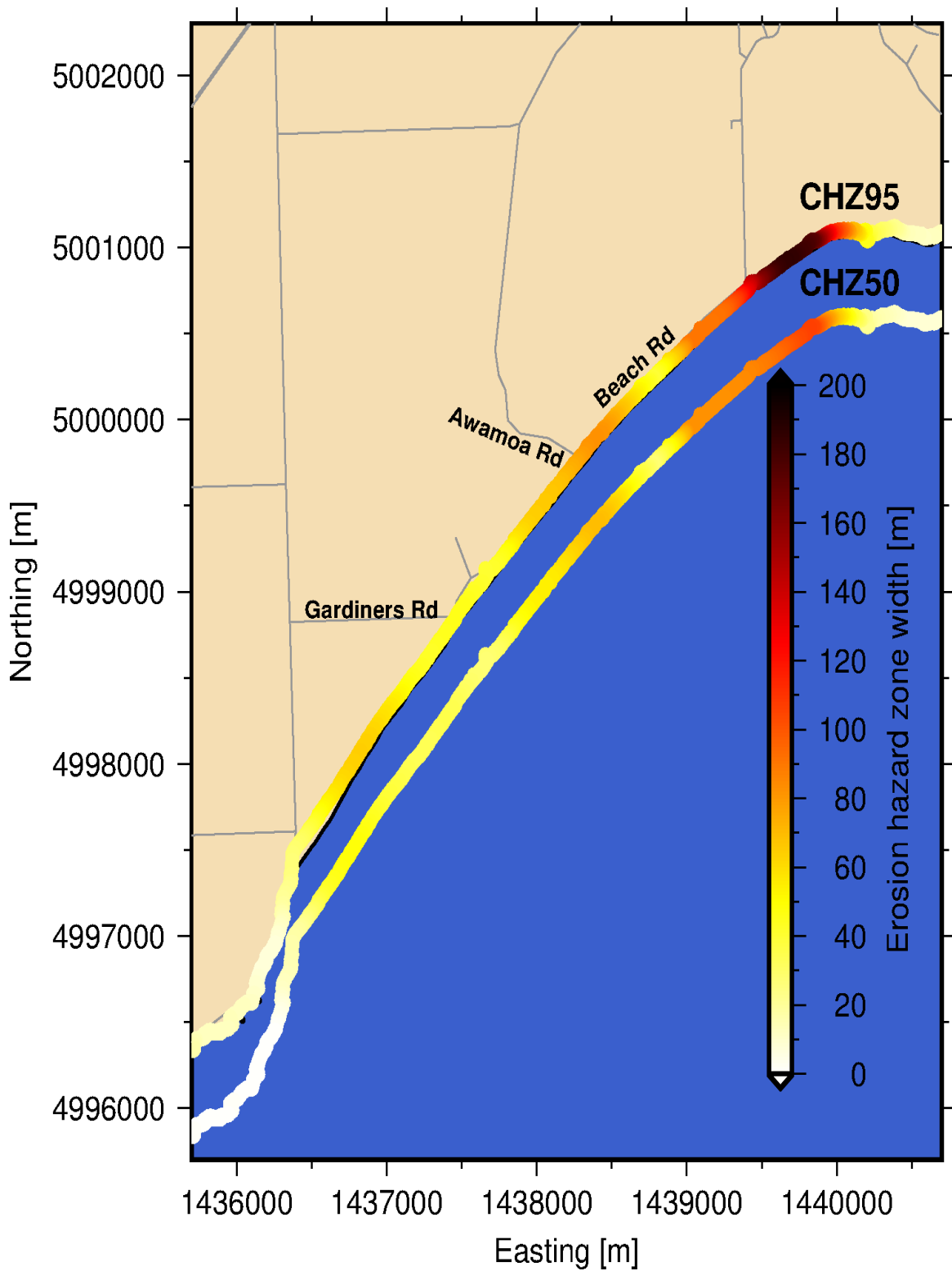


Figure 3-39: Coastal hazard zone width for 95th percentile (CHZ95) and for 50th percentile (CHZ50) for 100-year prediction for Beach Road. Note the CHZ50 points are offset to the south.

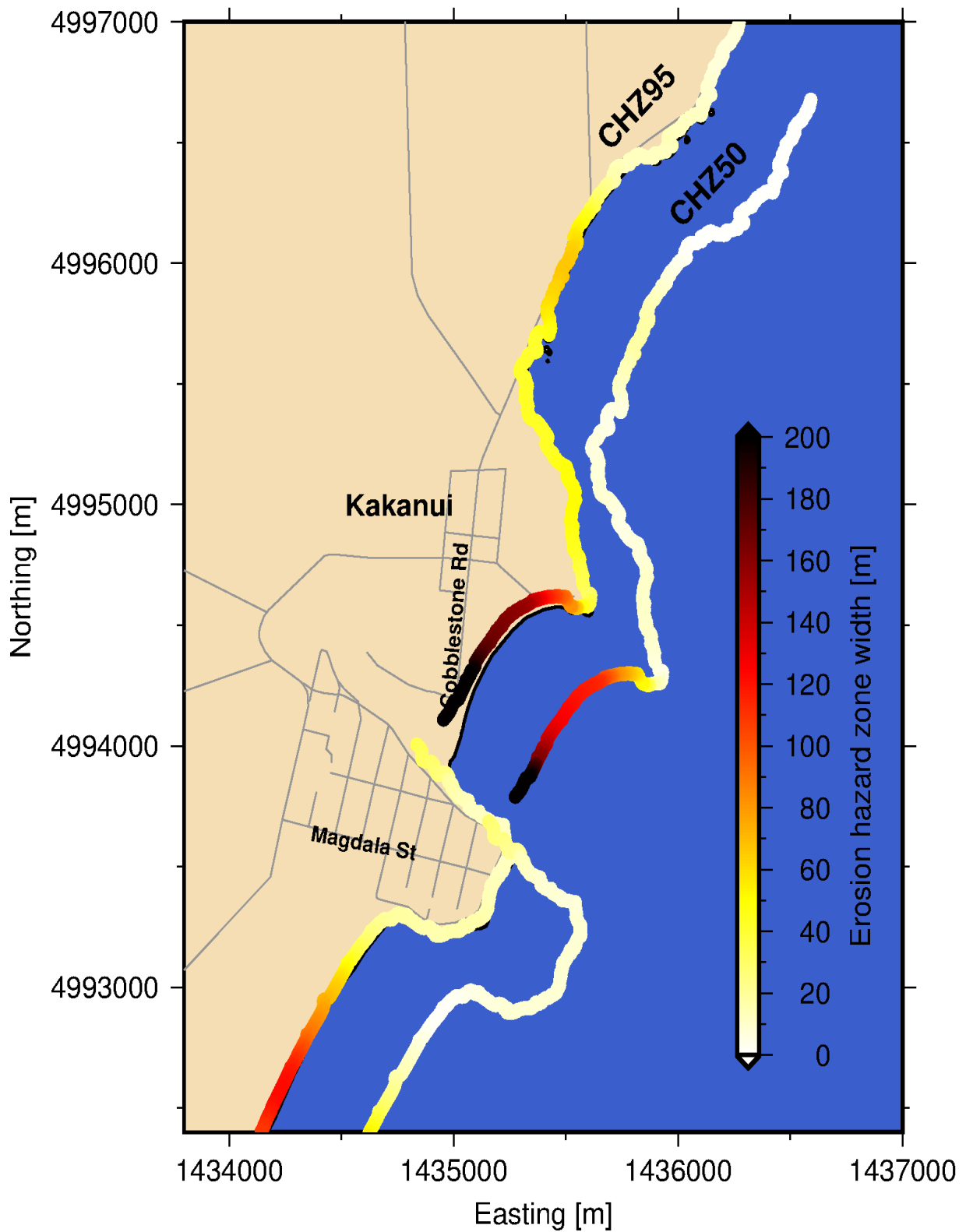


Figure 3-40: Coastal hazard zone width for 95th percentile (CHZ95) and for 50th percentile (CHZ50) for 100-year prediction for Kakanui. Note the CHZ50 points are offset to the southeast.

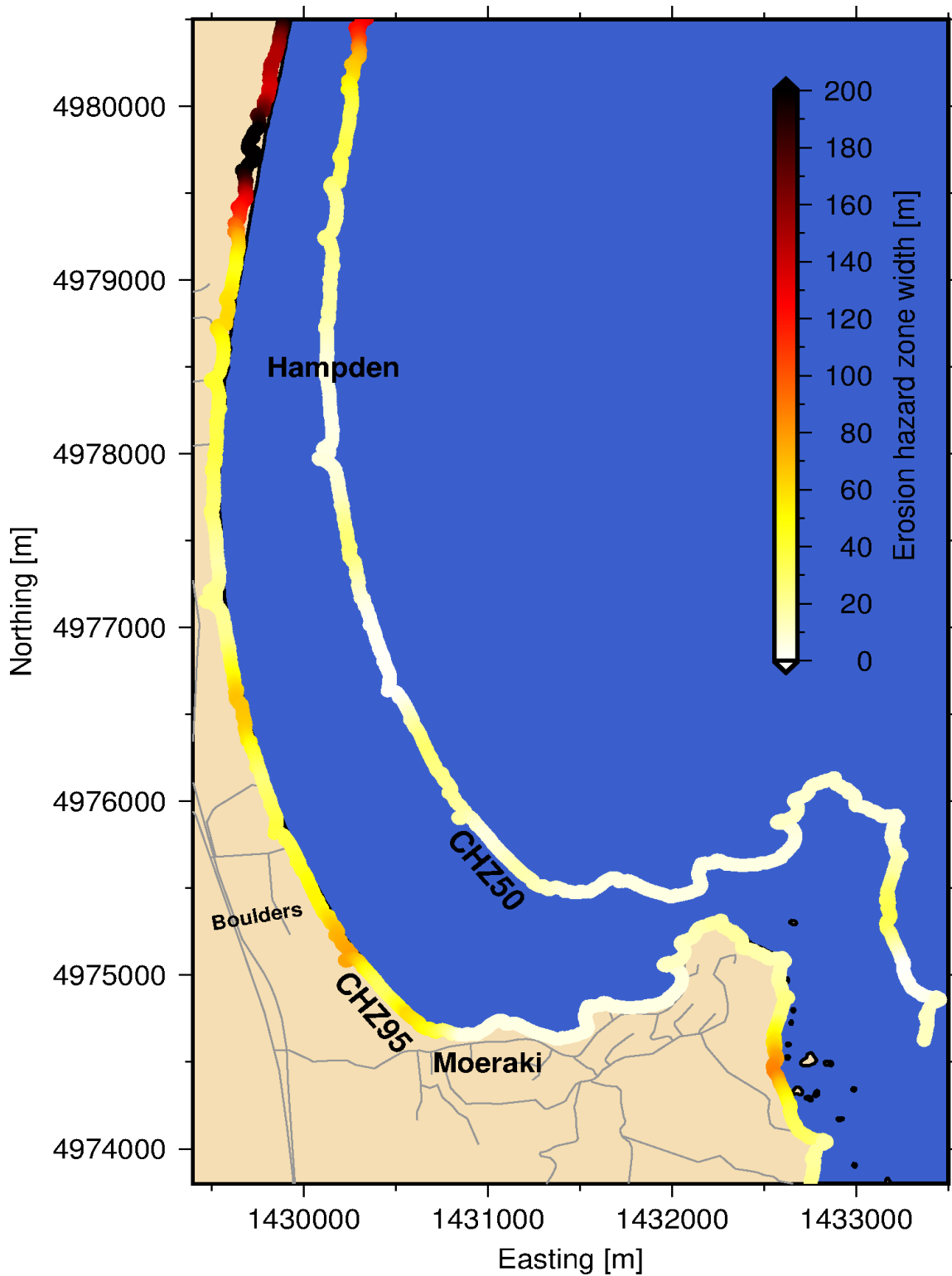


Figure 3-41: Coastal hazard zone width for 95th percentile (CHZ95) and for 50th percentile (CHZ50) for 100-year prediction for Hampden and Moeraki. Note the CHZ50 points are offset to the northeast.

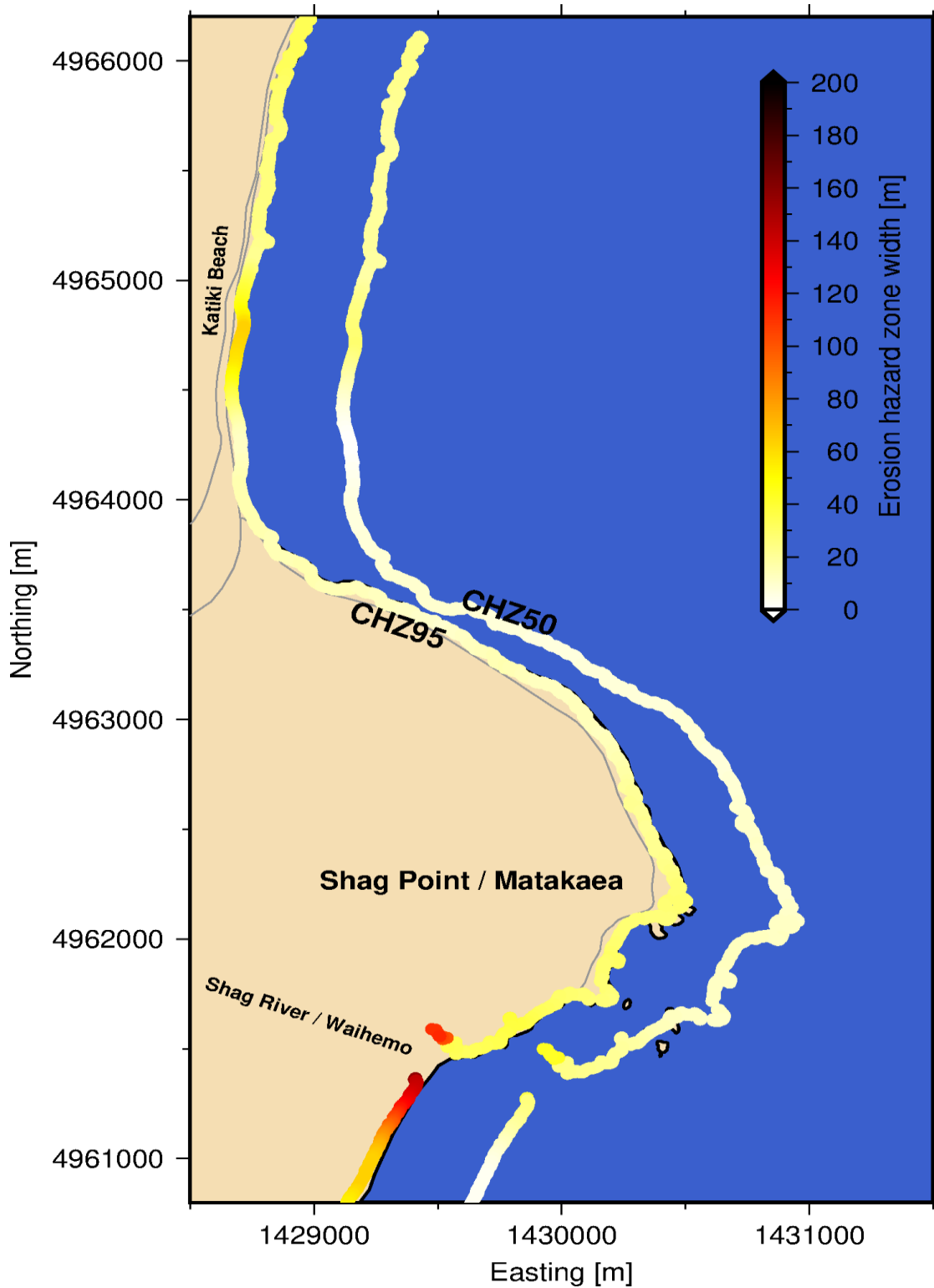


Figure 3-42: Coastal hazard zone width for 95th percentile (CHZ95) and for 50th percentile (CHZ50) for 100-year prediction for Shag Point / Matakaea. Note the CHZ50 points are offset to the southeast.

4 Discussion

4.1 Overview of the results

This study analysed the inundation and erosion hazards along the Waitaki District coast. The study found that while the erosion hazard is widespread, the inundation hazard only affects relatively small parts of the district (mostly Kakanui Estuary). This finding is consistent with the previous study of Todd (1997).

Limitations were found in the analysis of coastal inundation by Lane et al. (2008), and these limitations affect the reliability of the inundation prediction used in the coastal inundation hazard zone definition used herein. The limitations of the analysis of Lane et al. (2008) are non-conservative (i.e., they result in an inundation zone that is likely underpredicted) for the open-coast shore, where storm waves break, but are conservative on floodplains adjacent to estuaries. Improved extreme water level estimates are likely to show a reduction in the predicted inundation extent in Kakanui. Accurate predictions of wave runup are critical not only for inundation estimates in built-up areas but also for the small coastal settlements (e.g., Kaika and Karita) and infrastructure that is close to the shore (e.g., Katiki Road and Beach Road). Developing and implementing improved calculations for both extreme water levels and wave runup is out of scope for this project but should be considered in future studies.

The coastal erosion hazard zone was calculated using measured long-term erosion rates combined with potential short-term shoreline retreat due to storm-cut or cliff slumping/collapse. In areas where sufficient information was available, the contribution of the acceleration of sea-level rise has been taken into account. Simulation of the evolution of the cliffs north of Oamaru was undertaken using a morphological model, and this showed that acceleration in sea-level rise should have little impact on the cliff retreat.

The coastal hazard width proposed for the 100-year outlook with 95% confidence (CHZ95) is 65 m wide just north of Oamaru near Waitaki Boys High School and is similar to the proposed zoning by Johnstone (2001). Further north, to account for faster retreat rates and the occurrence of larger slumps on the cliffs, the CHZ95 width is close to 100 m, which is similar to the 100 m zone previously proposed for the Waitaki District Council.

It is noted that the erosion hazard zone estimates provided herein are based on a hybrid-probabilistic approach using the shoreline retreat data and short-term storm movement detected from aerial and satellite imagery and expert judgement where data is lacking and, in area north of Oamaru, also on a simulation of the cliff evolution with accelerated sea-level rise. The results presented here can be reproduced and refined when new data becomes available.

4.2 Impact of accelerated sea-level rise on the erosion hazard

Our SCAPE model simulations indicated that acceleration of sea-level rise over the next 100 years should have little effect on the erosion rate of the cliffs north of Oamaru. While this finding may appear counterintuitive, it is consistent with the expected dynamics of the cliffs. During fair weather, these cliffs are fronted by a gravel beach that can reach 5 m above mean sea level, and waves never reach the cliff toe, even at high tide; moreover, the gravel beach also acts as a retaining wall for the lower part of the cliff. During large and extreme coastal storms, this gravel beach is effectively removed, allowing waves to crash directly onto the cliff, undercutting it and producing large slumps. The gravel beach reforms quickly after the storm, again protecting the cliffs from waves. This is

anecdotally confirmed by the lack of cliff retreat observed on profiles between 1994 and 1999. As sea-level rises and the shore retreats, the beach height and the substrate profile under the beach are expected to lift to match the rise in sea-level, thus the protective function of the beach should be maintained. However, this finding is not applicable to other parts of the coast where the backshore cliff is lower and the beach sediment size smaller.

At the northern end of Katiki Beach and at Kakanui, a Bruun-type model was applied to separate the background erosion rate from that attributed to historical sea-level rise. However, Bruun-type models do not account for the effect of geological controls, so they are likely to overestimate the impact of sea-level rise on beaches tightly enclosed by headlands, such as at Kakanui, and beaches perched above nearshore reefs and tidal platforms, as is the case with the southern half of Katiki Beach.

4.3 Effectiveness of coastal protection to reduce erosion hazard

Small-scale coastal protection, such as short spans of riprap or concrete seawall, have not been taken into account in this analysis. This is mostly because these structures are often built with a shallow footing (e.g., ~1 m deep at Katiki), and therefore they will have a limited lifespan. Many dislodged blocks of riprap litter the shoreline of Katiki Beach, which is a sobering example of the inability of these structures to hold the shoreline along Beach Road (e.g., Figure 4-1 and Figure 4-2). Moreover, repeated LiDAR surveys (2004 and 2016) show that even the heavy armouring used at Oamaru degraded and settled over the intervening 12 years (Figure 3-24). This experience warns that where structures may be chosen for protecting additional assets in the future, heavy, deeply-footed armouring and high maintenance would be required.

4.4 Coastal monitoring

In the hotspots of erosion, a monitoring program would help to better capture the hazard characteristics (e.g. steady slow retreat of the shore versus storm driven rapid erosion) and understand the long-term trend of the shoreline, the role of individual storms, and the response of the coast to annual and inter-annual variability of the wave climate. Towards this, we recommend extending the network of surveyed profiles to include profiles at Beach Road, Kakanui, Moeraki Boulders and Katiki Beach, and to repeat these annually. An alternative approach to profile surveying would be to use airborne LiDAR or a mobile laser scanner to capture the full 3d topography of the shore.

Records of water level and waves would also allow analysis of the relationship between storm intensity and coastal erosion and inundation in greater detail. Wave and water level hindcasts used in this study could be verified with local data, and any bias in the hindcast could be captured in revisions of the inundation hazard zone.

Water level records kept in key estuaries and water ways (e.g., Oamaru port, Kakanui estuary) would clarify the contributions to inundation from river floods, storm surge, and wave runup and overwash.



Figure 4-1: Riprap section on Beach Road viewed on satellite imagery of 02/09/2006. The riprap (circled in black) was installed prior to 2003. Imagery source: DigitalGlobe.



Figure 4-2: Riprap section on Beach Road viewed on satellite imagery of 03/10/2012. The view is the same as shown on Figure 4-1. Note the material of the failed riprap scattered on the foreshore (circled in black). Imagery source: DigitalGlobe.

5 Conclusion

This study analysed the coastal hazards in the Waitaki District. Results show that the coastal erosion hazard is widespread, with more than 60% of the coast in the district retreating, while any significant coastal inundation hazard was limited to Kakanui.

The inundation hazard zones presented herein are based on the inundation extents of Lane et al. (2008), since that is as far as the scope of this work extended. Critical limitations were found in the Lane et al. analysis. In particular, no consideration was given to infragravity waves, and wave runup were underestimated. This limitation constrains the use of the inundation hazard zone to low-lying inland areas not exposed to open-coast wave action (e.g., Kakanui estuary floodplain, Oamaru harbour); it does not properly allow evaluation of the coastal inundation hazard in areas where wave breaking and runup is likely to be significant (e.g., Kaika, Karita, Katiki Road and Beach Road). Further work is recommended to refine extreme water levels and wave runup together and revise the inundation hazard zones in such areas.

A coastal erosion hazard zone was defined using a projection of the future shoreline position over 100 years taking into account historical retreat rates, sea-level rise and slope failure. Taking a conservative approach, the coastal hazard zone width typically ranged from 5 m to 145 m but reached 300 m at some locations.

Much infrastructure and many assets are located within the erosion hazard zones. No new erosion hotspots were identified, with continued erosion expected at the current hotspots of Katiki Beach, Beach Road, Kakanui, North Oamaru, and Kaika and Karita settlements. Any plans to stabilise these shores with protective structures would need to ensure that the structures are properly designed, constructed and maintained to maximise their lifespan. With perhaps the exception of the heavily armoured Oamaru shore, existing protection works along the District's coast are generally not functional in the long-term; indeed, some minor shoreline retreat has been observed even on the larger structures near Oamaru.

Monitoring of beach morphology at erosion hotspots is recommended on an annual basis and will enable refined estimates of the hazard zone widths and to better plan the nature and timing of erosion mitigations. Monitoring of water level and waves is also recommended to better assess the inundation hazard and the erosion impact of large storms.

6 Acknowledgements

The authors would like to thank the Waitaki District Council for being available for discussion during our field visit, showing us the erosion hotspots, sharing information. The authors would like to thank Richard Reinen-Hamill for his insightful review comments on a draft of the report.

7 References

- Boak, E., Turner, I. (2005) Shoreline Definition and Detection: A Review. *Journal of Coastal Research* 21(4): 688 – 703. <https://doi.org/10.2112/03-0071.1>.
- Bruun, P. (1962) Sea-level Rise as a Cause of Shore Erosion. Engineering progress at the University of Florida. Florida Engineering and Industrial Experiment Station.
- Carruther, J. (1871) Oamaru Harbour Works. Report to the Hon. Mr Gisborne, Wellington. *New Zealand journal of the House of Representatives*. Appendix to the Journals D-5b: 7:8.
- Dickson, M., Bristow, C., Hicks, M., Jol, H., Stapleton, J., Todd, D. (2009) Beach Volume on an Eroding Sand–Gravel Coast Determined Using Ground Penetrating Radar. *Journal of Coastal Research* 25(5): 1149 – 1159.
- Gallop, S. L., Bosserelle, C., Pattiaratchi, C. B., Eliot, I. (2011) Rock topography causes spatial variation in the wave, current and beach response to sea breeze activity. *Marine Geology* 290(1–4): 29–40. <https://doi.org/10.1016/j.margeo.2011.10.002>.
- Gibb, J.G. (1978) Rates of Coastal Erosion and Accretion in New Zealand. *New Zealand Journal of Marine and Freshwater Research* 12 (4): 429-56.
- Gibb, J.G., Adams, J. (1982) A sediment budget for the East Coast between Oamaru and Banks Peninsula, South Island, New Zealand. *New Zealand Journal of Geology and Geophysics* 25: 335-352.
- Gorman, R., Hicks, M., Walsh, J. (2002) Canterbury open-coast wave refraction and longshore transport study. *NIWA Client Report* ENC02509, prepared for Environment Canterbury, NIWA, Christchurch, 47 p.
- Gorman, R.M., Bryan, K.R., Laing, A.K. (2003) A wave hindcast for the New Zealand region: near-shore validation and coastal wave climate. *New Zealand Journal of Marine and Freshwater Research* 37(3): 567–588.
- Gouldby, B., Méndez, F.J., Guanache, Y., Rueda, A., Mínguez, R. (2014) A methodology for deriving extreme nearshore sea conditions for structural design and flood risk analysis, *Coastal Engineering* 88: 15-26.
- Hannah, J., Bell, R.G. (2012) Regional sea level trends in New Zealand. *Journal of Geophysical Research: Oceans* 117(C1): C01004.
- Hicks, D.M. (2011) Downstream effect of a large hydro-power scheme on a gravel-bed braided river and alluvial-fan coast: Waitaki River, New Zealand. In *Proceedings of River, Coastal and Estuarine Morphodynamics*, Beijing, China, September 2011.
- IPCC. (2013) Climate Change 2013: The Physical Science Basis. Contribution of Working Group I to the Fifth Assessment Report of the Intergovernmental Panel on Climate Change. Cambridge: Cambridge University Press. Retrieved from www.ipcc.ch/report/ar5/wg1/.

- Jackson, C., Alexander, C., Bush, D. (2012) Application of the AMBUR R package for spatio-temporal analysis of shoreline change: Jekyll Island, Georgia, USA. *Computers & Geosciences* 41: 199-207. ISSN 0098-3004, <https://doi.org/10.1016/j.cageo.2011.08.009>.
- Johnstone, N. (2001) North Otago Coastal Hazard Review. Report prepared for the Otago Regional Council. ISBN: 0-908922-67-1.
- Kopp, R.E., Horton, R.M., Little, C.M., Mitrovica, J.X., Oppenheimer, M., Rasmussen, D.J., Strauss, B.H., Tebaldi, C. (2014) Probabilistic 21st and 22nd century sea-level projections at a global network of tide-gauge sites. *Earth's Future* 2(8): 383–406.
- Lane, E., McMillan, H., Gillibrand, P., Enright, M., Carter, J., Arnold, J., Bind, J., Roulston, H., Goff, J., Gorman, R. (2008) Otago Regional Council Storm Surge Modelling Study. *NIWA Client Report: CHC2008-047*. Prepared for Otago Regional Council, June 2008.
- McCall, R.T., Masselink, G., Poate, T.G., Roelvink, J.A., Almeida, L.P. (2015) Modelling the morphodynamics of gravel beaches during storms with XBeach-G. *Coastal Engineering*, 41: 52-66. ISSN 0378-3839, <https://doi.org/10.1016/j.coastaleng.2015.06.002>.
- Measures, R., Cochrane, T., Caruso, B., Walsh, J., Horrell, G., Hicks, M., Wild, M. (2014) Analysis of Te Waihora lake level control options - A Whakaora Te Waihora science project. *NIWA Client Report CHC2014-076* prepared for Ngāi Tahu and Environment Canterbury, June 2014.
- Ministry for the Environment (2017) Preparing for Coastal change: A summary of coastal hazards and climate change guidance for local government. Available on the Ministry for the Environment website: www.mfe.govt.nz.
- Pattle, W.N. (1974) Coastal Processes and beach Development; Cape Wanbrow —Shag Point. MA Thesis, University of Canterbury.
- Robertson N. (2017) Kakanui floods video uploaded 21 July 2017. <https://www.youtube.com/watch?v=X6E2FmFQDUg&t=43s>.
- Roelvink, J.A., Renier, A.R., van Dongeren, A.R., van Thiel, de Vries, J.S.M., McCall, R. (2009) Modeling storm impacts on beaches, dunes and barrier islands. *Coastal Engineering* 56: 1133-1152.
- Rueda, A., Camus, P., Tomas, A., Vitousek, S., Méndez, F.J. (2016) A multivariate extreme wave and storm surge climate emulator based on weather patterns. *Ocean Modelling* 104: 242–251.
- Rueda, A., Cagigal, L., Antolinez, J.A., Albuquerque, J., Méndez, F.J. (In review) New Zealand Wave Climate Variability Based On Weather Patterns. Presented at the 1st International Workshop on Waves, Storm Surges and Coastal Hazards, Liverpool, Sept. 2017.
- Sheng, P.Y., Lapetina, A., Gangfeng, M. (2012) The reduction of storm surge by vegetation canopies: Three-dimensional simulations. *Geophysical Research Letters* 39: L20601. doi:10.1029/2012gl053577.

- Stephens, S.A., Allis, M., Robinson, B., Gorman, R. (2015) Storm tide and wave runup in the Canterbury region. *NIWA Client Report HAM2015-129* prepared for Environment Canterbury.
- Stephens, S.A., Robinson, B. (2016) Analysis of the Green Island sea-level record 2002-2015. *NIWA Client Report HAM2016-016* prepared for Otago Regional Council.
- Stockdon, H.F., Holman, R.A., Howd, P.A., Sallenger, A.H. (2006) Empirical parameterization of setup, swash, and runup. *Coastal Engineering* 53: 573-588.
- Todd, D.J. (1997) Otago Regional Tsunami and Storm Surge Study, Final Report. Report prepared for the Otago Regional Council by Tonkin and Taylor Ltd.
- Walkden, M.J.A., Hall, J.W. (2005) A predictive mesoscale model of the erosion and profile development of soft rock shores. *Coastal Engineering* 52(6): 535-563.
- Walkden, M., Dickson, M., Thomas, J., Hall, J. (2015) Simulating the Shore and Cliffs of North Norfolk. Chapter 7 of *Broad scale coastal simulation: new techniques to understand and manage shorelines in the third millennium*, Springer (editors: Nicholls, R., Dawson, R., and Day, S).
- Walters, R.A., Goring, D.G., Bell, R.G. (2001) Ocean tides around New Zealand. *New Zealand Journal of Marine and Freshwater Research* 35: 567–579.
- Wild, M., Bell, R., Walsh, J. (2005) Otago extreme sea level analysis. *NIWA Client Report CHC2005-114A*, August 2005.

8 List of supplementary material supplied separately from this report

Shapefile of digitized shoreline: Ambur_All_Shorelines_NZTM.shp

Shapefile of Calculated erosion rates: Shoreline_Retreat_Rates_Final.shp

Shapefiles with Coastal Hazard zone for 50-year and 100-year for both the 50th percentile and 95th percentile:

- CHZ50_50y_Final.shp.
- CHZ95_50y_Final.shp.
- CHZ50_100y_Final.shp.
- CHZ95_100y_Final.shp.

GIS raster files and figures for extreme water level inundation in Oamaru, Kakanui, Hampden and Moeraki for the 20-year, 50-year, 100-year and 500-year ARI and for sea-level rise scenarios of 0.0 m, 0.3 m, 0.5 m, 0.7 m, 0.9 m, 1.1 m and 1.3 m above present mean level of the sea.